

**Carbon-isotope stratigraphy of the East Isthmus Bay (Port au
Port and St. George groups) and Broom Point (Cow Head Group)
sections, western Newfoundland, Canada**

By

© Sebastian Scorrer

A thesis submitted to the

School of Graduate Studies

in partial fulfilment of the requirements for the degree of

Master of Science

Department of Earth Sciences

Memorial University of Newfoundland

April 2018

St. John's, Newfoundland and Labrador

ABSTRACT

The carbon-isotope stratigraphy of two carbonate sections spanning the Upper Cambrian to lowermost Ordovician from western Newfoundland were investigated for their potential for regional and global correlation with coeval carbonate sections.

The East Isthmus Bay (EI) section consists of carbonates from the uppermost Cambrian (Furongian) Berry Head Formation (~ 160 metres thick), and the lowermost Ordovician (Tremadocian) Watts Bight Formation (~ 30 metres thick) that accumulated in a shallow-marine setting on the Laurentian platform/passive margin in western Newfoundland, Canada. Petrographic investigation shows that the sampled carbonates have retained at least their near-primary sedimentary fabrics, though there is minor recrystallisation in the lower section.

The Broom Point (BP) section encompasses the Broom Point North (~ 20 metres sampled) and Broom Point South (~ 120 metres sampled) sections. The sections cover the Shallow Bay (Furongian) and Green Point (Tremadocian) formations, these carbonates formed further down the slope in slightly deeper water. Petrographic examination of the carbonates implies the retention of near-primary sedimentary fabrics.

Correlation between the Sr and Mn concentrations of carbonates from both sections suggests the Broom Point carbonates have been more impacted by diagenesis than their East Isthmus Bay counterparts due to the higher correlation ($R^2_{BP} = 0.4$, $R^2_{EI} = 0.18$, respectively). The East Isthmus Bay $\delta^{13}\text{C}$ values show insignificant correlation with their Sr ($R^2_{EI} = 0.04$), Mn ($R^2_{EI} = 0.001$), and Fe ($R^2_{EI} = 0.02$) counterparts, implying preservation of at least near-primary carbon-isotope compositions. On the other hand, the Broom Point section shows considerable correlation of Sr and Mn with their $\delta^{13}\text{C}$ counterparts ($R^2_{BP} = 0.54$

and $R^2_{BP} = 0.29$, respectively), implying considerable alteration of the primary geochemical signatures. Though a poor correlation is seen between $\delta^{13}\text{C}$ and Fe ($R^2_{BP} = 0.14$) in the Broom Point carbonates and insignificant correlation is seen between the $\delta^{18}\text{O}$ and $\delta^{13}\text{C}$ values in both the investigated sections ($R^2_{EI} = 0.0003$, $R^2_{BP} = 0.06$).

The petrographic and geochemical examination suggests that a reliable carbon-isotope profile can be reconstructed from the $\delta^{13}\text{C}$ signatures of the East Isthmus Bay section. On the contrary the geochemical analyses do not support the preservation of near-primary $\delta^{13}\text{C}$ signatures from the Broom Point section, emphasising the importance of using geochemical analyses alongside petrographic examination to inspect the degree of preservation of $\delta^{13}\text{C}$ signatures of carbonate rocks.

The East Isthmus Bay section is largely fossil poor but the $\delta^{13}\text{C}$ profile shows a pattern with distinct variations that can be matched with those of the Laurentian Lawson Cove Auxiliary Boundary Stratigraphic Section and Point (ASSP) section, Utah, USA. Therefore, a conclusive conodont biozonal match was possible to reconstruct by matching the $\delta^{13}\text{C}$ profile with its counterpart from the Lawson Cove ASSP section. At the base of the East Isthmus Bay section, the $\delta^{13}\text{C}$ profile exhibits a broad excursion (the top of the HerlInmaria-Red Tops Boundary, HERB Event), which can be matched with the base of the *Eoconodontus* Zone (mid-Furongian), followed by an enrichment trend through the *Cordylodus intermedius* Zone (top Furongian). A positive anomaly (*Hirsutodontus simplex* spike or HSS) is recorded in the upper *Cordylodus intermedius* Zone (the top Cambrian), and a prominent positive peak characteristic for the upper *Cordylodus lindstromi* Zone is recorded from the top of the investigated section. The $\delta^{13}\text{C}$ values of the Newfoundland carbonates are generally $\sim 1\text{ ‰}$ VPDB lower than the Lawson Cove values, which is likely attributed to a relative higher productivity and/or organic burial in the Utah region.

The investigated carbon-isotope stratigraphy revealed four main excursions: (1) an upper negative excursion (~ 2.5 ‰ VPDB), thought to be associated with the Cambrian–Ordovician boundary, (2) a lower broad negative excursion (~ 2 ‰ VPDB) which can be correlated to the latest Furongian HERB Event. (3) A positive excursion of ~ 1 ‰ VPDB seen at the base of the *Cordylodus proavus* conodont Zone and finally (4) a distinct gradual rise in positive $\delta^{13}\text{C}$ values known as the *Hirsutodontus simplex* Spike (or HSS). These four excursions can be seen on various sections worldwide spanning the uppermost Cambrian to lowermost Ordovician.

This work is dedicated to;
Mrs. P. J. Scorrer, Dr. T. J. Scorrer,
and
Mr. J. T. M. Scorrer who sadly passed during the completion of this work.

ACKNOWLEDGEMENTS

The author wishes to express his sincere appreciation to Professor Karem Azmy for his supervision of this study and critical reading of the thesis. Special thanks also to Dr. Svend Stouge and Dr. Gabriella Bagnoli for their assistance and support during the field sampling of this study, and again to Dr. Svend Stouge for his constructive comments on the thesis. This project was supported by funding (to Karem Azmy) from Petroleum Exploration Enhancement Program (PEEP) and (to Svend Stouge) the Carlsberg Foundation, Denmark.

The author also wishes to thank Allison Pye (Stable Isotope Lab) and Inês Nobre Silva (Trace Element Lab) for technical assistance in chemical analyses.

TABLE OF CONTENTS

ABSTRACT	ii
DEDICATION.....	v
ACKNOWLEDGEMENTS	vi
LIST OF FIGURES	x
LIST OF TABLES	xii
LIST OF APPENDICES	xii
CHAPTER I.....	1
INTRODUCTION.....	1
1.1 Scope and Purpose of Study	1
CHAPTER II	6
GEOLOGIC SETTING AND STRATIGRAPHY	6
2.1 Geologic Setting	6
2.2 Stratigraphy	8
2.2.1 Port au Port Group.....	8
2.2.1.1 Berry Head Formation	10
2.2.2 St. George Group.....	10
2.2.2.1 Watts Bight Formation.....	10
2.2.3.1 Shallow Bay Formation	13
2.2.3.2 Tuckers Cove Member	14
2.2.3.3 Green Point Formation.....	14
2.2.3.4 Broom Point Member	16
2.2.4 This Study.....	16
2.2.4.1 East Isthmus Bay Section	17
2.2.4.2 Broom Point Section	19
2.2.4.2.1 Broom Point North section	20
2.2.4.2.2 Broom Point South section	20
2.2.4.3 Broom Point Biostratigraphy.....	21
2.2.4.3.1 Broom Point North section	21
2.2.4.3.2 Broom Point South section	22
CHAPTER III	23
METHODS AND THEORY	23
3.1 METHODOLOGY.....	23

3.1.1 Sampling Protocol.....	23
3.1.2 Petrographic Analysis	23
3.1.3 Geochemical Analysis.....	25
3.2 CATHODOLUMINESCENCE.....	25
3.2.1 Concept and Applications	25
3.2.2 Apparatus.....	29
3.3 STABLE ISOTOPE ANALYSIS	29
3.3.1 Carbon Isotopes	30
3.3.2 Oxygen Isotopes	31
3.3.3 Procedure (Gas Bench Carbonate Method)	32
3.4 INDUCTIVELY COUPLED PLASMA MASS SPECTROMETER	33
3.4.1 Trace Element Analysis.....	33
3.4.2 Analytical Protocol	33
CHAPTER IV	35
RESULTS	35
4.1 East Isthmus Bay section	35
4.2 Broom Point sections.....	37
4.3 Petrography	37
4.2 Geochemistry	38
4.2.1 Major and Trace Elements	38
4.2.2 Carbon and Oxygen Isotopes.....	42
4.2.3 Carbon Isotope Stratigraphy.....	43
4.2.4 Manganese and Strontium.....	45
CHAPTER V	47
DISCUSSION	47
5. Discussion.....	47
5.1 East Isthmus Bay section	47
5.1.1 Evaluation of Sample Preservation.....	47
5.1.2 Major and Minor Trace Elements and Stable Isotopes	48
5.1.3 Carbon Isotope Stratigraphy.....	50
5.2 Broom Point sections.....	51
5.2.1 Evaluation of Sample Preservation.....	51
5.2.2 Major and Minor Trace Elements and Stable Isotopes	52
5.3 East Isthmus Bay section match to the Lawson Cove ASSP section, Utah, USA...54	
5.4 Global Correlation of the East Isthmus Bay Section Carbon-Isotope Profile.....55	

CHAPTER VI.....	59
CONCLUSIONS	59
6.1 East Isthmus Bay section	59
6.2 Broom Point sections.....	60
REFERENCES.....	61
CHAPTER VII	83
Manuscript submitted to Canadian Journal of Earth Sciences (in review)	83

LIST OF FIGURES

Figure 1.1. Map of western Newfoundland, Canada, showing the location of the investigated sections.

Figure 2.1. A schematic framework of the stratigraphic units spanning the East Isthmus Bay section.

Figure 2.2. Stratigraphic framework of the investigated upper Cambrian and lowermost Ordovician East Isthmus Bay section.

Figure 2.3. Photographs of various sedimentary features of the East Isthmus Bay carbonates

Figure 2.4. A stratigraphic framework of the Cow Head Group Broom Point (modified from James and Stevens, 1986).

Figure 2.5. Stratigraphic framework of the investigated Upper Cambrian and lower Ordovician section at Broom Point.

Figure 2.6. Localities where the boundary between the Berry Head and Watts Bight formations are exposed on the Port au Port Peninsula (Modified from Ji and Barnes, 1994).

Figure 3.1. Photomicrographs showing the resultant staining from the potassium ferricyanide and alizarine red solution.

Figure 3.2. Diagram showing the process that causes cathodoluminescence in minerals (Boggs *et al.*, 2001).

Figure 4.1. Photomicrographs of various petrographic features of the East Isthmus Bay carbonates.

Figure 4.2. Photomicrographs of various petrographic features of the Broom Point carbonates.

Figure 4.3. Scatter plots showing correlation of Mn with Sr, and Sr, Mn, and Fe with their $\delta^{13}\text{C}$ counterparts for the investigated samples.

Figure 4.4. Scatter plot showing the correlation of $\delta^{13}\text{C}$ values with their $\delta^{18}\text{O}$ counterparts.

Figure 4.5. Stratigraphic framework with the carbon-isotope, Mn and Sr profiles of the investigated East Isthmus Bay section.

Figure 4.6. Stratigraphic framework with the carbon-isotope profiles of the investigated sections at Broom Point.

Figure 5.1. Correlation of the $\delta^{13}\text{C}$ profiles of the East Isthmus Bay section, western Newfoundland, Canada, with that of Lawson Cove, Utah, USA.

Figure 5.2. Carbon-isotope stratigraphic correlation of Cambrian–Ordovician strata between Laurentia, China, Australia, USA, and Argentina.

LIST OF TABLES

Table 3.1. Cathodoluminescence colours of principle carbonate minerals.

Table 3.2. Examples of organic, physical and chemical processes associated with carbonate diagenesis.

Table 4.1. Summary of geochemical statistics from the investigated section and the Green Point GSSP section (Miller *et al.*, 2011; Azmy *et al.*, 2014).

LIST OF APPENDICES

Appendix 1. Sample, elemental, and isotopic geochemical compositions of the East Isthmus Bay carbonates.

Appendix 2. Sample, elemental, and isotopic geochemical compositions of the Broom Point carbonates.

CHAPTER I

INTRODUCTION

1.1 Scope and Purpose of Study

Chemostratigraphy has a great potential for refining the global stratigraphic correlations of sequences (e.g., Jing *et al.*, 2008; Azmy *et al.*, 2014, 2015; Li *et al.*, 2017) particularly those with poor or no biostratigraphic resolution. The near-primary stable isotope signatures of well-preserved carbonates have been found to be reliable tools of isotope correlations (e.g., Veizer *et al.*, 1999, Azmy *et al.*, 2014). The variations in the reconstructed $\delta^{13}\text{C}$ profiles of well-reserved carbonates reflect the changes in eustatic sealevel, which allow the correlation of sedimentary sequences, not only from the same basin (e.g., Azomani *et al.*, 2013; Olanipekun *et al.*, 2014), but also on a global basis at high resolution (e.g., Veizer *et al.*, 1999; Jing *et al.*, 2008; Azmy *et al.*, 2010; Miller *et al.*, 2011, 2014). The eustatic sea-level changes during the late Cambrian and early Ordovician have significantly influenced the redox conditions and organic productivity along the eastern margin of Laurentia, which influenced the $\delta^{13}\text{C}$ signatures of the associated carbonates (e.g., Azmy *et al.*, 2014, 2015; Wang *et al.*, 2017). The Upper Cambrian carbonate sections from East Isthmus Bay, near Port au Port, and from Broom Point (Fig. 1.1; western Newfoundland, Canada) are potential candidates to examine those variations through the reconstruction of a reliable near-primary carbon-isotope profile that reflects the palaeoenvironmental changes.

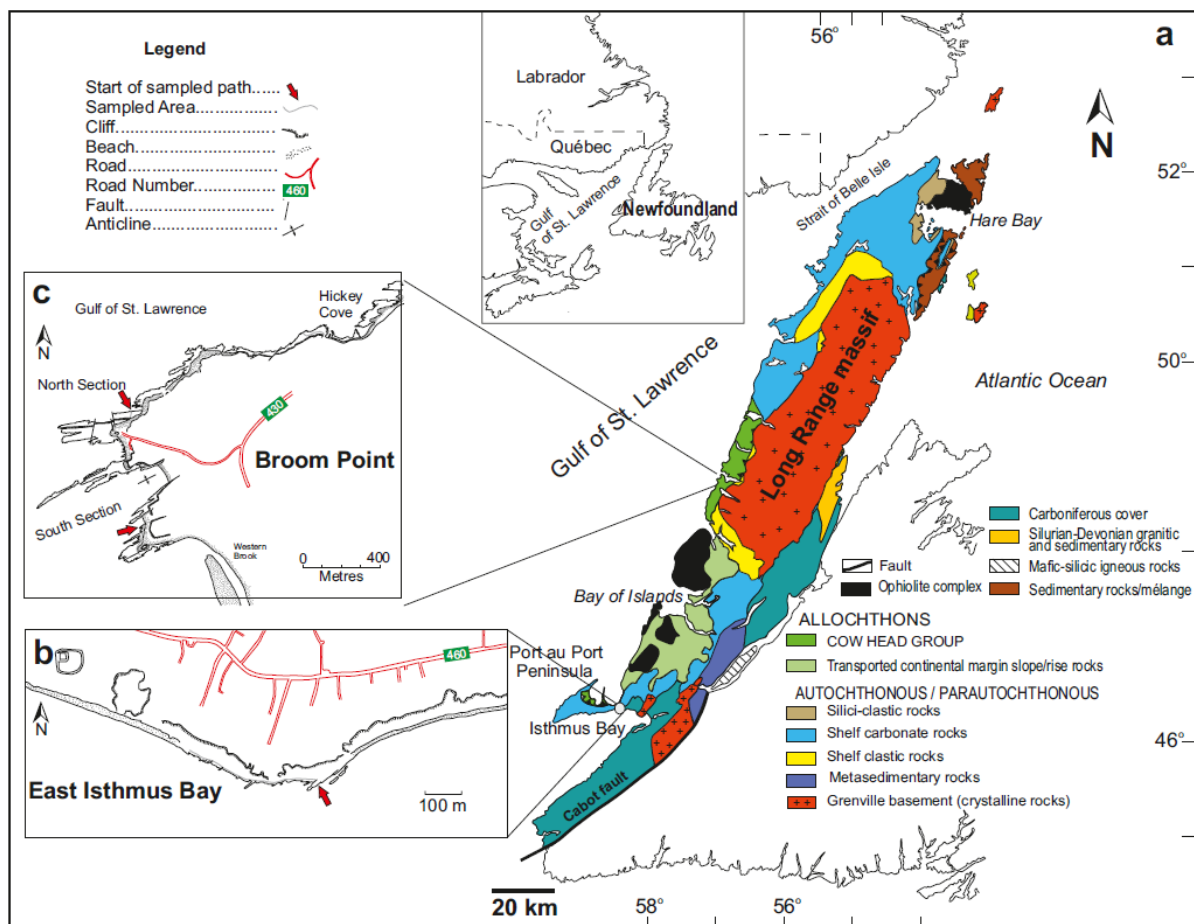


Fig. 1.1. (a) Map of western Newfoundland, Canada, showing the location of the investigated sections, and (b) East Isthmus Bay section's coastline (48° 33' 5.5" N; 58° 42' 4.5" W). (c) Broom Point sections coastline (Broom Point North, 49° 50' 15.9" N; 57° 52' 06.9" W; Broom Point South, 49° 49' 53.0" N; 57° 52' 02.0" W). Detailed in text.

In the last decade, the $\delta^{13}\text{C}$ profiles of the marine carbonates of Port au Port Peninsula, western Newfoundland (e.g., Salzman *et al.*, 2004; Hurtgen *et al.*, 2009), documented the presence of the wide spread distinct carbon-isotope event called the Steptoean positive carbon isotope excursion (or SPICE) in the Petit Jardin Formation at Felix Cove, Port au Port Peninsula. The excursion has been dated by trilobites (*Aphelaspis*, *Dunberbergia*, and *Elvinia* zones), on the south coast of Port au Port Peninsula (Fig. 1.1) to the Steptonian Stage of the

Upper Cambrian (Westrop, 1992; Cowan and James, 1993; Knight and Boyce, 2002; Salzman *et al.*, 2004). Hurtgen *et al.*, (2009) presented both $\delta^{34}\text{S}$ and $\delta^{13}\text{C}$ isotope data from the Port au Port Group and recorded two $\delta^{13}\text{C}$ excursions, where one was referred to the SPICE Event (Salzman *et al.*, 2004). The authors investigated the March Point and Felix Cove formations of the Port au Port Group and their studies focused on sections likely in the steep coastal cliff exposed along the south coast of the Port au Port Peninsula. However, this study sheds light on the younger carbonates outcropped at the southwestern coast of Newfoundland.

Miller *et al.*, (2011) studied carbonates younger than the SPICE Event from multiple sections on a global scale. A high-amplitude, negative carbon-isotope excursion known as the Hellnmaria-Red Tops Boundary or HERB Event, was investigated in sections from Utah (USA), Queensland (Australia), and Newfoundland (Canada). The HERB Event is represented by a negative $\delta^{13}\text{C}$ excursion that consists of several high-amplitude $\delta^{13}\text{C}$ peaks in Upper Cambrian sections, which can be used for global correlations. In the Green Point, western Newfoundland, a drop of $\sim 4\text{‰}$ VPDB was observed, and a fall of similar $\delta^{13}\text{C}$ values was also documented in the other sections (e.g., Ripperdan *et al.*, 1992; Buggisch *et al.*, 2003; Jing *et al.*, 2008; Miller *et al.*, 2014; 2015b; Azmy *et al.*, 2018). The Green Point slope deposits are poorly fossiliferous, but the HERB Event occurs at the base of the *Eoconodontus notchpeakensis* conodont Subzone in Utah (Miller *et al.*, 2011).

Azmy and Lavoie (2009) constructed the $\delta^{13}\text{C}$ -isotope profile for the St. George Group (Lower Ordovician), western Newfoundland and Azmy *et al.*, (2010) discussed its correlation along the Laurentian margin with northeast Greenland. This investigation studies the Upper Cambrian to Lower Ordovician carbonates exposed at Broom Point and East of Isthmus Bay on the southwestern coast of Newfoundland.

Azmy *et al.*, (2014) investigated the carbon-isotope stratigraphy of the Cambrian–Ordovician boundary of the Green Point Formation at the Global Boundary Stratotype Section and Point (GSSP) section (Green Point, western Newfoundland). The geochemical investigations indicated the preservation of near-primary signatures of the carbonates, and thus the reliability of the $\delta^{13}\text{C}$ values for chemostratigraphic correlations of those carbonates. No significant $\delta^{13}\text{C}$ excursions have been documented until near the boundary where a composite excursion was revealed. This unique excursion can be used to aid the correlation of the Cambrian–Ordovician boundary in other carbonate sequences (Azmy *et al.*, 2014, 2015).

Recently, Azmy (2018) studied the upper Furongian (uppermost Cambrian) carbonate rocks of Martin Point (western Newfoundland). The study combined multiple petrographic and geochemical screening tools to confirm the preservation of at least near-primary $\delta^{13}\text{C}$ signatures. The Martin Point carbon-isotope profile identified two main negative excursions, a lower excursion, associated with the HERB event, and an upper excursion corresponding to the Cambrian–Ordovician boundary.

Due to the barren nature of the East Isthmus Bay section in respect to fossils, this study will also investigate the possibility of improving the age resolution of these intervals due to their low biostratigraphic resolution (Glumac, 2002a) by using carbon isotope excursions as markers to correlate with equivalent fossiliferous sections, whose age has been determined by the combination of the carbon isotope record and biostratigraphic indicators (Glumac, 2002a, 2002b; Miller *et al.*, 2014).

The chemostratigraphic investigations in western Newfoundland will allow refining the regional and global correlations and better understand the evolution of the marine palaeoenvironment during the late Cambrian and early Ordovician. The current study focuses on the carbonates of East Isthmus Bay (Berry Head to Watts Bight Formation) and Broom

Point (Shallow Bay to Green Point Formation) sections that spans the uppermost Cambrian, western Newfoundland, and the main objectives are:

1. To investigate and compare the petrographic and geochemical preservation of carbonates at Broom Point and East Isthmus Bay.
2. To present the carbon-isotope stratigraphy of the late Cambrian, Berry Head Formation of the Port au Port Group extending into the Lower Ordovician, Watts Bight Formation of the St. George Group to cover the interval immediately above the $\delta^{13}\text{C}$ curve of Hurtgen *et al.*, (2009).
3. To reconstruct reliable carbon-isotope profiles that allows basinal and global correlations of the HERB Event.
4. To discuss correlation of the conodont biozonation scheme with the mainly barren (fossil-poor) carbonates of the Berry Head and Watts Bight formations (East Isthmus Bay section) of western Newfoundland by matching the $\delta^{13}\text{C}$ isotope variations.
5. To correlate the results of this study with the results from other studies spanning the same period on a global scale (uppermost Cambrian to Lower Ordovician).

A manuscript (attached at the end of thesis) discussing the correlation of the $\delta^{13}\text{C}$ profile East Isthmus Bay section (western Newfoundland Canada) with the equivalent Lawson Cove counterpart (Utah, USA) has been submitted to the Canadian Journal of Earth Sciences (CJES) for publication.

CHAPTER II

GEOLOGIC SETTING AND STRATIGRAPHY

2.1 Geologic Setting

The Furongian (Upper Cambrian) to Tremadocian (Lower Ordovician) carbonates in western Newfoundland represent the Canadian segment of the extensive peritidal to shallow-marine carbonates that covered most of the Laurentian palaeocontinent (James *et al.*, 1989; Knight and Boyce, 2002; Lavoie *et al.*, 2003, 2013). Western Newfoundland is the north-easternmost extension of the Appalachian fold belt (Stevens, 1970; Williams, 1995; Hibbard *et al.*, 2007) and it belongs to the tectonostratigraphic Humber zone of the Appalachian orogen comprising a record of continental platform and margin deposits of Laurentia in association with the opening of the Iapetus Ocean (Williams, 1975; 1979; Cawood *et al.*, 2001). The Humber Zone consists of crystalline basement overlain by rift-related, passive margin and foreland basin sedimentary successions (Williams, 1995; Cawood *et al.*, 2001; Waldron *et al.*, 1998). In the Humber Zone, slices of Neoproterozoic to Upper Ordovician rocks are deformed and thrust over the St. Lawrence cratonic platform (St-Julien and Hubert, 1975; Williams, 1979; Waldron *et al.*, 1998; Lavoie *et al.*, 2003).

The Laurentian plate formed by active rifting of the supercontinent Rodinia, associated with the opening of the Iapetus Ocean, in the Neoproterozoic (570–550 Ma) (Cawood *et al.*, 2001; Hibbard *et al.*, 2007), which resulted in an irregular-shaped continental margin (Thomas, 1977). In the early Cambrian to early Middle Ordovician, the irregular palaeo-southern margin of Laurentia underwent a rapid transgression over the thermally subsiding passive margin, which initiated marine sedimentation of shallow water siliciclastic and carbonate rocks in the warm tropical waters (James *et al.*, 1989; Knight *et al.*, 2007, 2008; Lavoie and Dix, 2012; Lavoie *et al.*, 2013). These shallow-water autochthonous and

parautochthonous siliciclastics and carbonates sedimentary rocks were deposited on the shelf that was close to the apex of the St. Lawrence Promontory and along the Newfoundland Embayment (see Fig. 1.1; James *et al.*, 1989; Hibbard *et al.*, 2007; Knight *et al.*, 2008).

Thus, western Newfoundland involves the sedimentary rocks that accumulated on the large passive-margin carbonate platform, Cambrian–Middle Ordovician in age, which is overlain by Middle Ordovician siliciclastic foreland-basin deposits. These sedimentary rocks, referred to respectively as the Labrador, Port au Port and St. George groups from the early Middle Ordovician (Knight *et al.*, 2008), were deposited on a long-lived (50 Myr) passive margin that was formed after further rifting (c. 540–535 Ma) (Cawood *et al.*, 2001). The rifting is seen by fault-bounded, terrestrial clastic and volcanic, Late Proterozoic rocks of the lower Labrador Group (Fig. 2.1). These siliciclastic sedimentary rocks of the Labrador Group (Fig. 2.1) are overlain by the high-energy carbonate platform sedimentary rocks of the Port au Port Group in the middle to late Cambrian that later (early to earliest Middle Ordovician) evolved into the low-energy deposits of the St. George Group (James *et al.*, 1989; Knight, 2007; Knight *et al.*, 2008; Lavoie *et al.*, 2013), which marks the gradual sealevel rise during the early Ordovician.

The Taconic orogeny caused compression and uplift (peripheral bulge) of the St. George Group carbonate platform, allowing erosion of the carbonates (Jacobi, 1981; Knight *et al.*, 1991). The subaerial exposure resulted in the formation of the St. George Unconformity (Fig. 2.1), which is the most well-known marker of the transition from passive margin to foreland basin (Hibbard *et al.*, 2007; Knight *et al.*, 2007). The initial closure of the Iapetus Ocean (the Taconian deformation) resulted in the collapse of the carbonate platform and formed a rapidly evolving foreland basin (Cawood and Botsford, 1991; Hibbard *et al.*, 2007; Knight *et al.*, 2008). The foreland basin developed in three stages (Stenzel *et al.*, 1990) (1) deposition of shallow-water carbonates after fragmentation, (2) uplift and erosion of the

platform, followed by (3) collapse (Stenzel *et al.*, 1990). A subsequent, sealevel rise allowed the deposition of shelf carbonates of the younger Table Head Group (Fig. 2.1; Stouge, 1984; Stenzel *et al.*, 1990; Knight *et al.*, 1991, 2007). The shelf was smothered by an influx of siliciclastic flysch, of the Goose Tickle Group (Stevens, 1970; Stouge, 1984; Quinn 1988, 1995; Stockmal *et al.*, 1998; Knight *et al.*, 2007). Today, these deposits are extensively preserved in coastal and inland exposures in western Newfoundland (Knight and Boyce, 2002).

2.2 Stratigraphy

On the west coast of Newfoundland, the peritidal to shallow marine, Middle Cambrian to Lower Ordovician carbonate rocks are referred to as the Port au Port and St. George groups (Fig. 2.1; James and Stevens, 1986; James *et al.*, 1989; Lavoie *et al.*, 2013).

2.2.1 Port au Port Group

The Port au Port Group comprises the March Point, Petit Jardin (with five members) and Berry Head formations (Fig. 2.1; James and Stevens, 1986; James *et al.* 1989; Lavoie *et al.* 2013). The sequence generally consists of limestones, dolomitic limestones and dolomites which contain shallow-marine carbonate components such as limemud, bioclastics, ooids, and oncoids (Chow and James, 1987a; Knight and James, 1987) associated with abundant microbial stromatolite and thrombolite building organisms (cyanobacteria) in the Cambrian accumulated in intertidal to subtidal environments. In the Lower Ordovician, extensive *Renalcis* mounds appeared (Pratt and James, 1982, 1986; Knight, 2008). The biostratigraphic ages of the Port au Port Group carbonates are constrained from the trilobite *Bolaspidella* Zone (Series 3; Cambrian) at the base through the Furongian Series (Cambrian) into lower Middle Ordovician (Whiterockian). They are mainly based on shelly fossil assemblages of

trilobites, cephalopods, gastropods, brachiopods (e.g., Westrop, 1992; Rohr *et al.*, 2000; Boyce *et al.*, 2011), and conodonts (Barnes and Tuke, 1970; Stouge, 1982; Ji and Barnes, 1994; Boyce and Stouge, 1997).

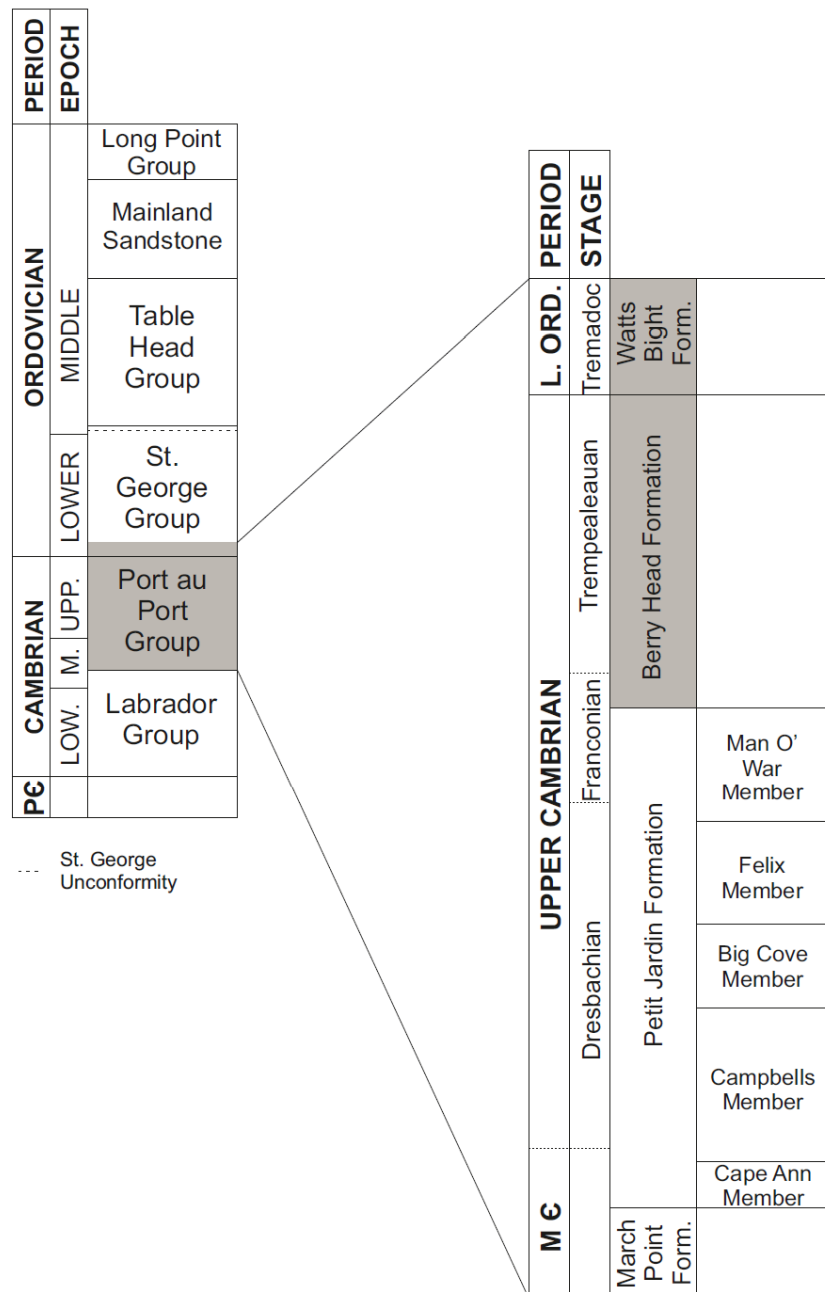


Fig. 2.1. A schematic framework of the stratigraphic units spanning the East Isthmus Bay section. Highlighted area shows the approximate investigated interval.

2.2.1.1 Berry Head Formation

The Berry Head Formation (latest Cambrian) at East Isthmus Bay is generally composed of light-grey to grey, buff dolostone with cyclic peritidal sequences of dark stromatolitic grey limestones/dolomitic limestones that become abundant in the upper section (Fig. 2.2). These dolostone are very fine-grained (dolomicrites), mainly laminated (as thin as 10 cm) and occasionally bioturbated. Lithofacies of the investigated section vary from microbial laminated limestones to wavy (Fig. 2.3a) and planar bedded dolostone. The limestones are infrequently bioturbated, and often include stromatolite and thrombolite mounds of various sizes (Fig. 2.3b-c). Shales are rare, but sometimes interrupt facies as thin partings up to 30 cm thick. Towards the top of the Berry Head Formation, black chert nodules occur, and their colour is attributed to their organic matter contents. The formation is poorly fossiliferous, except for stromatolite and thrombolite mounds, which are common from the middle to the upper parts of the formation.

2.2.2 St. George Group

The Lower Ordovician St. George Group is a succession of limestone and dolostones, that generally reflect lower energy conditions than the underlying Cambrian, Port au Port Group (Fig. 2.1). The group is subdivided, from bottom to top, into the Watts Bight, Boat Harbour, Catoche, and Aguathuna formations (Fig. 2.1; James and Stevens, 1986).

2.2.2.1 Watts Bight Formation

The base of the formation is defined at the conformable contact with the underlying Berry Head Formation. Peritidal limestone and dolostone are present at the base of the Watts Bight Formation but the formation is mainly composed of a dolomitized succession of subtidal carbonates, which are muddy and commonly bioturbated (Pratt and James, 1982;

James and Stevens, 1986; Knight and James, 1987). The middle and the upper parts of the formation are fossiliferous, but neither are present at the currently investigated section.

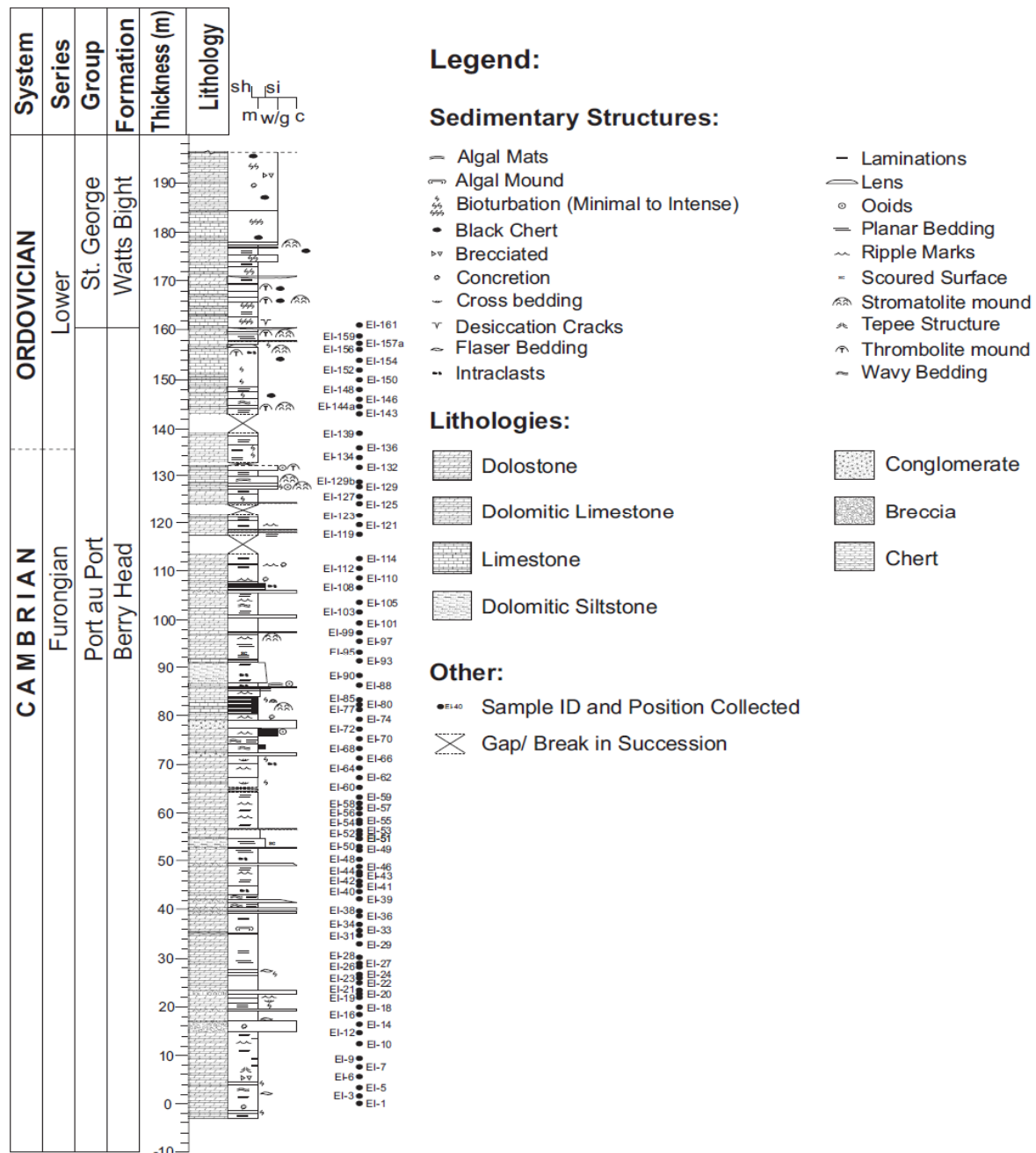


Fig. 2.2. Stratigraphic framework of the investigated upper Cambrian and lowermost Ordovician East Isthmus Bay section, western Newfoundland. Samples and their relative stratigraphic positions are marked.

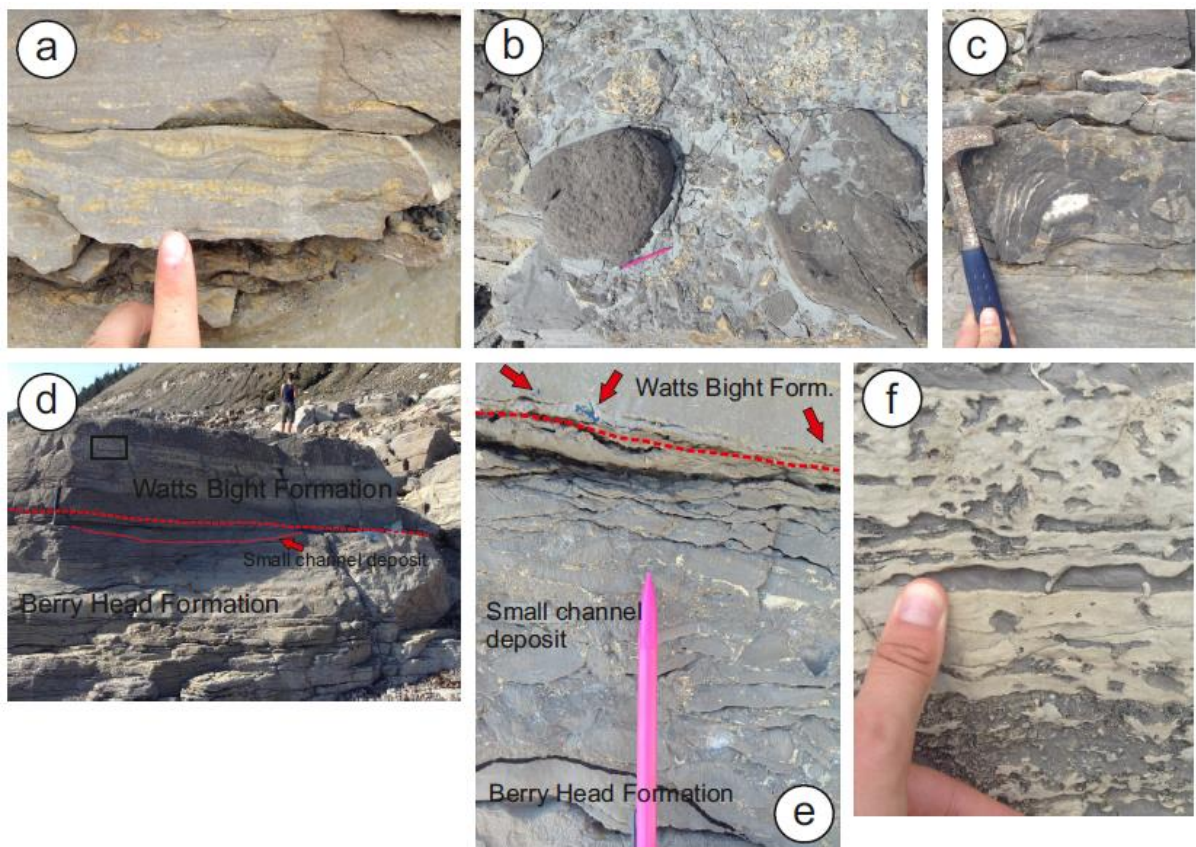


Fig. 2.3. Photographs of various sedimentary features of the East Isthmus Bay carbonates. (a) shows wavy bedding within dolostone, (b) stromatolite/ thrombolite mound just below the Berry Head–Watts Bight Formation boundary (~ 158 m, see Fig. 2.2), (c) a stromatolite (~ 82 m, Fig. 2.2), (d) the exposure of the boundary (red dashed line) between the Berry Head and Watts Bight formations seen at East Isthmus Bay, and (e) a close up of the boundary. The red arrow points at the blue paint displaying the boundary marked by Ji and Barnes (1994). Red dashed line showing the boundary between the Berry Head and Watts Bight formations. (f) Close up photograph of dolomitized ‘burrows’ seen in the base of the Watts Bight Formation, black box (d).

2.2.3 Cow Head Group

Rapid facies changes, lenticular units and abundant syndepositional erosion characterises the Cow Head Group (James and Stevens, 1986). This group includes the Shallow Bay and Green Point formations (Fig. 2.4).

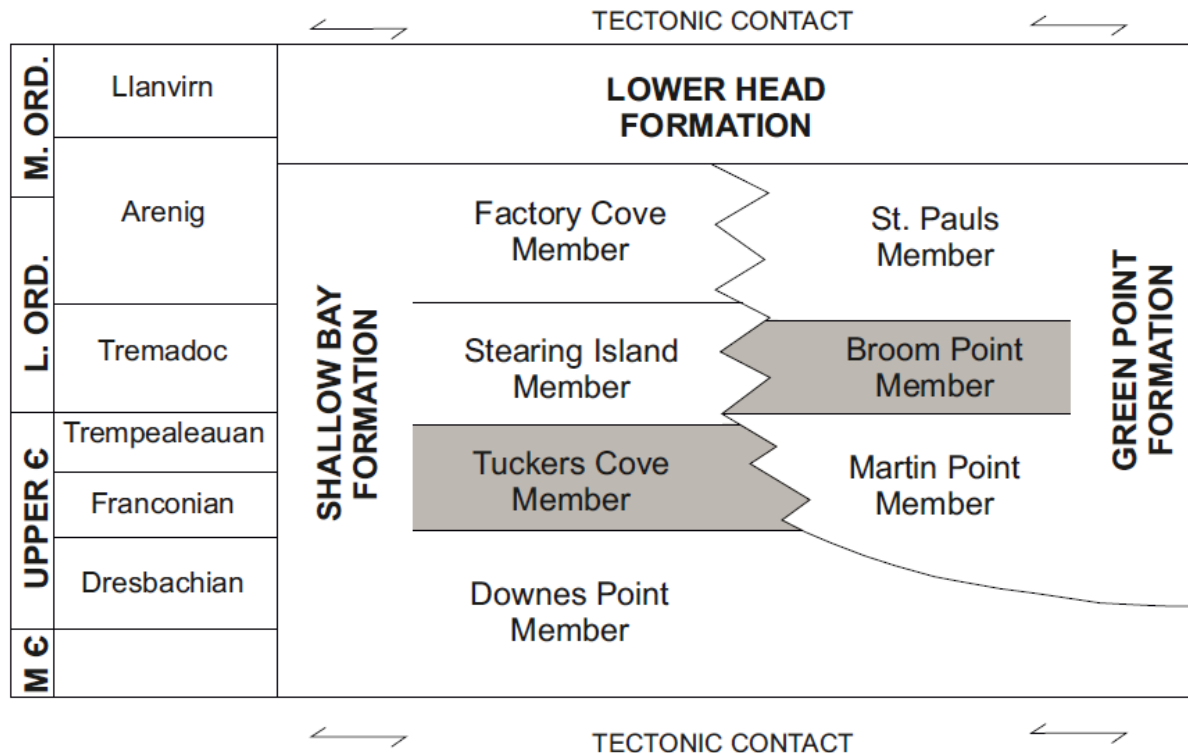


Fig. 2.4. A stratigraphic framework of the Cow Head Group Broom Point (modified from James and Stevens, 1986).

2.2.3.1 Shallow Bay Formation

The Shallow Bay Formation consists of thick (up to ~ 2 m) limestone conglomerate beds, calcarenite with interbedded limestone and shale more common in the upper part (James and Stevens, 1986). The formation is overlain by the Lower Head Formation (Fig. 2.4) and the upper boundary, with the Lower Head Formation, can be seen at the lowest tides, in Factory Cove, Cow Head Peninsula (James and Stevens, 1986), and at Lower Head.

The thickness of the Shallow Bay Formation ranges from 100 to 300 m, though ~ 90 metres was sampled at Broom Point South in this study. The formation is subdivided, from bottom to top, into four members: Downes Point Member, Tuckers Cove Member, Stearing Island Member, and the Factory Cover Member.

2.2.3.2 Tuckers Cove Member

These strata are a series of interbedded quartzose calcarenite, conglomerate and minor partings of ribbon limestone, sandstone, siltstone and shale (James and Stevens, 1986). The Tuckers Cove Member was the only member of the Shallow Bay Formation exposed, and accessible for sampling, at the Broom Point North and South sections (Fig. 2.5).





2.2.3.3 Green Point Formation

The Green Point Formation is mainly the fine-grained equivalent of the Shallow Bay Formation (James and Stevens, 1986), and comprises the distal fine-grained siliciclastic-carbonate hemipelagic sedimentary rocks of the Cow Head Group allochthonous sequence, with a few lenticular to continuous conglomerate carbonates (Fig. 2.5, James and Stevens, 1986).

The formation ranges in thickness from 400 to 500 m (James and Stevens, 1986), though only ~ 70 m of the formation is exposed at Broom Point. It overlies the lower parts of the Shallow Bay Formation at some localities (James and Stevens, 1986).

The Green Point Formation is subdivided into three members, in a stratigraphic order: Martin Point, Broom Point and St. Paul's members (James and Stevens, 1986). Only the Broom Point Member of the Green Point Formation is present at Broom Point and is further described below.

Lithologies:


 Dolostone
  Conglomerate
 Parted limestone
  Shale

Sedimentary Structures:

 Channel fill Lenticular bedding

Other:

● BP- 17 Sample ID and Position Collected

 Gap/ Break in Succession

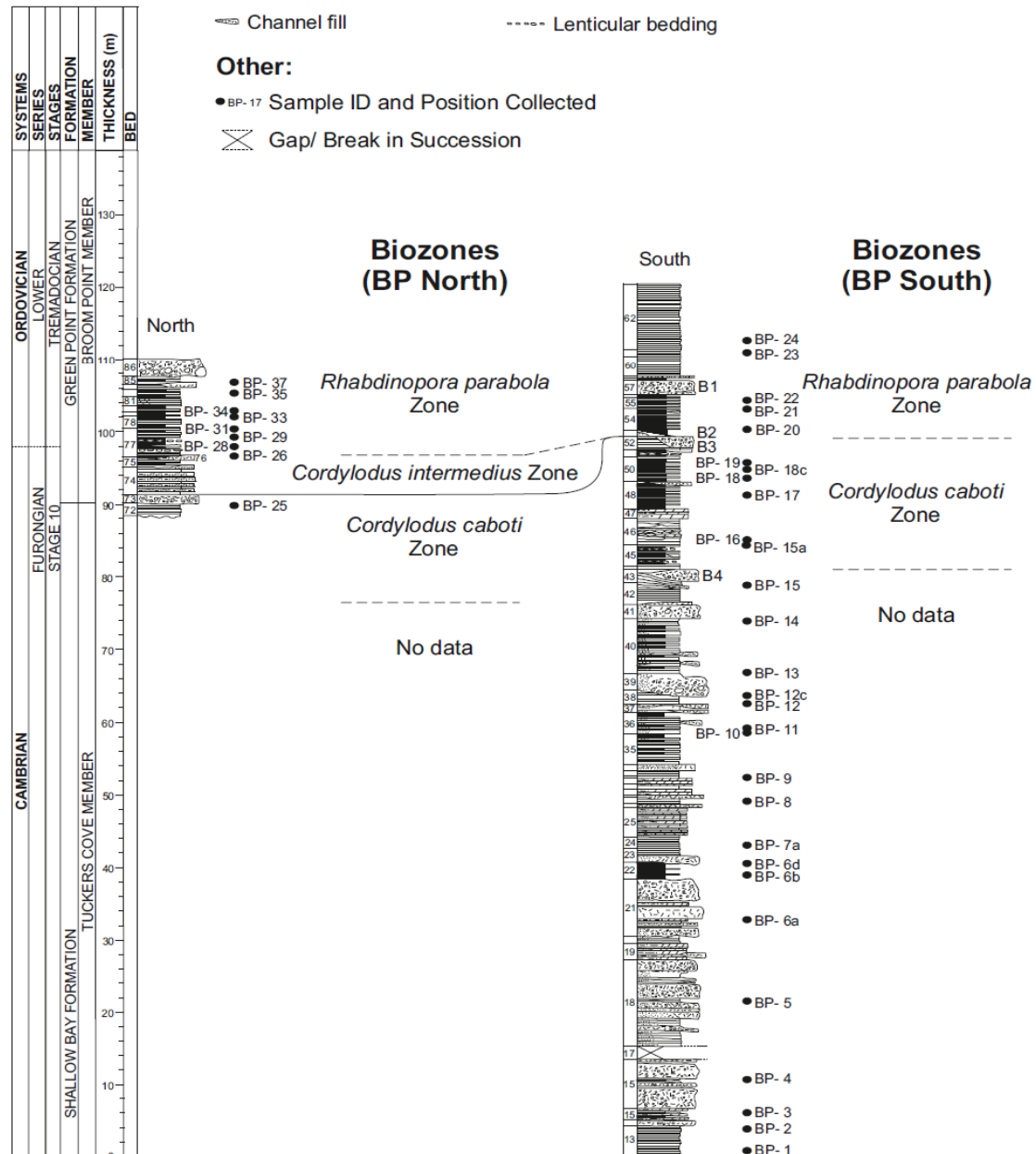


Fig. 2.5. Stratigraphic framework of the investigated Upper Cambrian and lower Ordovician section at Broom Point, western Newfoundland, with the samples and their stratigraphic levels marked. The biozones of both Broom Point North and Broom Point South are also marked.

2.2.3.4 Broom Point Member

The Broom Point Member is ~ 80 m thick, mainly ribbon to parted limestone with minor siltstone, and conglomerate units in the middle of the Green Point Formation (James and Stevens, 1986). The ribbon to parted limestone may be a single unit or several separated by shale (James and Stevens, 1986). The formation starts at the base of Bed 73, in Broom Point North, and towards the base of Bed 48, in Broom Point South (Fig. 2.5).

2.2.4 This Study

Exposures of the boundary between the Berry Head Formation and the Watts Bight Formation are found on the Port au Port Peninsula at; East Isthmus Bay, West Isthmus Bay, Jerrys Nose and a highway cut west of Lower Cove (Fig. 2.6; cf. sections 1, 2, 4, and 7 of Ji and Barnes, 1994 for details).

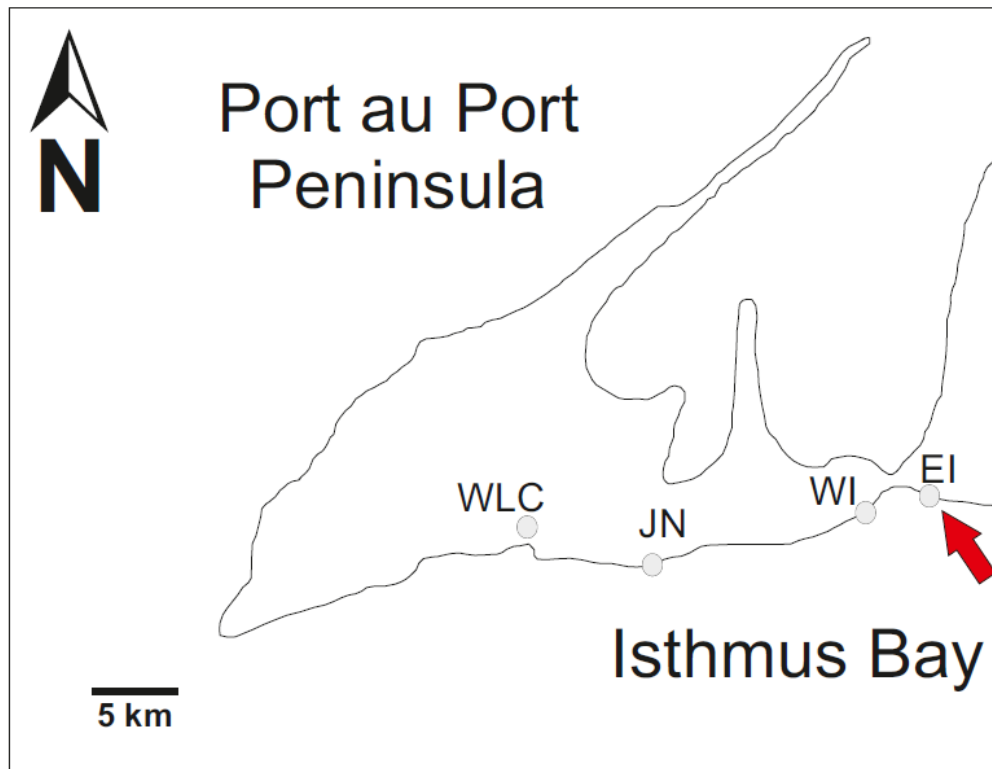


Fig 2.6. Localities where the boundary between the Berry Head and Watts Bight formations are exposed on the Port au Port Peninsula (modified from Ji and Barnes, 1994). EI: East Isthmus Bay, WI: West Isthmus Bay, JN: Jerrys Nose, WLC: Highway cut west of Lower Cove. Red arrow points to study area (EI, known as East Isthmus Bay section in this study).

2.2.4.1 East Isthmus Bay Section

The investigated section East of Isthmus Bay consists of the uppermost Cambrian Berry Head Formation (approximately 160 metres thick), and the lowermost Ordovician Watts Bight Formation (lowermost 30 metres), with the latter conformably overlying the former (Fig. 2.1; Fig. 2.3d). The lithostratigraphy of the investigated section of East Isthmus Bay (Fig. 1.1), which was briefly described by Ji & Barnes (1994), is located approximately 1000 m southwest of Romaines, near Port au Port. The section starts at the corner of the east coast of Isthmus Bay (Fig. 1.1) and continues for approximately 1000 m northwest along the shore to terminate at end of the rocky coast (Ji & Barnes, 1994). Ji and Barnes (1994)

undertook a conodont study on the Port au Port Peninsula and marked the positions of their collected samples, one of these marked sampling levels (sample Z1-27A, the Berry Head–Watts Bight Formation boundary, Fig. 2.3e) was successfully located in the sampling scheme of the current study. The spot was resampled (EI-161) in the current investigation to be taken as a marker of the contact between the Berry Head and the Watts Bight Formation (161 m, Fig. 2.2).

The Berry Head Formation and the conformably overlying Watts Bight Formation (Tremadocian, Lower Ordovician), are fully exposed in the coastal cliffs. The base of the Berry Head Formation (Port au Port Group) is not completely exposed at the section since the lowermost part is covered, also with some ‘gaps’ in the upper part of the formation (Fig. 2.2). Only the lowermost 30 metres of the Watts Bight Formation is exposed at the East Isthmus Bay section.

The section of the Berry Head Formation at the East Isthmus Bay section consists of dominantly peritidal dolostone and dolomitic limestone, with minor limestone, oolites, subordinate shale and small breccias beds. The dolostone are medium to thick bedded, laminated, burrowed and bioturbated, with some desiccation cracks. The dolomitic limestone is grey, with pale yellow light grey weathering, with chert and minor oolitic horizons. The Watts Bight Formation (St. George Group) consists of subtidal, dark grey, medium to thick bedded, heavily bioturbated limestone. Dolomitic limestone with peritidal, often laminated, dolostone interbeds also occur. Massive, high-energy thrombolitic mound complexes are also exposed.

The whole succession lacks shallow-water faunas, except for scarce conodonts (see Ji and Barnes, 1994) and bioturbation of some units. Generally speaking, the formation is poorly fossiliferous, except for the stromatolite mounds and thrombolite mounds (Fig. 2.3b-c), which start to appear above ~ 80 m in the East Isthmus Bay section (see Fig. 2.2). There

are multiple short intervals, or gaps, where the rocks are not exposed in the succession. Two seen at approximately 64 m (Fig. 2.2) in the section where ~ 20 cm of the section is lost, with four much larger gaps seen at ~ 114 m, 122 m, 132 m and 139 m. These intervals may represent soft fine-grained units prone to weathering, such as shale or siltstone, which has since been eroded away.

Ji and Barnes (1994) indicated that the Berry Head Formation and the lower part of the Watts Bight Formation have sparse conodont faunas, and that subtidal to peritidal rocks yielded conodonts, whereas supratidal rocks were barren (Ji and Barnes, 1994). Their conodont study also dated the upper Berry Head Formation (Port au Port Group) to range from the latest Cambrian to the earliest Ordovician, and the Watts Bight Formation to the early Tremadoc to middle Tremadoc (Ji and Barnes, 1994). Although the Berry Head Formation was barren of conodont, a low diverse fauna composed of *Cordylodus lindstromi*, *Semiacontiodus nogamii* and *Teridontus nakamurai* was found in the lower Watts Bight Formation (Ji and Barnes, 1994, their Fig. 5.2). The appearance of *Cordylodus lindstromi* demonstrates that the lowermost strata of the Watts Bight Formation are Ordovician (e.g., Barnes, 1988; Ji and Barnes, 1994; Cooper *et al.*, 2001).

The overlying Watts Bight Formation (St. George Group) consists of subtidal, dark grey, medium to thick bedded, heavily bioturbated limestone. Dolomitic limestone with peritidal, often laminated and/or bioturbated (Fig. 2.3f), dolostone interbeds also present. Massive, high-energy thrombolitic mound complexes are also exposed.

2.2.4.2 Broom Point Section

The lithostratigraphy of the Broom Point section has been well documented and discussed in detailed by earlier studies (e.g., Kindle and Whittington, 1958; James and Stevens, 1986) and will therefore be only summarised here.

The Broom Point sections are located between Cow Head and Martin Point, the investigated Broom Point section in the current study encompasses the Broom Point North and Broom Point South (Fig. 1.1).

2.2.4.2.1 Broom Point North section

The Broom Point North section extends along the coast from Hickey Cove to Mudge Cove (Fig. 1.1). The Downes Point, Tuckers Cove, Broom Point, and St. Pauls members are all included in the Broom Point North section, though the part of the section sampled in this study (Fig. 2.5) only covers ~ 20 m of the Broom Point Member, which is dominated by shaly mudstones, parted limestones and conglomerates. The sampled interval (between beds 72 and 86) covers the previously marked Cambrian–Ordovician boundary.

2.2.4.2.2 Broom Point South section

The Broom Point South section forms a small point between Sandy Cove and Western Brook (Fig. 1.1). This study sampled ~ 120 m of the section (Fig. 2.5) that comprises the Downes Point Member at the base, overlain by the Tuckers Cove Member of the Shallow Bay Formation. The Tuckers Cove Member is overlain by the Broom Point Member of the Green Point Formation. The boundary of the two units is sharp, consisting of a conglomerate (Bed 41, Fig. 2.5, James and Stevens, 1986) at the top of the Tuckers Cove Member, containing trilobites in the blocks. The overlying Green Point Formation is composed of a succession of dominantly ribbon to parted limestone, grey, green to black shale, and conglomerates. The limestones are thin bedded, varying from lime mudstone and wackestone and laminated lime mudstone. The breccias/conglomerates contain mainly clasts of peloidal grainstone and recrystallised limestone with minor amounts of chert and quartz clasts (James and Stevens, 1986). The lowest beds at Broom Point South form the eastern limb of an

anticline where the core is eroded and now forms the beach at Sandy Cove (Fig 1.1), and thus the basal contact is not exposed (James and Stevens, 1986).

2.2.4.3 Broom Point Biostratigraphy

The Broom Point interval comprises the Broom Point North and Broom Point South sections. The two sections have been investigated by Fortey *et al.*, (1982), Bagnoli *et al.*, (1987) and Barnes (1988). However, only a limited portion of the two sections has been documented, because the focus was on the Cambrian–Ordovician Boundary and for a period the Broom Point South section was considered a candidate as GSSP section for the global Cambrian–Ordovician Boundary. Due to the recent discovery of a hiatus in the Broom Point South section it was abandoned as GSSP candidate and the Green Point section was chosen instead (e.g., Barnes, 1988; Cooper *et al.*, 2001).

2.2.4.3.1 Broom Point North section

The succession from bed 60 to unit 95 was collected and investigated in detail by Forety *et al.*, (1982), Bagnoli *et al.*, (1987), respectively, and summarized by Barnes (1988). In this investigation the collected interval in the Broom Point Section North covers the beds 72 to 85 (Fig. 2.5), i.e. the graptolite bearing strata composed by ribbon limestone. The conodont zones below include *Cordylodus caboti* in beds 72, 73 and *Cordylodus intermedius* Zone from bed 74 to low bed 75. The *Cordylodus intermedius* Zone is overlain by the *Rhabdinopora parabola* graptolite Zone (beds 77-85, Fig. 2.5, but the zone is extending up to unit 95 in the section).

2.2.4.3.2 Broom Point South section

The Broom Point South section has been investigated biostratigraphically starting from bed 41. Beds 41 to 45 (Fig. 2.5) are tentatively referred to the *Eoconodontus notchpeakensis* conodont Zone (Barnes, 1988). The interval from bed 45 and up to 52 comprise the *Cordylodus proavus*–*Cordylodus caboti* zones. The units 54 and 55 belong to the *Rhabdinopora parabola* graptolite Zone. The interval at units 53/54 is composed of two conglomerate beds (B3/B2, Fig. 2.5) and the *Cordylodus intermedius* Zone is missing at these two conglomerates.

CHAPTER III

METHODS AND THEORY

3.1 METHODOLOGY

3.1.1 Sampling Protocol

One hundred and thirty carbonate samples were collected (at sampling intervals between 20 and 100 cm) from three sections spanning late Cambrian to Early Ordovician at East Isthmus Bay (48° 33' 5.5" N; 58° 42' 4.5" W) and Broom Point North (49° 50' 15.9" N; 57° 52' 06.9" W) and South (49° 49' 53.0" N; 57° 52' 02.0" W), western Newfoundland (Fig. 1.1). Hand sized samples were collected from the carbonate mudstone intervals of the coastline outcrops at the sites, recorded and bagged. The finest-grained material (lime mudstone where possible), composed of calcite or dolomite, was collected from the unaltered, laminated beds where possible to avoid allochthonous clasts (e.g., Azmy *et al.*, 2014) for petrographic and geochemical analyses. The sampling was focused on the shallow-water micrite and dolomicrite to utilize the retained near-primary geochemical signatures for the reconstruction of seawater carbon-isotope evolution by numerous studies (e.g., Fairchild *et al.*, 1990; Magaritz *et al.*, 1991; Marshall, 1992; Schidlowski and Aharon 1992; Brasier *et al.*, 1994; Kaufman *et al.*, 1993; Narbonne *et al.*, 1994; Kaufman and Knoll 1995; Knoll *et al.*, 1995; Glumac and Walker, 1998; Buggisch *et al.*, 2003; Azmy *et al.*, 2006; among others).

3.1.2 Petrographic Analysis

Thin sections were cut, stained with a mixture of potassium ferricyanide and alizarine red solution (Dickson, 1966) and petrographically examined using a standard polarizing

microscope and cathodoluminescence (CL). The solution caused the calcite in the samples to stain red (Fig. 3.1a) and the dolomite blue (Fig. 3.1b). Mirror-image slabs of each thin section were prepared and polished for microsampling.

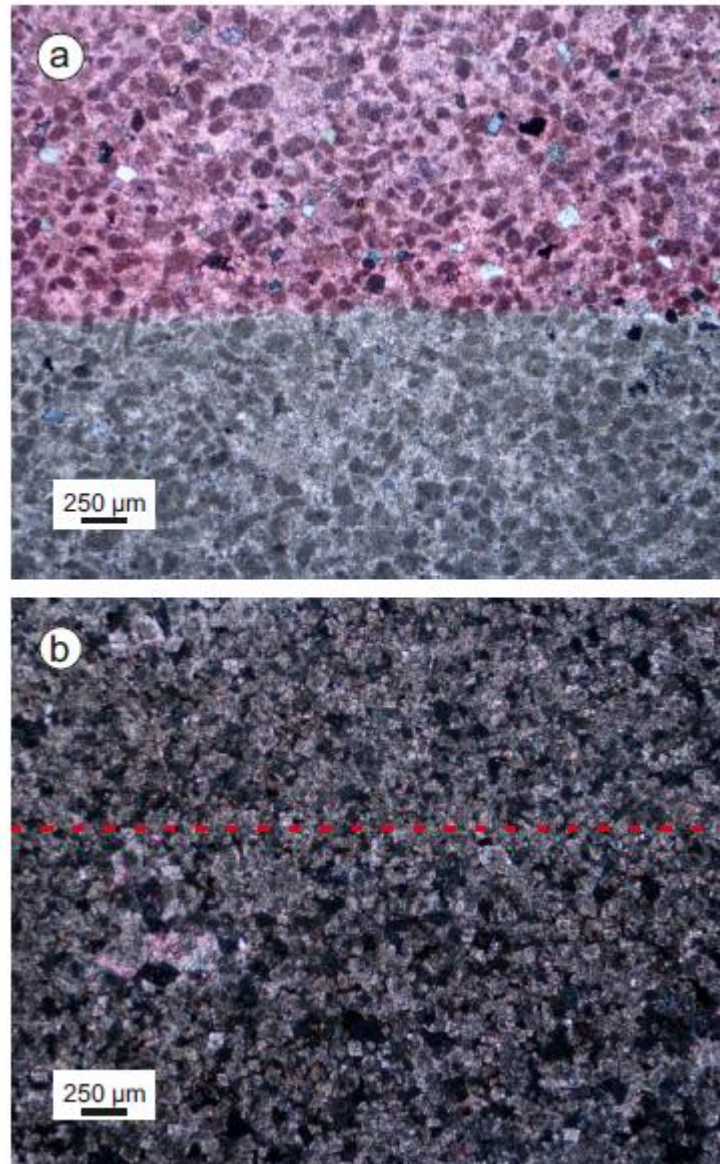


Fig. 3.1. Photomicrographs showing the resultant staining from the potassium ferricyanide and alizarine red solution on (a) calcite dominated sample (BP-6a) and (b) dolomite dominated sample (EI-28), the blue staining is more subtle.

3.1.3 Geochemical Analysis

The polished mirror-image slabs of the samples were washed with deionized water and dried at 40°C overnight. The micritic spots were identified in the thin sections during petrographic examinations and marked on the corresponding mirror-image slabs. The finest grained material (micritic where possible) was microsampled, where approximately 10 mg of carbonate was extracted from the clean slabs using a low-speed microdrill under a binocular microscope. For stable isotope analyses (carbon and oxygen isotopes), about 200 µg of sample powder was run for C- and O-isotope analyses (see chapter 3.3.3 for full stable isotope procedure). For elemental analyses, ~ 10 mg of sample was run for major and trace for analyses (see chapter 3.4.2 for elemental procedure).

3.2 CATHODOLUMINESCENCE

3.2.1 Concept and Applications

Cathodoluminescence (CL) is the visible radiation (colour) produced in a mineral exposed to high-energy bombardment by electrons. If bombarded with sufficient energy electrons can become energised and move from the valance band to the higher-energy conduction band. They remain in the conduction band for a brief time (10^{-8} s) before losing energy and returning to the lower-energy valance band. Before returning to the valance band they can be held in electron traps where photons are released (Fig. 3.2). The wavelengths of the emitted photons are usually within the visible light range; thus, luminescence occurs. Though emissions may also occur in the ultraviolet and infrared range (Boggs and Krinsley, 2010).

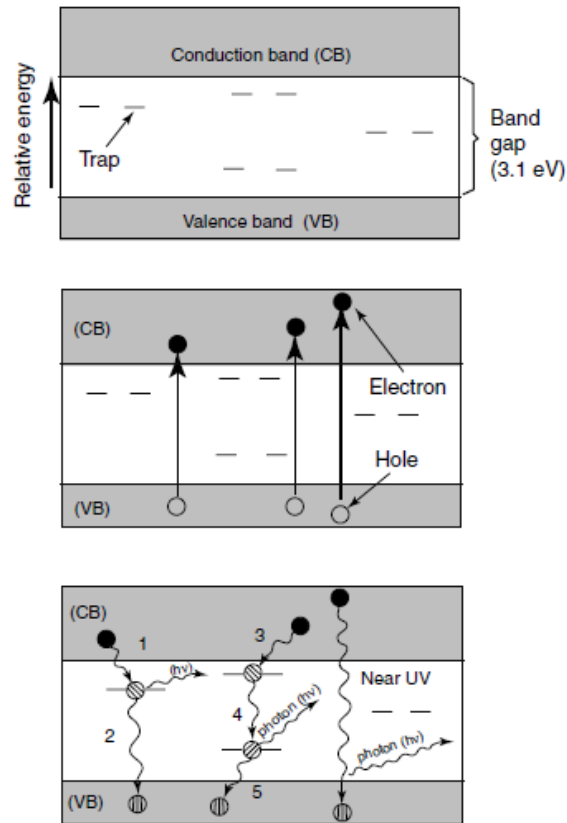


Fig. 3.2. Diagram showing the process that causes cathodoluminescence in minerals (Boggs *et al.*, 2001). CB: Conduction band; VB: Valance band.

Many elements influence the luminescence of diagenetic carbonates. These elements can be activators, sensitizers or quenchers of CL (Machel and Burton, 1991). Activators are ions that promote luminescence in a mineral, while quenchers do the opposite in inhibiting CL in a mineral. Ions that coexist with another activator ion to promote the CL response to that activator are known as sensitizers such as Pb^{2+} and Ce^{2+} . The most important activator ion is Mn^{2+} , whereas Fe^{2+} is the principle quencher ion, thus suggesting the Fe/Mn ratio is the main control of luminescence of carbonate minerals (Boggs and Krinsley, 2010). Other activator ions include Pb^{2+} (also an important sensitizer for Mn^{2+}), Cu^{2+} , Zn^{2+} and REEs (e.g., Sm^{2+} , Eu^{2+} , Tb^{3+} , etc.), which may play roles in causing CL activation in some carbonate rocks

(Machel and Burton, 1991). Other CL quenchers are Ni^{2+} and Co^{2+} (Machel, 1985).

Dependent on the carbonate mineral (calcite, aragonite or dolomite), the colours seen vary (see Table 3.1). Luminescence colours seen across all principle carbonate minerals are; orange, yellow, red, blue, and green.

Table 3.1. Cathodoluminescence colours of principle carbonate minerals calcite, aragonite and dolomite (modified from Boggs and Krinsley, 2010).

Mineral	Activator ions(s)	CL colours
Calcite	Mn^{2+}	Orange-yellow, yellow-orange, orange, violet(?)
	REE	Green, cream white, blue
Aragonite	Mn^{2+}	Yellow-green, green
Dolomite	Mn^{2+}	Yellow, red

Cathodoluminescence can be recorded by a spectrometer or more commonly visually investigated. The CL images of carbonates (calcite or dolomite) are mainly described as “orange” ‘bright red’, ‘dull’ or ‘non-luminescent’ (Machel, 1985). Most young abiotic marine carbonates (low in Mn and Fe) do not display cathodoluminescence or possibly exhibit very dull CL (e.g., Machel, 1985).

Diagenesis of carbonates may involve organic, physical, and chemical processes (Table 3.2). The vast majority of CL studies focus on the analysis of diagenetic features generated by chemical processes.

Table 3.2. Examples of organic, physical and chemical processes associated with carbonate diagenesis.

Organic Processes	Physical Processes	Chemical Processes
E.g., boring, shell breakage by organisms	E.g., compaction, bed thinning, grain breakage	E.g., dissolution, cementation, neomorphism

The discussion and application of cathodoluminescence petrography did not come into geological use until the mid-1960s (Machel and Burton, 1991, Boggs and Krinsley, 2010), but is now a popular tool used in a variety of geological studies, mainly that of sedimentary rocks, including carbonate rock studies. The CL imaging's role in carbonate studies is mainly the investigation of diagenesis (others include; identification of carbonate grains, textures, and structures). The CL image provides important compositional, textural and structural information of a sample that is not available from other techniques (such as plane polarized and crossed polars). The origins and subsequent diagenetic histories can be flagged by CL characteristics of carbonate grains and cements (Hiatt and Pufahl, 2014). Variations in the chemistry of diagenetic fluids during cement precipitation results in zones of different compositions in the crystals. Application of CL allows the identification of the pattern and evaluation of zoning in cements to interpret burial history and the nature of diagenetic pore waters (Boggs and Krinsley, 2010). Applications of CL in carbonate rock studies include:

1. Carbonate Diagenesis
2. The identification of carbonate grains, textures, and structures
3. Shape of dolomite crystals, zoning in dolomite crystals, and other textural features in dolomites

4. The burial history of carbonate sediments
5. Characteristics of cements, particularly zoned cements
6. Internal features of microfossils and ooids
7. Properties of diagenetic fluid including fluid chemistry, temperature and pressure, and redox conditions
8. Environment of dolomitization
9. Neomorphic processes in carbonates such as recrystallisation of dolomite
10. Development of porosity and crystal growth and replacement (Boggs and Krinsley, 2010).

Thus, the examination of the carbonated under CL is a potential preliminary tool to identify the degree of chemical preservation of the samples from the CL image exhibited.

3.2.2 Apparatus

Cathodoluminescence (CL) observations were performed using a Technosyn 8200 MKII cold cathode instrument operated at 8 kV accelerating voltage and 0.7 mA current.

3.3 STABLE ISOTOPE ANALYSIS

Isotopes of the same element have slight differences in mass due to the different number of neutrons in the nucleus, resulting in variances in physical and chemical properties. Generally, these differences are greater for elements of low atomic number. In a molecule of two or more isotopes, the lighter isotope is more reactive than the heavier isotope as it possesses weaker bonds. Fractionation is the term given when the ratio of two isotopes changes during a reaction or process (Tucker and Wright, 1990).

3.3.1 Carbon Isotopes

Carbon has two stable isotopes: ^{12}C (the more abundant isotope; 98.89%) and ^{13}C (1.11%). Global carbon can be divided into two reservoirs that is (1) the oxidised reservoir (as CO_2 , HCO_3^{2-} and carbonate minerals) and (2) the reduced one (organic compounds, fossil fuels and the native element), there is a constant exchange between the two reservoirs (Tucker and Wright, 1990; Faure and Mensing, 2005). Atmospheric CO_2 forms a link between relatively ^{12}C -enriched organic compounds produced by photosynthesis and carbonates (exchange reactions with aqueous HCO_3^{2-}) causing relative ^{13}C -enrichment (Tucker and Wright, 1990). Calcium carbonates precipitates in isotopic equilibrium with the atmospheric CO_2 dissolved in seawater and the other aqueous species ($\text{CO}_2(\text{aq})$, H_2CO_3 , $[\text{HCO}_3]^-$, $[\text{CO}_3]^{2-}$) and this is controlled also by other factors such as vital effect (organic primary productivity via photosynthesis by microorganisms, which is also related to ocean surface water temperature), non-atmospheric CO_2 formed by oxidation of organic matter (due to change in sealevel), and mineralogy (calcite vs aragonite) (Faure and Mensing, 2005). The near-primary $\delta^{13}\text{C}$ of carbonates can be altered by diagenesis during the burial history but this requires CO_2 -rich diagenetic fluids which are not very common and/or significant recrystallisation through multiple stage dissolution and precipitation process. They may explain the preservation of at near-primary carbon-isotope signatures in micritic carbonates that did not experience significant alteration (Faure and Mensing, 2005). Measurements of carbon isotopes are made with a mass spectrometer (Ionic Ratio Mass Spectrometer, IRMS) and expressed relative to the synthetic international standard, Vienna Pee Dee Belemnite (VPDB).

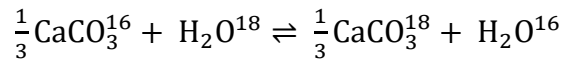
The carbon isotopic composition of dolomite reflects the nature of the precursor carbonate unless the process of dolomitization occurs in conditions of high water/rock interaction ratios (under open system conditions). In these open systems, solutions have

enough dissolved CO₂ to reset the carbon-isotope signature of the precursor carbonate (Tucker and Wright, 1990; Boggs, 2009).

3.3.2 Oxygen Isotopes

Oxygen has three stable isotopes: ¹⁶O (99.763%), ¹⁷O (0.0375%) and ¹⁸O (0.1995%).

Oxygen fractionation between calcium carbonate and water has been thoroughly well established. It was first investigated by Urey (1947) leading to the application palaeothermometry in marine carbonates. The fractionation of oxygen isotopes is temperature sensitive. The isotope exchange reaction between calcium and water:



Where the factor $\frac{1}{3}$ is needed to represent the number of oxygen atoms present in water in the calcium carbonate molecule. If the reaction is at equilibrium, the law of mass action applies and is expressed by the equation:

$$K = \frac{[\text{CaCO}_3^{18}]^{\frac{1}{3}} [\text{H}_2\text{O}^{16}]}{[\text{CaCO}_3^{16}]^{\frac{1}{3}} [\text{H}_2\text{O}^{18}]}$$

or rewritten as:

$$K = \frac{[\text{CaCO}_3^{18}]/[\text{CaCO}_3^{16}]^{\frac{1}{3}}}{\frac{1}{3}[\text{H}_2\text{O}^{18}]/[\text{H}_2\text{O}^{16}]}$$

Where K is the equilibrium constant and the reactants quantities and products are expressed as moles (Faure and Mensing, 2005). Like carbon, measurements of oxygen isotopes are made with a mass spectrometer, though can be expressed as Standard Mean Ocean Water

(SMOW) or Vienna SMOW (VSMOW) and in carbonate analyses, as in this study, relative to Vienna Pee Dee Belemnite (VPDB).

3.3.3 Procedure (Gas Bench Carbonate Method)

Carbonate powdered samples were weighed at approximately 0.200 mg and placed into rounded-bottom 12 ml glass vials. The vials were covered with Exetainer screw caps with pierceable septa. The vials were then placed in a heated sample holder held at 50°C. Using the GC Pal Autosampler, the vials were flushed with He (UHP grade) for 5 minutes using a double-holed needle connected by tubing to the He gas source. Samples were then automatically injected with 0.1 ml of phosphoric acid (100%) and a minimum of 1 hour was allowed for samples to react.

The samples were analysed using the Thermo Electron Delta V Plus isotope ratio mass spectrometer. The GC Pal was used to sample the headspace in each vial using a double-holed needle. The needle was flushed with a He carrier gas. The sample gas from the vial and the He were then carried through the capillary tubing into the Thermo Electron Gas Bench II. Using a sampling loop, portions of the sample gas were injected onto a 30 m x 0.32 mm GS-Q fused silica capillary GC column in the Gas Bench II to separate the gases desired. Nafion water traps remove water from the gas stream. The Gas Bench II acts as an interface between the sampling in the vials and the mass spectrometer. The gas stream, containing the CO₂ sample gas, is carried by the He carrier gas into the source of the Delta V plus isotope ratio mass spectrometer in the stream of helium, where the gas was ionized and measured for isotope ratios. The “raw” isotope ratios determined by the IsodatNT 3.0 software are imported into LIMS for Light Stable Isotopes. LIMS is then used to calibrate (or normalise) the run, using the known standards, to determine the isotope ratio of the unknown samples.

Uncertainties of analyses were better than 0.1 ‰ based repeated measurements of international standards, such as NBS-19 ($\delta^{18}\text{O} = -2.20\text{‰}$ and $\delta^{13}\text{C} = +1.95\text{‰}$ vs. VPDB) and L-SVECS ($\delta^{18}\text{O} = -26.64\text{‰}$ and $\delta^{13}\text{C} = -46.48\text{‰}$ vs. VPDB), and internal standards during each run of samples.

3.4 INDUCTIVELY COUPLED PLASMA MASS SPECTROMETER

3.4.1 Trace Element Analysis

The degree of preservation in carbonates can be evaluated by some of their major and trace element compositions. Diagenetic alteration changes the concentrations of those elements, for example increase the concentration of some elements in calcite (e.g., Mn and Fe) but decreases those of others (e.g., Sr and Na). The measurements of elemental compositions of the investigated carbonates were carried out in the ICP-MS laboratory at Memorial University of Newfoundland, using a Perkin Elmer Sciex ELAN DRC II Quadrupole Inductively Coupled Plasma Mass Spectrometer and analysed for a variety of elements. Standards included international (e.g., DLS-88a) and multi-element external calibration solutions, and Sc, Rh, Re and Th as internal standards to correct instrument drift. Uncertainties of analyses are determined by repeated measurements of international standard CCH-1 (a carbonate reference material). The relative uncertainties of these measurements are less than 5 %, and results (Appendices 1 and 2) are normalized to a 100 % carbonate basis (e.g., Brand and Veizer, 1980; Veizer et al. 1999; Azmy *et al.*, 2014).

3.4.2 Analytical Protocol

For each of the samples selected for trace element analyses, the following procedure was applied:

- 1- Approximately 10 mg of sample powder was extracted and weighed.
- 2- Sample powder was partially digested in 2 ml of 8 M (~ 5 % v/v) HNO₃ acid in closed vials overnight at room temperature.
- 3- Sample solution was weighed and then diluted with 10 ml of 0.2 M HNO₃, left for about 2 days (this dilution is also part of the digestion process).
- 4- For the final dilution, supernatant of each sample solution was pipetted out into clean vials, ~ 5 ml of 0.2 M nitric acid was added to the sample (~ 3000 times total dilution) prior to ICP-MS analysis.

CHAPTER IV

RESULTS

4.1 East Isthmus Bay section

The visual examination of lithology while logging the section imply a shallow-water environment of deposition. This supported by rhythmic to cyclic, peritidal dolostones and minor oolites (Berry Head Formation), and subtidal dolomitic limestone (Watts Bight Formation). Ooids were observed in some thin sections (e.g., Samples EI-72, EI-129, and EI-132; Fig. 4.1a), which have been interpreted in previous Port au Port Group studies to accumulate *in situ* (Cowan and James, 1993). The development of massive, high-energy thrombolytic mound complexes in the upper part of the section compliments the interpretation of a shallow marine depositional setting. Thrombolites are a Cambrian and Lower Ordovician phenomenon, filling the shallow-subtidal niche left after the abrupt extinction of the archaeocyathids in the Early Cambrian (Kennard and James, 1986).

The East Isthmus Bay section is approximately 200 m thick (Fig. 2.2), consisting mainly of limestones, dolomitic limestones and dolostones. The dolostone lithofacies consist of fine-grained dolomicrites, with few slightly coarser grained beds. Sedimentary structures include minor bioturbation, laminations to fine bedding, and intraclasts. The limestone lithofacies include grey limestone that ranges from mudstones (micritic) to packstone, with stromatolite and thrombolite complexes common and rare shale interbeds. Dolomitic limestone often shows moderate to intense bioturbation (Fig. 2.3f).

The lower part of the section (~ 80 m) consists of dolostones with sporadic breccia and conglomerate beds (up to 2 m thickness), the former light grey to grey, buff in appearance, and thinly bedded and fine-grained, occasionally displaying minor bioturbation. The middle interval (next ~ 80 m) of the section (approximately 80 to 160 m; Fig. 2.2) is

composed of limestones and dolostones, with stromatolite and thrombolite mounds common in some horizons (Fig. 2.2, Fig. 2.3b-c), dolostones are very similar to lower part of the section, with wavy (Fig. 2.3a) to planar thin beds with recognisable gaps at ~ 114 m, ~ 122 m, and ~ 140 m (Fig. 2.2) that might have formed by erosion of softer shale beds, as they are rarely seen throughout the section. The upper ~ 35 metres of the section mainly consists of dolomitic limestones and limestones, which are heavily bioturbated (Fig. 2.3f). The change between the middle and the upper section (the change between the Berry Head and the Watts Bight formations) is marked by a small channel deposit (Fig. 2.3d-e).

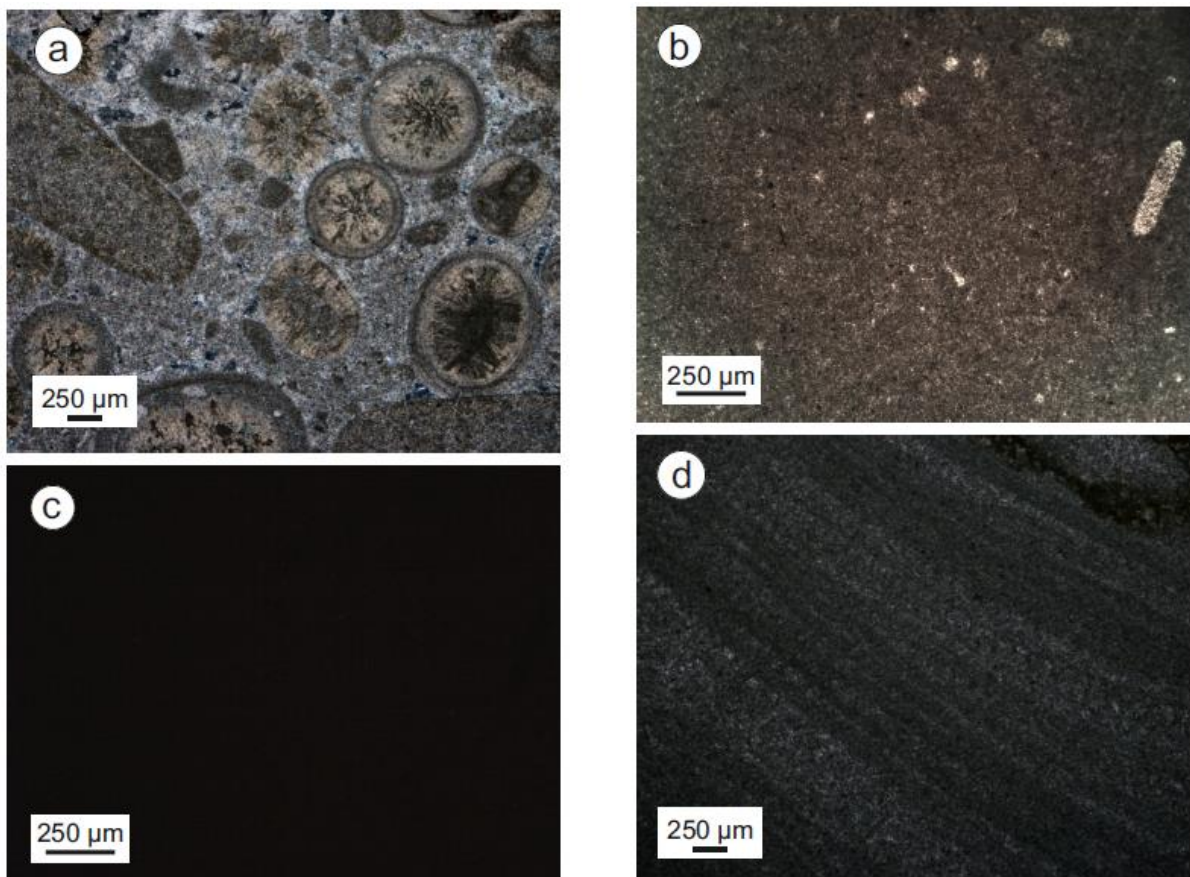


Fig. 4.1. Photomicrographs of various petrographic features of the East Isthmus Bay carbonates showing (a) radial-concentric ooids (Sample EI-132, XPL), (b) micritic lime mudstone (Sample EI-139, PPL), (c) CL image of (b) that appears non-luminescent (Sample EI-139), and (d) near-micritic laminated limestone (Sample EI-77, XPL).

4.2 Broom Point sections

This study investigated about 120 metres of the Broom Point section, just over 20 m of Broom Point North (BPN) and 120 m of Broom Point South (BPS, Fig. 2.5). The lowest 40 m of the Broom Point South section is dominated by micritic limestones and conglomerate interbeds. A thick shale bed (Bed 22; Fig. 2.5) is then encountered before a small section (~ 12 m) of micritic and grainstone limestones with few thin conglomerate interbeds. This is followed by a sequence of limestones with interbedded shales, which is then separated by thick (up to ~ 2 m, e.g., Bed 39) conglomerate deposits. Limestones in the following sequence (~ 40 m) occasionally show lenticular bedding and are often interbedded with shales, with regular conglomerate beds, which vary in thickness laterally. The investigated part of the Broom Point North section is the equivalent of this sequence. Both sections end with a large conglomerate deposit (Bed 86, BPN, and Bed 57, BPS; Fig. 2.5). The final ~ 10 m of the studied section at Broom Point South consists of well bedded, micritic limestones.

4.3 Petrography

Petrographic examination shows that the sampled carbonates from both sections have mainly retained at least their near-primary texture (Fig. 4.1a-d, Fig. 4.2a-d) except for some minor recrystallisation caused by dolomitization in parts of the East Isthmus Bay succession. They appear dull to non-luminescent under CL (Figs. 4.1c). The investigated carbonates, at East Isthmus Bay, are dominated by dolostones with minor oolitic grainstone interbeds. The bottom of the East Isthmus Bay section is dolomitized and composed mainly of fenestral dolomicrites with minor beds of crystalline dolomite and breccia. Thin interbedded limestones and shale dominate the Broom Point sections, thick conglomerate beds (avoided when sampling) are common in the Broom Point section.

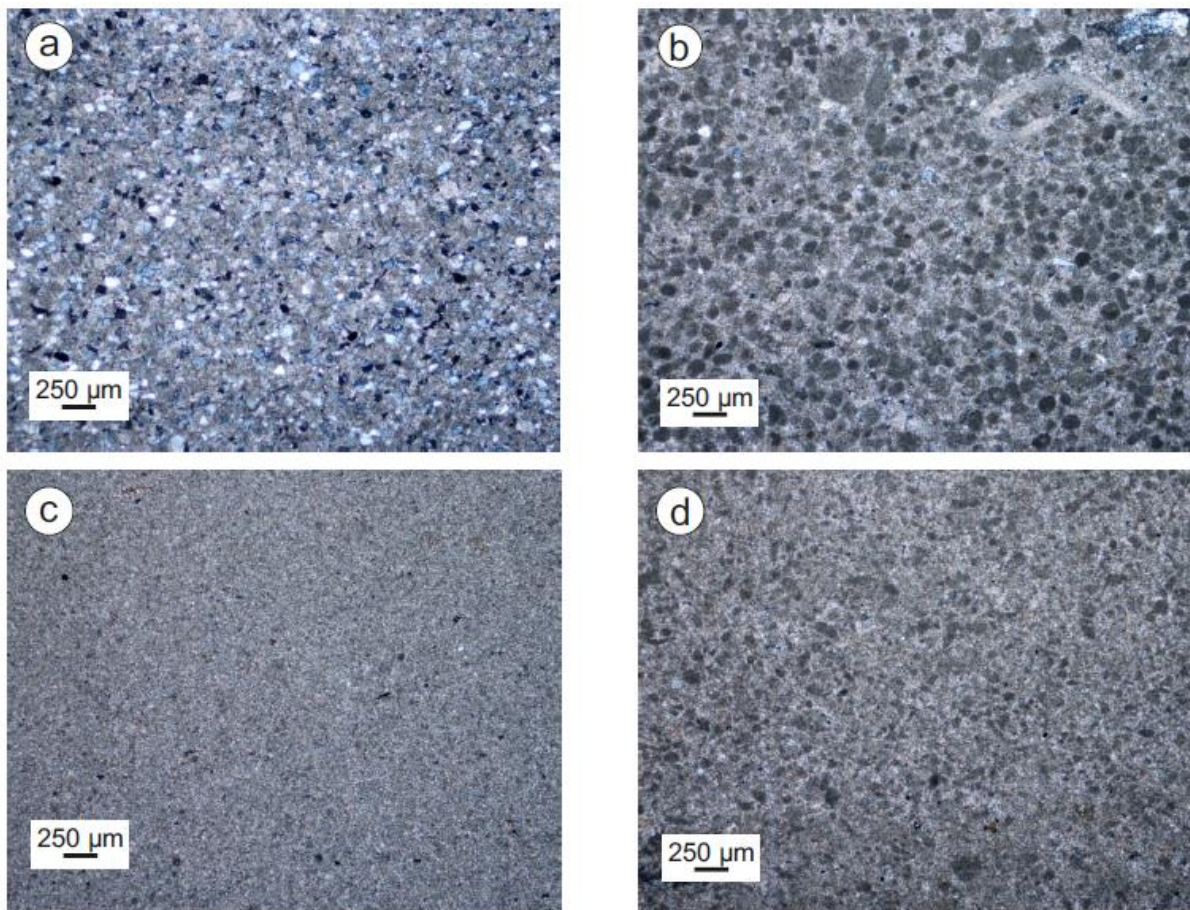


Fig. 4.2. Photomicrographs of various petrographic features of the Broom Point carbonates showing (a) dolomite, recrystallization in bed 13 (Sample BP-1, XPL), (b) shell fragment and various other bioclasts (Sample BP-9, XPL), (c) near-micritic limestone (Sample BP-12c, XPL), and (d) preservation of near-primary fabric (Sample BP-31, XPL).

4.2 Geochemistry

4.2.1 Major and Trace Elements

The geochemical characteristics of the investigated carbonates are tabulated in Appendices 1 and 2 and their statistics are summarized in Table 4.1. The mean Sr composition (214 ± 184 ppm, $n = 32$) of the investigated carbonates of the East Isthmus Bay (EI) section is lower than that of the Broom Point (BP: 416 ± 145 ppm, $n = 18$) and the Green

Point (GP: 273 ± 73 ppm, $n = 62$) counterparts (Table 4.1, Azmy *et al.*, 2014). However, it is noteworthy that no trace element results have been yet documented for carbonate below the Cambrian–Ordovician (C–O) Boundary in Green Point (cf. Miller *et al.*, 2014). On the other hand, the mean Mn content (Table 4.1) of the East Isthmus Bay carbonates (199 ± 121 ppm, $n = 32$) are comparable to that of the Broom Point counterparts (164 ± 85 ppm, $n = 18$) although those values are lower than that documented for the C–O carbonates of GP (392 ± 220 ppm, $n = 62$, Azmy *et al.*, 2014). The mean MgCO_3 % value is significantly higher in the EI carbonates (27.7 ± 16.9 , $n = 32$) than in the BP and GP carbonates (BP: 1.5 ± 0.4 , $n = 18$; GP: 3.0 ± 6.8 , $n = 62$).

The Sr and Mn values exhibit generally a poor correlation in the East Isthmus Bay carbonates ($R^2_{\text{EI}} = 0.18$), though the correlation is considerable for the samples from the Broom Point section ($R^2_{\text{BP}} = 0.4$, Fig. 4.3a). However, the results indicate that both Sr ($R^2_{\text{EI}} = 0.04$, Fig. 4.3b) and Mn ($R^2_{\text{EI}} = 0.001$, Fig. 4.3c) from the East Isthmus Bay section show insignificant correlation with their $\delta^{13}\text{C}$ counterparts. On the other hand, the Broom Point section shows a relatively considerable positive correlation of Sr with their $\delta^{13}\text{C}$ counterparts ($R^2_{\text{BP}} = 0.54$, Fig. 4.3b) and a moderate negative correlation between Mn and $\delta^{13}\text{C}$ ($R^2_{\text{BP}} = 0.29$, Fig. 4.3c). Moreover, Fe shows very poor correlation with the $\delta^{13}\text{C}$ counterparts in the East Isthmus Bay carbonates and similarly in the Broom Point carbonates ($R^2_{\text{EI}} = 0.02$ and $R^2_{\text{BP}} = 0.14$ respectively, Fig. 4.3d). The Sr and Mn concentrations are also insignificantly correlated with their $\delta^{18}\text{O}$ counterparts in the East Isthmus Bay section ($R^2_{\text{EI}} = 0.06$ and 0.05 , respectively). In addition, the Mn/Sr values are poorly correlated with their $\delta^{13}\text{C}$ ($R^2_{\text{EI}} = 0.001$) and $\delta^{18}\text{O}$ ($R^2_{\text{EI}} = 0.005$) counterparts in the East Isthmus Bay section (Fig. 4.3e). On the other hand, the Broom Point carbonates show significant correlation between the Mn/Sr values and $\delta^{13}\text{C}$ values ($R^2_{\text{BP}} = 0.3$, Fig. 4.3e), despite the poor between Mn/Sr and their $\delta^{18}\text{O}$ counterparts ($R^2_{\text{BP}} = 0.007$, Fig. 4.3e).

Table 4.1. Summary of geochemical statistics from the investigated section and the Green Point GSSP section (Miller *et al.*, 2011; Azmy *et al.*, 2014), western Newfoundland.

		BP	IB	Total	GP
$\delta^{13}\text{C}$ (‰)	<i>n</i>	38	92	130	84
VPDB	STDV	1.0	0.5	0.8	1.4
	Median	-0.3	-1.2	-1.1	-
	Average	-0.4	-1.2	-0.9	-0.9
	Max	1.6	0.2	1.6	1.7
	Min	-2.3	-2.5	-2.5	-4.7
$\delta^{18}\text{O}$ (‰)	<i>n</i>	38	92	130	84
VPDB	STDV	0.2	1.2	1.1	0.5
	Median	-6.6	-6.8	-6.7	-
	Average	-6.6	-7.0	-6.9	-7.4
	Max	-6.2	-5.1	-5.1	-5.5
	Min	-7.2	-11.3	-11.3	-8.7
CaCO_3 %	<i>n</i>	18	32	50	62
	STDV	0.4	16.9	18.5	6.4
	Median	98.6	63.5	97.6	-
	Average	98.5	72.3	81.7	97.4
	Max	99.0	99.4	99.4	99.1
	Min	97.5	58.2	58.2	62.0
MgCO_3 %	<i>n</i>	18	32	50	62
	STDV	0.4	16.9	18.5	6.8
	Median	1.4	36.5	2.4	-
	Average	1.5	27.7	18.3	3.0
	Max	2.5	41.8	41.8	38.0
	Min	1.0	0.6	0.6	0.9
Mn (ppm)	<i>n</i>	18	32	50	62
	STDV	85	121	110	220
	Median	158	163	163	-
	Average	164	199	187	392
	Max	380	565	565	1054
	Min	70	40	40	90
Sr (ppm)	<i>n</i>	18	32	50	62
	STDV	145	184	196	73
	Median	376	149	253	-
	Average	416	214	287	273
	Max	721	918	918	510
	Min	227	37	37	177
Fe (ppm)	<i>n</i>	18	32	50	-
	STDV	996	1907	1628	-
	Median	1733	1696	1733	-
	Average	2008	2155	2102	-
	Max	4726	7182	7182	-
	Min	888	180	180	-

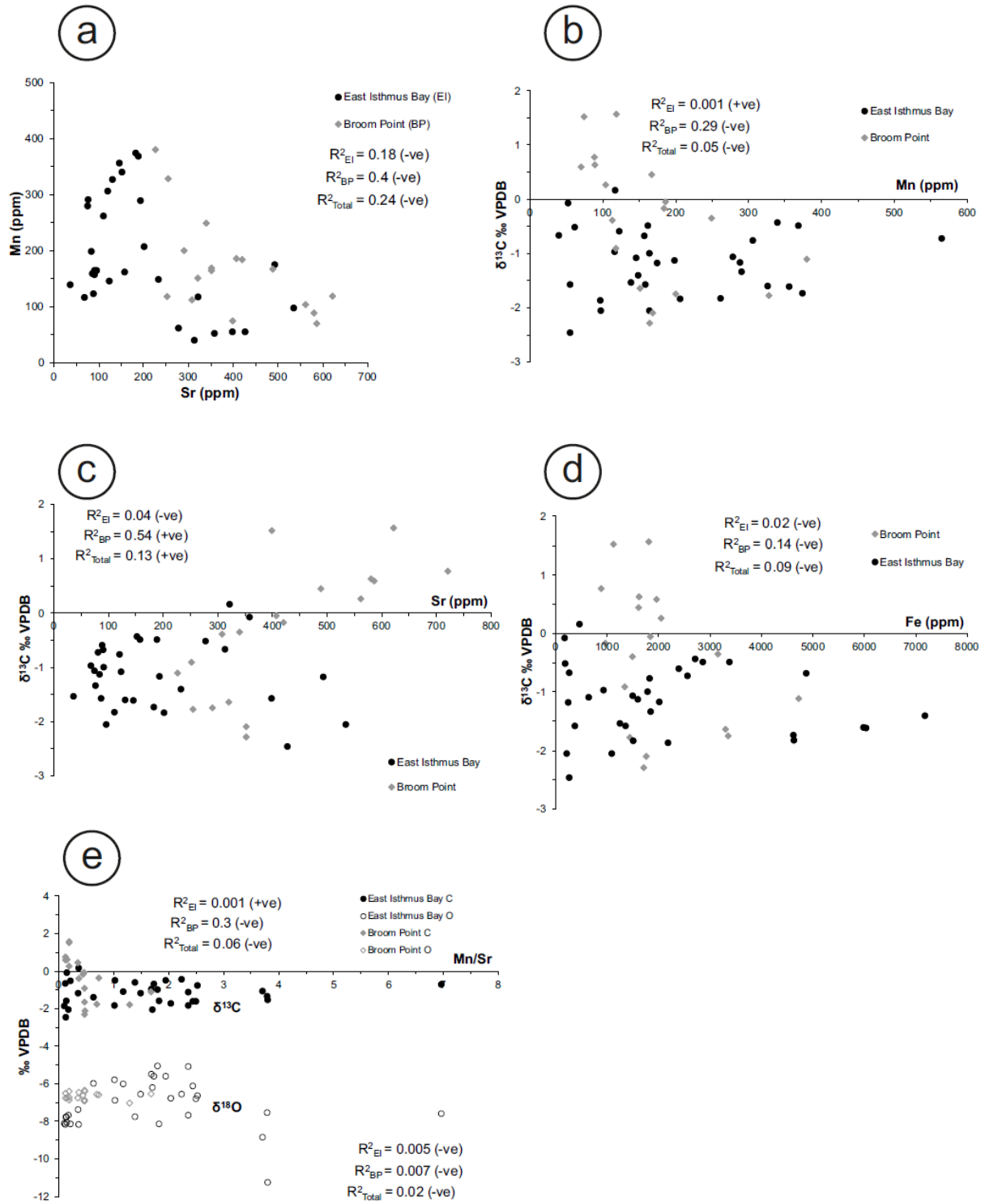


Fig. 4.3. Scatter plot showing correlation of (a) Mn with Sr, and (b) Sr, (c) Mn, and (d) Fe with their $\delta^{13}C$ counterparts for the investigated samples. (e) Mn/Sr with both $\delta^{13}C$ and $\delta^{18}O$ for the investigated carbonates of the East Isthmus Bay and Broom Point sections.

4.2.2 Carbon and Oxygen Isotopes

The $\delta^{13}\text{C}$ of the East Isthmus Bay section carbonates range from -2.47 to 0.16 ‰ VPDB, with the $\delta^{18}\text{O}$ values showing a larger range of values as expected (-11.3 to -5.1 ‰ VPDB, Table 4.1). The Broom Point carbonates show a wider range of $\delta^{13}\text{C}$ values (-2.29 to 1.62 ‰ VPDB). The mean $\delta^{13}\text{C}$ (Table 4.1) of the investigated EI carbonates (-1.2 ± 0.5 ‰ VPDB, $n = 92$) is more depleted than that of the BP carbonates (-0.4 ± 1 ‰ VPDB, $n = 38$) but comparable to that of the GP counterparts (-0.9 ± 1.4 ‰ VPDB, $n = 84$; Azmy *et al.*, 2014). However, the $\delta^{18}\text{O}$ values are comparable for all the investigated carbonates (Table 4.1) and those documented for the GP counterparts (EI: -7.0 ± 1.2 ‰ VPDB, $n = 92$; BP: -6.6 ± 0.2 ‰ VPDB, $n = 38$; GP: -7.4 ± 0.5 ‰ VPDB, $n = 84$, Table 4.1; Azmy *et al.*, 2014). The $\delta^{13}\text{C}$ values of the investigated carbonates show insignificant correlation with those of the $\delta^{18}\text{O}$ ($R^2_{\text{Total}} = 0.001$, $R^2_{\text{EI}} = 0.0003$; $R^2_{\text{BP}} = 0.02$, Fig. 4.4) and most of values fall within the range documented for best-preserved carbonates of the late Cambrian (Veizer *et al.*, 1999).

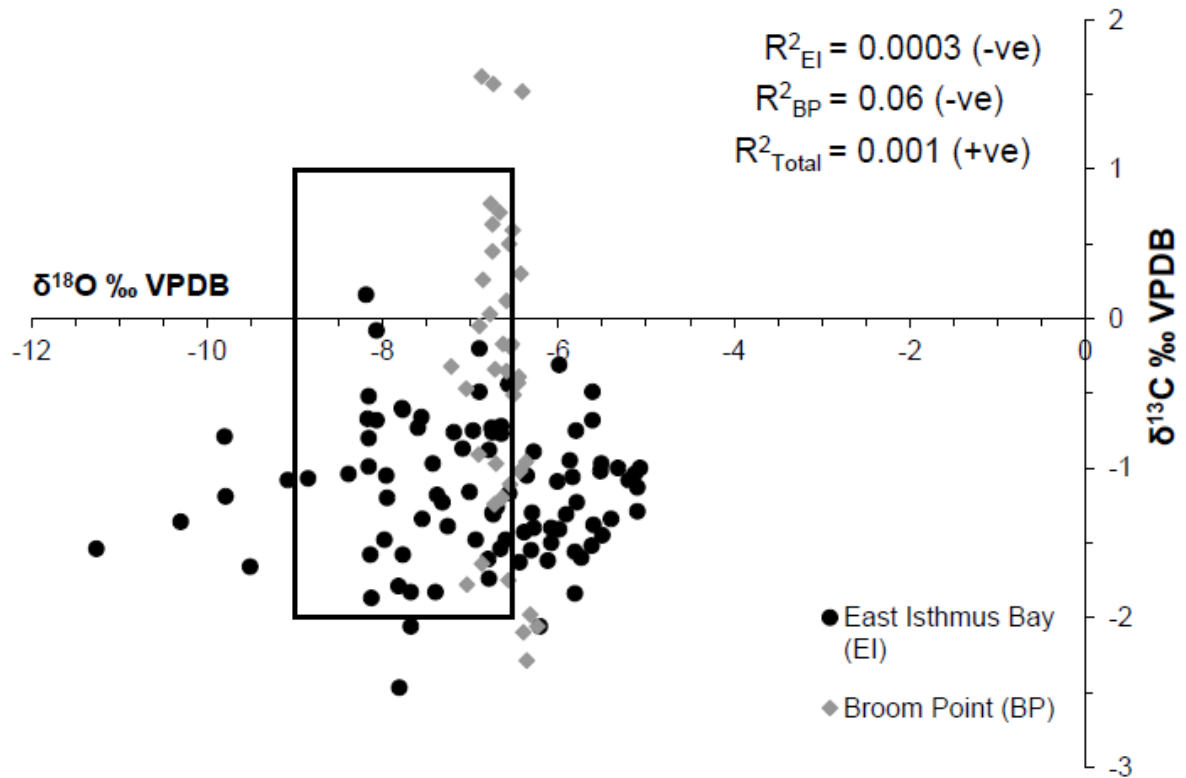


Fig. 4.4. Scatter plot showing the correlation of $\delta^{13}\text{C}$ values with their $\delta^{18}\text{O}$ counterparts. The square represents the composition documented for the best-preserved carbonates from the Late Cambrian (Veizer et al. 1999).

4.2.3 Carbon Isotope Stratigraphy

The carbon-isotope profile of the East Isthmus Bay section (Fig. 4.5) shows two negative excursions. The lower excursion is broad (~ 2 ‰ VPDB), recorded in the lowermost portion of the section (Fig. 4.5) possibly around the level of the HERB Event, and a distinct sharp negative excursion (~ 2.5 ‰ VPDB) towards the top near the Cambrian–Ordovician boundary (Fig. 4.5). Two positive excursions of note can be seen in the East Isthmus Bay section, a positive excursion of ~ 1 ‰ VPDB is also displayed at $\sim 58\text{m}$, and a second, a gradual increase in positive $\delta^{13}\text{C}$ values (~ -1.6 to ~ -1 ‰ VPDB) seen between approximately 100 to 110 m.

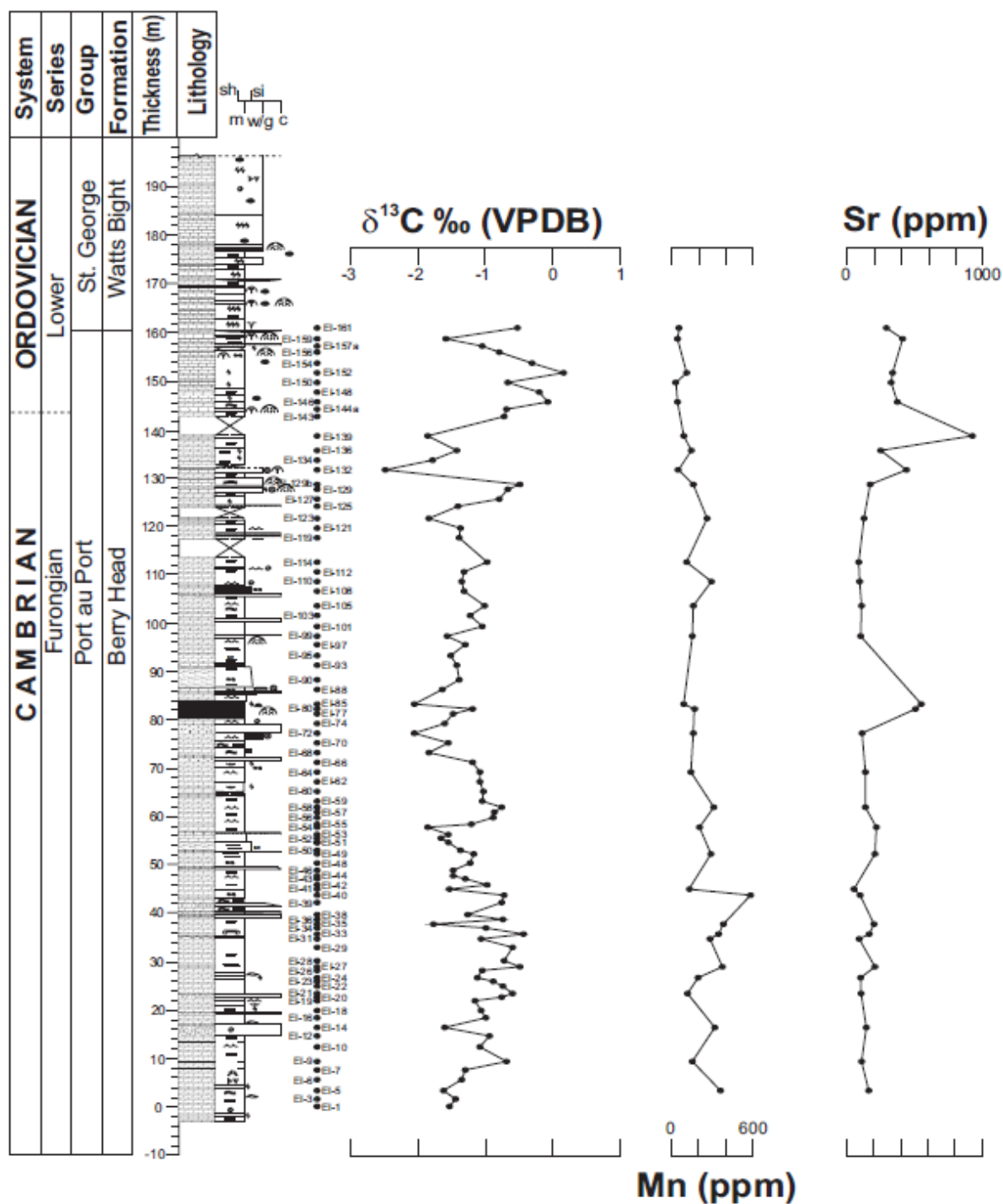


Fig. 4.5. Stratigraphic framework and detailed measured section with the positions of investigated samples along with the carbon-isotope, Mn and Sr profiles of the investigated Upper Cambrian to lowermost Ordovician, East Isthmus Bay section, western Newfoundland.

On the contrary, the Broom Point South carbon-isotope profile (Fig. 4.6) shows no clear or distinct excursions except for a possible negative excursion (~ 1.75 ‰ VPDB) in the upper section (~ 95 m) and a possible broad counterpart of ~ 2 ‰ VPDB (peaking at approximately 20 m). These two excursions could match the two negative excursions in the East Isthmus Bay section, though this is not clear (Fig. 4.6). The biostratigraphy reveals a hiatus in the Broom Point South section (beds 53/53, at ~ 100 m), where the *Cordylodus intermedius* conodont Zone is missing (Fig. 2.5), which interrupts the carbon-isotope profile. The small carbon-isotope curve created from the Broom Point North section shows two negative excursions (Fig. 4.6).

4.2.4 Manganese and Strontium

The Mn concentrations show an overall gradual decrease upward, in the East Isthmus Bay section, with the lowest values in the upper part of the section (Fig. 4.5). There is little variation between 100 and 300 ppm from the lowermost interval to 120 m on the section, except for a single high value of ~ 550 ppm at 44 m, but the Mn concentration decreases generally below 100 ppm for the remainder of the section (Fig. 4.5; Appendix 1). On the contrary, the Sr concentrations are nearly constant at ~ 200 ppm in the lower to middle intervals, except for a large interrupting peak at 83 m of ~ 500 ppm, but they are consistently higher (~ 400 ppm) in the upper interval (above the ~ 120 m horizon), except for one peak of ~ 900 ppm at 140 m (Fig. 4.5; Appendix 1). The Broom Point Mn and Sr concentrations have no clear trends (Appendix 2).

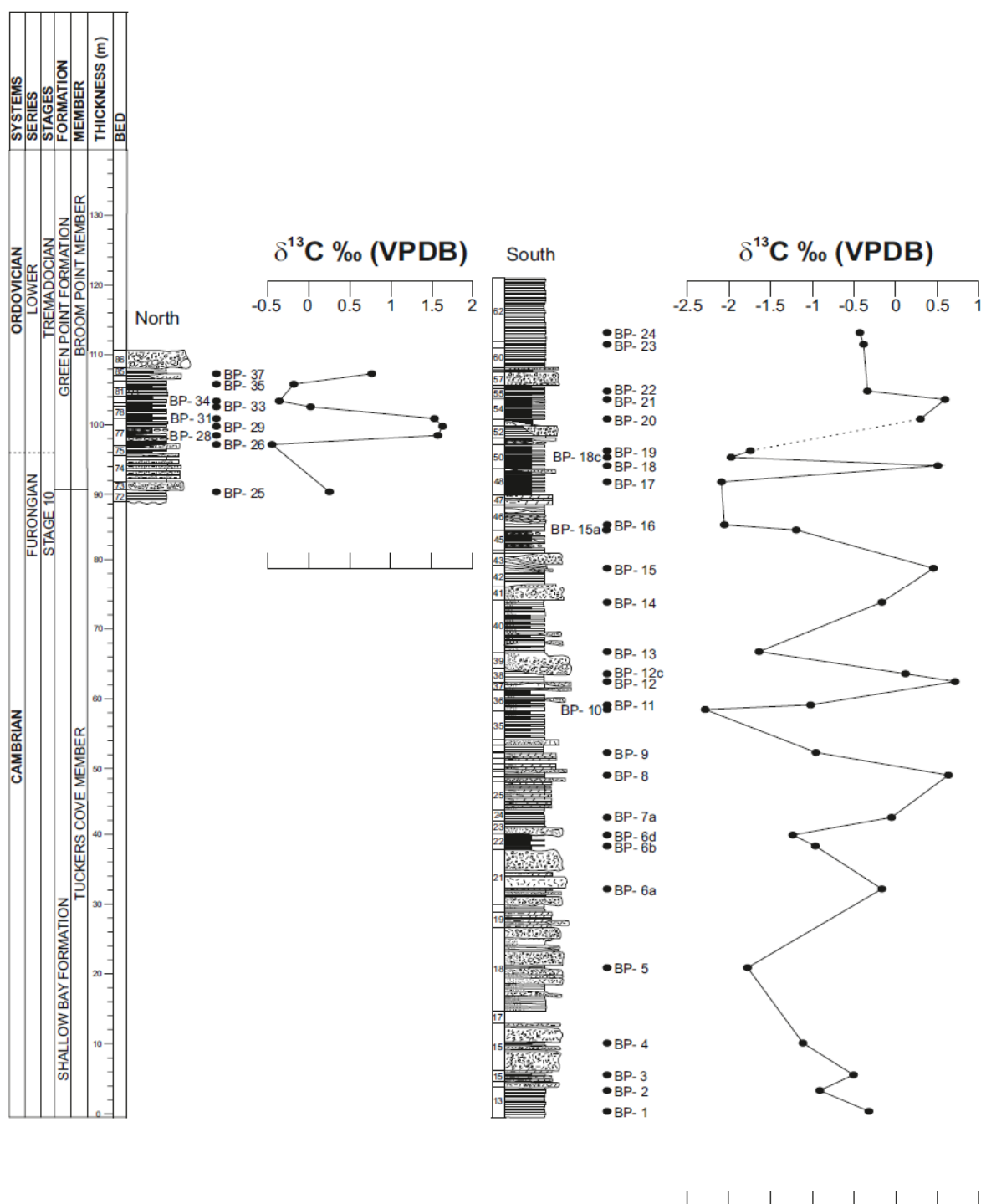


Fig. 4.6. Stratigraphic framework and the positions of investigated samples along with the carbon-isotope profiles of the investigated Upper Cambrian to lowermost Ordovician sections at Broom Point, western Newfoundland (left: Broom Point North; right: Broom Point South). Dashed line in Broom Point South's carbon-isotope profile indicates hiatus where *Cordylodus intermedius* conodont Zone is missing (see Chapter 2.2.4.2).

CHAPTER V

DISCUSSION

5. Discussion

The scarcity of preservation of ancient sediments, particularly those from the Palaeozoic, makes the evaluation of the petrographic and geochemical preservation of the investigated carbonates a foundation for carbon-isotope chemostratigraphic correlations.

Carbon isotope stratigraphy relies on near-primary $\delta^{13}\text{C}$ variations in carbonates. The $\delta^{13}\text{C}$ signatures may reflect environmental changes or diagenetic controls because ancient sediments, particularly those of the Palaeozoic, are susceptible to diagenetic alteration during burial history. The low level of dissolved CO_2 in diagenetic fluids makes the $\delta^{13}\text{C}$ signatures, at times, retain at least their near-primary values if low water/rock interaction was maintained. Therefore, the evaluation of the degree of preservation of the geochemical signatures in carbonates is one of the main pillars for reconstructing a near-primary carbon-isotope profile that can be utilised for reliable, high resolution, global chemostratigraphy correlations among different sedimentary basins.

Multiscreening techniques (i.e. petrography, cathodoluminescence, and geochemical analyses) have been applied to examine the preservation of the East Isthmus Bay and Broom Point carbonates.

5.1 East Isthmus Bay section

5.1.1 Evaluation of Sample Preservation

Petrographic investigation shows that the sampled carbonates from the studied section have mainly retained at least their near-primary sedimentary fabrics (Fig. 4.1a–d), except for minor recrystallisation caused by dolomitization in the lower parts of the succession,

suggesting a high degree of petrographic preservation. Although most of the East Isthmus Bay section consists of dolomites (mainly dolomicrites), the reset of $\delta^{13}\text{C}$ signatures requires high water-rock interaction ratio, which is always associated with significant recrystallisation and significant increase in crystal size (Veizer, 1983; Banner and Hanson, 1990). The micritic/near-micritic grain size (Fig. 4.1b, d) of investigated carbonates and the preservation of fabric, such as the ooids internal structure (Fig. 4.1a, radial-concentric ooids, Chow and James, 1987a) argue against significant reset of the $\delta^{13}\text{C}$ signatures. The relative contents of the Mn and Fe in carbonates have been found to control their luminescence (CL) under a cathodoluminoscope (Machel and Burton, 1991). High Mn concentrations in carbonates cause bright CL whereas, on the contrary, the enrichment of Fe quenches the luminescence and results in dull to non-CL (Machel and Burton, 1991). The dull CL exhibited by the investigated carbonates (Fig. 4.1c) supports the preservation of near-primary geochemical signatures, which is consistent with the near-micritic grainsize and fabric retention. However, cathodoluminescence of carbonates must be taken with caution because high Fe contents can cause non-luminescence in altered carbonates (see Rush and Chafetz, 1990). Therefore, other techniques are always applied to confirm the preservation of carbonates.

5.1.2 Major and Minor Trace Elements and Stable Isotopes

It is well established that, during burial of sediments, the diagenetic fluids react with marine sediments under anoxic conditions through dissolution-reprecipitation processes that result in recrystallisation (generally associated with aggrading neomorphism) and changes in the geochemical composition of the diagenetic carbonate phase where Mn and Fe is enriched in the secondary carbonate, but Sr is progressively depleted (Veizer, 1983; Veizer *et al.*, 1999). Therefore, correlation of the Mn and Sr values with their $\delta^{13}\text{C}$ counterparts have been found to be a reliable tool for the evaluation of the geochemical preservation of carbonates

(e.g., Derry *et al.*, 1992; Kaufman and Knoll, 1995; Azmy *et al.*, 2014). The Sr and Mn contents exhibit generally poor correlation for the East Isthmus Bay section carbonates ($R^2_{EI} = 0.18$, Fig. 4.3a). In addition, the Sr, Mn, and Fe contents (diagenetic proxies) exhibit insignificant correlation with their $\delta^{13}\text{C}$ counterparts ($R^2_{EI} = 0.04$, 0.001, and 0.02, respectively; Fig. 4.3b-d) suggesting the preservation of at least near-primary carbon-isotope compositions of the investigated carbonates. This combined with the fact that the investigated samples were extracted from mainly carbonate mudstones and dolomicrites generally retaining micritic to near-micritic grain size and their sedimentary fabrics (Fig. 4.1a-d), suggest a high degree of textural preservation, which is also supported by their non- to dull CL (Fig. 4.1c).

Impact of diagenesis on the $\delta^{13}\text{C}$ composition of carbonates is relatively less than that on the $\delta^{18}\text{O}$ counterparts particularly at low water/rock interaction ratio because diagenetic fluids do not usually have high dissolved CO_2 , which may reset the $\delta^{13}\text{C}$ signatures significantly (Veizer, 1983; Banner and Hanson, 1990). Thus, the reset of $\delta^{13}\text{C}$ signature requires high water-rock interaction ratio, which is always associated with significant recrystallisation and increased crystal size. The micritic to near-micritic grain size of investigated carbonates at the East Isthmus Bay section (Fig. 4.1a-d) argue against significant reset of the $\delta^{13}\text{C}$ signatures. On the contrary, the diagenetic waters can still significantly alter the $\delta^{18}\text{O}$ signatures of carbonates at low water-rock interaction ratios because the diagenetic fluids are predominantly water, which oxygen is one of the atoms that constitute its molecule. The lack of correlation between the $\delta^{18}\text{O}$ values of the investigated carbonates with their $\delta^{13}\text{C}$ counterparts ($R^2_{EI} = 0.0003$, Fig. 4.4) argues for the preservation of at least near-primary $\delta^{13}\text{C}$ signatures, which is also consistent with the occurrence of those values falling within the range documented for the best-preserved carbonates of the late Cambrian to early Ordovician (Veizer *et al.*, 1999, Fig. 4.4).

Freshwater diagenesis is another alteration process that delivers ^{13}C -depleted carbon from soil CO_2 together with ^{18}O -depleted oxygen from meteoric water (Allan and Matthews, 1982). Such diagenesis is often associated with meteoric cements that have low values of both $\delta^{13}\text{C}$ and $\delta^{18}\text{O}$ and generates the apparent covariance of the C- and O-isotopic values (e.g., Allan and Matthews, 1982; Marshall, 1992). The poor correlation between the $\delta^{18}\text{O}$ and $\delta^{13}\text{C}$ values of the investigated East Isthmus Bay carbonates (Fig. 4.4) and the falling of most of these values within the range documented for the best preserved marine carbonates of the late Cambrian (Fig. 4.4; Veizer et al. 1999) strongly support the preservation of at least near-primary signatures of the investigated carbonates.

5.1.3 Carbon Isotope Stratigraphy

Stratigraphic profiles of carbon isotopes are generated from near-primary signatures. Eustatic changes in sealevel influence oxygen levels in water column and accordingly organic productivity, which is reflected in the $\delta^{13}\text{C}$ composition of the associated marine carbonates (e.g., Veizer *et al.*, 1999; Halverson *et al.*, 2005; Azmy *et al.*, 2006). Alteration of organic matter results in depletion of $\delta^{13}\text{C}$ signatures and is usually associated with recrystallisation of carbonates and visible increase in crystal size. If the $\delta^{13}\text{C}$ signatures of the investigated samples were influenced by alteration of organic matter during diagenesis, the negative excursions (Fig. 4.5) would be randomly distributed in the profile rather than correlated specifically with the Cambrian–Ordovician boundary and stratigraphic level of the lower HERB Event (Buggisch *et al.*, 2003; Miller *et al.*, 2011, 2014). Also, no diagenetic process or model has been known, yet, to cause similar global consistent negative carbon-isotope excursions at those stratigraphic levels in equivalent sections from depositional basins on several palaeocontinents (cf. Chen *et al.*, 1995; Landing *et al.*, 2011; Jing *et al.*, 2008; Miller *et al.*, 2011, 2014; Azmy *et al.*, 2014; Terfelt *et al.*, 2014). Since petrographic and

geochemical examination strongly suggest that the investigated carbonates from the East Isthmus Bay section retained at least near-primary $\delta^{13}\text{C}$ signatures, a reliable carbon-isotope profile can be reconstructed for global correlation with other equivalent sections spanning the late Cambrian–early Ordovician interval (Fig. 4.5) particularly when no significant sedimentary hiatuses or major faulting have been documented in the section (cf. James and Stevens, 1986; Cooper *et al.*, 2001; Terfelt *et al.*, 2012).

In summary, lack of significant recrystallisation, preservation of sedimentary fabric, high resolution of sampling (sampling interval as small as 20 cm), and insignificant correlation of $\delta^{13}\text{C}$ with diagenetic proxies, Mn, Sr and Fe, support the preservation of at least near-primary signatures for the reconstructed carbon-isotope profile of the investigated carbonates of the East Isthmus Bay, which makes the carbon-isotope profile (see Fig. 4.5) reliable for high resolution local and global chemostratigraphic correlations (e.g., Halverson *et al.*, 2005; Azmy *et al.*, 2008, 2014, 2015).

5.2 Broom Point sections

5.2.1 Evaluation of Sample Preservation

Petrographic examination of the Broom Point carbonates shows that the samples appear to have retained their near-primary sedimentary textures (Fig. 4.2a-d). With the preservation of shell fragments and other bioclasts in some samples (e.g., samples BP-6a and BP-9, Fig. 4.2b). The majority of the samples collected from the Broom Point sections consisted of limestone and the thin section stained red (Fig. 3.1a), with only one sample in the Broom Point section consisting of dolomite (sample BP-1, Fig. 4.2a).

5.2.2 Major and Minor Trace Elements and Stable Isotopes

When correlating the Sr and Mn concentrations of the Broom Point carbonates a moderate correlation ($R^2_{BP} = 0.4$, Fig. 4.3a) suggests that the BP carbonates have been more impacted by diagenesis than their East Isthmus Bay counterparts. As mentioned, diagenesis results mainly in depletion of Sr and $\delta^{18}\text{O}$ values but enrichment in Mn and Fe. Therefore, correlating these elements with $\delta^{13}\text{C}$ values can be used to examine the degree of preservation. The Sr values exhibit a considerable correlation with their $\delta^{13}\text{C}$ counterparts ($R^2_{BP} = 0.54$, Fig. 4.3b), suggesting significant alteration of the primary geochemical signatures. Furthermore, a moderate correlation has been found between the Mn and $\delta^{13}\text{C}$ ($R^2_{BP} = 0.29$, Fig. 4.3c), thus suggesting that the sampled material is not entirely dominated by preserved micritic fabrics like those of East Isthmus Bay section but have been significantly affected by diagenesis.

On the other hand, the Broom Point carbonates still exhibit insignificant correlation between their $\delta^{18}\text{O}$ and $\delta^{13}\text{C}$ values ($R^2_{BP} = 0.06$, Fig. 4.4). However, most of the values occur on the more enriched border of best preserved carbonates for the Late Cambrian (Veizer *et al.*, 1999) likely due to dolomitization (Land, 1983). As $\delta^{18}\text{O}$ values were altered during progressive diagenesis, this could further imply that the $\delta^{13}\text{C}$ values of the Broom Point carbonates are not near-primary.

In summary, despite the fabric preservation of some of the Broom Point carbonates, their trace element compositions do not support preservation of primary geochemical signatures and the resultant carbon-isotope profile (Fig. 4.6) is therefore not near-primary, thus cannot be utilized for correlations within the basin or beyond. This is evident from the ambiguous variations exhibited by the carbon-isotope profile that does not show consistent excursions that can be used for correlations compared with those of East Isthmus Bay (Fig. 4.5).

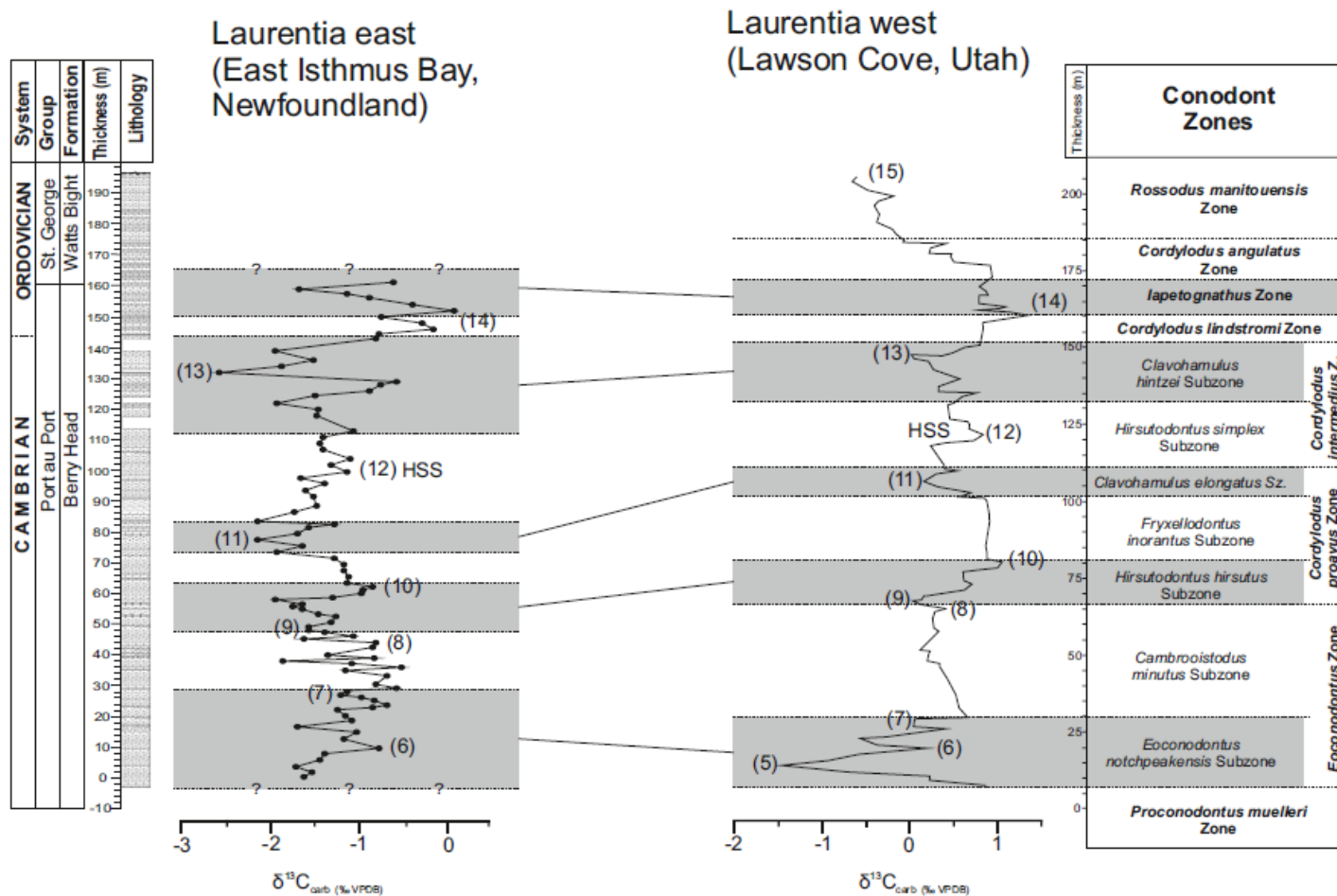


Fig. 5.1. The correlation of the $\delta^{13}\text{C}$ profiles of the East Isthmus Bay section, western Newfoundland, Canada, with that of Lawson Cove, Utah, USA. Conodont biostratigraphy in Utah is from Miller et al. (2015b). The construction of the conodont biostratigraphy at East Isthmus Bay is based on the carbon-isotope correlation. Detail in text.

5.3 East Isthmus Bay section match to the Lawson Cove ASSP section, Utah, USA

The systematic sampling of the investigated section allows the reconstruction of a continuous $\delta^{13}\text{C}$ profile from the Furongian (Stage 10, Upper Cambrian) into the Tremadocian (Lower Ordovician) in the East Isthmus Bay section (eastern Laurentia, Fig. 4.5) and the correlation with the coeval strata, from the Lawson Cove ASSP section, Utah, USA (western Laurentia; Miller *et al.*, 2011, 2014). The two sections consist of shallow-marine carbonates deposited on the platform of Laurentia, but the strata in the Lawson Cove section are much less dolomitized and provide a well-established, nearly complete conodont record tied to the $\delta^{13}\text{C}$ isotope profile (Miller *et al.*, 2015a, 2015b).

The $\delta^{13}\text{C}$ values at East Isthmus Bay are generally ~ 1 ‰ VPDB lower than those of the Lawson Cove counterparts (Fig. 5.1; Miller *et al.*, 2015b, their figure 14), which is likely attributed to the local palaeo-oceanographic conditions such as productivity and/or organic carbon burial. The palaeo-geographical different positions of the two sections on Laurentia (relatively shallower depositional setting) of the Lawson Cove section, represented by a thicker section, may have contributed to the higher $\delta^{13}\text{C}$ values. The $\delta^{13}\text{C}$ profiles of both sections (East Isthmus Bay and Lawson Cove) have comparable features of synchronous peaks of distinct negative and positive excursions that allow a possible correlation of the conodont-poor section in western Newfoundland (Fig. 5.1). For consistency, the numbering of carbon-isotope peaks on the profiles of the correlated sections in this study (Fig. 5.1) follows the format of Miller *et al.*, (2015b). The lower negative excursion (~ 2 ‰ VPDB) that peaks in the bottom of East Isthmus Bay section is close to the base of the *Eoconodontus* conodont Zone (Fig. 5.1), though this excursion is not complete in the investigated section, as the largest negative excursion (Peak 5) associated with the appearance *Eoconodontus notchpeakensis* has not been recorded but it can therefore be matched with the top of the HERB Event (Miller *et al.*, 2011, 2014; also known as TOCE – the Top of Cambrian

Excursion; Zhu *et al.*, 2006). The upper negative excursion (Fig. 5.1; Peak 13) can be reliably correlated with the upper subzone of the *Cordylodus intermedius* Zone (Upper Cambrian). The following sharp increase (Peak 14) appears to match the spike seen in the upper *Cordylodus lindstromi* Zone of the Lawson Cove, which is supported by the reported presence of *Cordylodus lindstromi* in the upper beds in the currently investigated section (Ji and Barnes, 1994). The intermediate but characteristic excursions (Peaks 9 to 11) can be matched respectively with the base and the upper part of the *Cordylodus proavus* Zone. The overlying positive peak (Peak 12), here named HSS (= *Hirsutodontus simplex* spike, i.e. following Chen *et al.*, 1995), lies within the lower *Hirsutodontus simplex* Subzone of the *Cordylodus intermedius* Zone.

This match using the near-primary $\delta^{13}\text{C}$ -isotope described above greatly improves the relative dating of the non-fossiliferous to fossil-poor, Furongian (Stage 10, Upper Cambrian) platform carbonates of the Berry Head Formation (Port au Port Group) in Newfoundland and its lateral equivalents along the eastern Laurentian margin.

5.4 Global Correlation of the East Isthmus Bay Section Carbon-Isotope Profile

The $\delta^{13}\text{C}$ profile of the Isthmus Bay section (Fig. 4.5) shows two main composite negative shifts: (1) the upper excursion is ~ 2.5 ‰ VPDB with its peak negative value correlated approximately with the upper *Cordylodus intermedius* conodont Zone (Fig. 4.5, Fig. 5.1, Azmy *et al.*, 2014) and (2) the lower broader excursion is ~ 2 ‰ with its peak correlated towards the base of the *Eoconodontus notchpeakensis* conodont Zone (Fig. 4.5, Fig. 5.1, Miller *et al.*, 2011; Terfelt *et al.*, 2014; Li *et al.*, 2017). Moreover, two further excursions, (3) a positive excursion (~ 1 ‰ VPDB) in the profile between this is the first of two positive excursions which is associated with the first appearance datum (FAD) of the

conodont *Cordylodus proavus* (*C. proavus* shift, Terfelt *et al.*, 2014) and (4) a second positive excursion is seen at ~ 108 m in the East Isthmus Bay section and displays the characteristic positive rise known as the *Hirsutodontus Simplex* Spike (HSS, Fig. 5.1). No unconformity has been known in the section to separate these excursions (cf. James and Stevens, 1986; Cooper *et al.*, 2001; Terfelt *et al.*, 2014). Those minor shifts can be correlated with their counterparts on the Lawson Cove Profile (e.g., Miller *et al.*, 2011)

The upper negative excursion on the East Isthmus Bay section carbon-isotope profile has sharp and narrower subpeaks comparable to those documented in earlier studies of the GSSP Cambrian–Ordovician boundary section (Azmy *et al.*, 2014) at Green Point (western Newfoundland) and found to be associated with a geochemical anomaly level (Azmy *et al.*, 2015) immediately below the Cambrian–Ordovician biostratigraphic boundary (Cooper *et al.*, 2001; Terfelt *et al.*, 2012; Miller *et al.*, 2011, 2014). The geochemical anomaly level marks a distinct change in the redox conditions and chemistry of the ocean water across the C–O boundary (Azmy *et al.*, 2015). This negative excursion has been also globally documented in other equivalent sections (Fig. 5.2) from basins of deposition on different palaeocontinents (e.g., Terfelt *et al.*, 2014) such as Black Mountain section, Australia (Ripperdan *et al.*, 1992), Xiaoyanqiao near Dayangcha (Jilin Province, China, Ripperdan *et al.*, 1993), Lawson Cove (Utah, USA, Nowlan, 1995), Kazakhstan (Nowlan, 1995), Argentina (Buggisch *et al.*, 2003), and China (e.g., Kalpin region of Tarim Basin, Jing *et al.*, 2008). However, the strength of the excursion (amplitude of peaks) varies in sections around the world due to the local disparities of organic primary productivity in response to sealevel changes.

The lower negative excursion consists also of couple subpeaks (Fig. 4.5, Fig. 5.1). The association of the excursion with the base of the *Eoconodontus notchpeakensis* Zone (Fig. 5.1) suggests a correlation with the global HERB Event (or TOCE) that occurred during the latest Cambrian (e.g., Terfelt *et al.*, 2014; Li *et al.*, 2017). The HERB excursion, though

incomplete in the investigated East Isthmus Bay section, has been globally documented in sections (Fig. 5.2) from different depositional basins such as Lawson Cove (USA, Miller *et al.*, 2011, 2014), Green Point (Newfoundland, Miller *et al.*, 2014), Dayangcha, Kalpin Cement Plant Section (China, Ripperdan *et al.*, 1993; Jing *et al.*, 2008), Cerro La Silla (Argentina, Buggisch *et al.*, 2003) and Black Mountain (Australia, Ripperdan *et al.*, 1992). The HERB Event was associated with a brief sealevel fall before its long-term rise. This rise in sealevel may have resulted in increased burial of organic-rich sediments and/or dysoxic conditions, leading to more depleted $\delta^{13}\text{C}$ values (Ripperdan *et al.*, 1992; Miller, 1992; Miller *et al.*, 2006; Fan *et al.*, 2009; Li *et al.*, 2017, Azmy, 2018). The middle positive shift on the $\delta^{13}\text{C}$ profiles correlates with the base of the *Cordylodus proavus* conodont Zone (*C. proavus* shift, Fig. 4.5, Fig. 5.1, Terfelt *et al.*, 2014). Although the event associated with this shift has not been named yet, it is still globally recognised in other equivalent sections from different depositional basins (Fig. 5.2, Terfelt *et al.*, 2014).

Figure 5.2 shows that the four main unique excursions in the East Isthmus Bay section and minor peaks in between can be used for high resolution chemostratigraphic correlation with coeval sections on a regional and global scale.

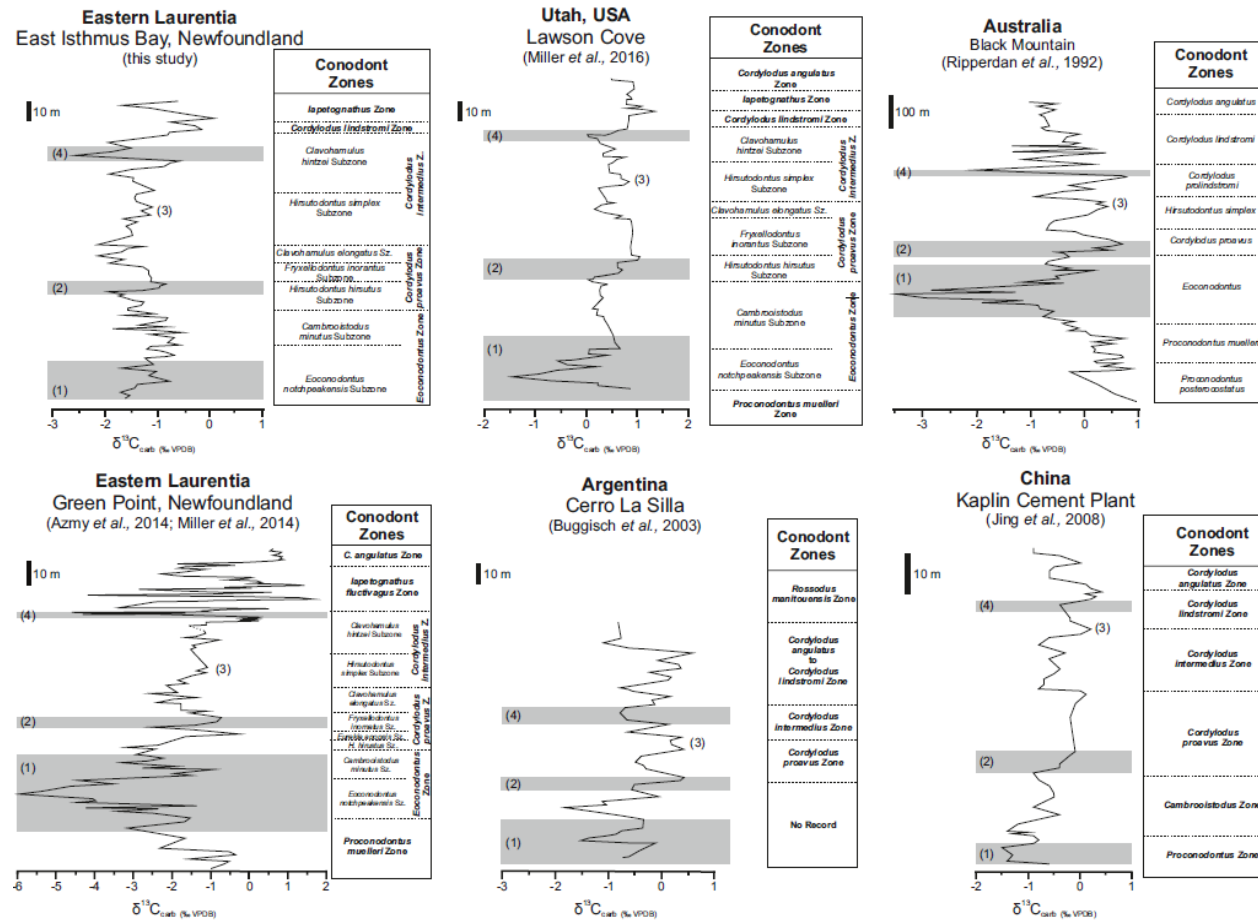


Fig. 5.2. Carbon-isotope stratigraphic correlation of Cambrian–Ordovician strata between Laurentia, China, Australia, USA, and Argentina. (1) HERB event, (2) suggested *Cordylodus proavus* positive shift, (3) suggested *Hirsutodontus Simplex* Spike, and (4) Upper negative excursion (as seen in East Isthmus Bay).

CHAPTER VI

CONCLUSIONS

6.1 East Isthmus Bay section

Samples were collected at narrow intervals from the carbonates of the East Isthmus Bay section of Berry Head and Watts Bight formations in western Newfoundland, Canada.

Petrographic examination of the East Isthmus Bay carbonates revealed the preservation of primary sedimentary fabrics and micritic to near micritic grainsize of the sampled carbonates. Cathodoluminescence investigation showed the carbonates exhibited dull to non-luminescence, suggesting the preservation of near-primary $\delta^{13}\text{C}$ values.

Trace element and stable isotope geochemistry suggests the $\delta^{13}\text{C}$ signatures of the East Isthmus Bay section are at least near-primary. The $\delta^{13}\text{C}$ profile shows two main negative excursions, a broad one in the lower section (Furongian, Upper Cambrian) and a sharper counterpart in the upper part of the section (uppermost Cambrian).

The main negative excursions and the bracketed minor peaks in between can be correlated with counterparts on the well-established equivalent profile of the Lawson Cove ASSP section, Utah, USA. The match suggests that the large lower negative excursion can be correlated with the *Eoconodontus notchpeakensis* Subzone of the *Eoconodontus* Zone (Furongian, Stage 10, Upper Cambrian) in the Lawson Cove section and the large upper negative excursion can be correlated with the top of the *Cordylodus intermedius* Zone (top Cambrian) in the Lawson Cove section. The positive and negative peaks between the two major negative excursions on the East Isthmus Bay carbon-isotope profile can be matched with equivalent counterparts in the Lawson Cove profile allowing for a secure match with the conodont biozonation scheme between the *Eoconodontus notchpeakensis* Subzone of the

Eoconodontus Zone and *Iapetognathus* Zone.

Local variations in palaeo-oceanographic conditions likely resulted in a slight decrease (~ 1 ‰ VPDB) in the $\delta^{13}\text{C}$ values at East Isthmus Bay relative to those of their Lawson Cove counterparts.

The current study provides a continuous carbon-isotope profile from the top of Port au Port Group extending into the base of the St. George Group that allows better regional correlation for the sections with poor biostratigraphic controls. The study also highlights the main unique excursions that can be used to aid high resolution chemostratigraphic correlations from depositional basins on a global scale.

6.2 Broom Point sections

Petrographic examination of the Shallow Bay and Green Point formation carbonates from Broom Point North and Broom Point South sections of western Newfoundland reveals that some of the carbonate samples have retained their near micritic texture, and primary sedimentary fabrics.

However, the geochemical proxies of diagenesis indicated significant alteration that was reflected by the considerable correlation of Mn, Sr and Fe with their $\delta^{13}\text{C}$ counterparts, which dismisses the reliability the Broom Point carbon-isotope profile for chemostratigraphic correlations.

This study emphasises the importance of using geochemical analyses to accompany petrographic examination to examine the degree of preservation of $\delta^{13}\text{C}$ signatures of carbonate rocks.

REFERENCES

- Allan, J. and Matthews, R. 1982. Isotope signatures associated with early meteoric diagenesis. *Sedimentology*, 29(6), pp. 797-817.
- Azmy, K. 2018. Carbon-isotope stratigraphy of the uppermost Cambrian in eastern Laurentia: implications for global correlation. *Geological Magazine*, pp. 1-13.
- Azmy, K. and Lavoie, D. 2009. High-resolution isotope stratigraphy of the Lower Ordovician St. George Group of western Newfoundland, Canada: implications for global correlation. *Canadian Journal of Earth Sciences*, 46(6), pp. 403-423.
- Azmy, K., Kaufman, A., Misi, A. and Oliveira, T. 2006. Isotope stratigraphy of the Lapa Formation, São Francisco Basin, Brazil: Implications for Late Neoproterozoic glacial events in South America. *Precambrian Research*, 149(3-4), pp. 231-248.
- Azmy, K., Kendall, B., Brand, U., Stouge, S. and Gordon, G. 2015. Redox conditions across the Cambrian–Ordovician boundary: Elemental and isotopic signatures retained in the GSSP carbonates. *Palaeogeography, Palaeoclimatology, Palaeoecology*, 440, pp. 440-454.
- Azmy, K., Kendall, B., Creaser, R., Heaman, L. and de Oliveira, T. 2008. Global correlation of the Vazante Group, São Francisco Basin, Brazil: Re–Os and U–Pb radiometric age constraints. *Precambrian Research*, 164(3-4), pp. 160-172.

- Azmy, K., Stouge, S., Brand, U., Bagnoli, G. and Ripperdan, R. 2014. High-resolution chemostratigraphy of the Cambrian–Ordovician GSSP: Enhanced global correlation tool. *Palaeogeography, Palaeoclimatology, Palaeoecology*, 409, pp. 135-144.
- Azmy, K., Stouge, S., Christiansen, J., Harper, D., Knight, I. and Boyce, D. 2010. Carbon-isotope stratigraphy of the Lower Ordovician succession in Northeast Greenland: Implications for correlations with St. George Group in western Newfoundland (Canada) and beyond. *Sedimentary Geology*, 225(1-2), pp. 67-81.
- Azomani, E., Azmy, K., Blamey, N., Brand, U. and Al-Aasm, I. 2013. Origin of Lower Ordovician dolomites in eastern Laurentia: Controls on porosity and implications from geochemistry. *Marine and Petroleum Geology*, 40, pp. 99-114.
- Bagnoli, G., Barnes, C.R., and Stevens, R.K., 1987, Tremadocian conodonts from Broom Point and Green Point, western Newfoundland: *Bollettino della Societa Paleontologica*, 25, pp. 145-158.
- Banner, J. L. and Hanson, G. N. 1990. Calculation of simultaneous isotopic and trace element variations during water-rock interaction with applications to carbonate diagenesis. *Geochimica et Cosmochimica Acta*, 54(11), pp. 3123–37.

- Barnes, C.R. and Tuke, M.F. 1970. Conodonts from the St. George Formation (Ordovician), northern Newfoundland. Geological Survey of Canada, Bulletin 187, pp. 79–97.
- Barnes, C.R., 1988. The proposed Cambrian–Ordovician global boundary stratotype and point (GSSP) in western Newfoundland, Canada. Geological Magazine, 125, pp. 381–414.
- Boggs, S. and Krinsley, D. (2010). Application of cathodoluminescence imaging to the study of sedimentary rocks. Cambridge: Cambridge University Press.
- Boggs, S. Jr. 2009. Petrology of Sedimentary rocks. University press, Cambridge, UK.
- Boggs, S., Jr., 2001. Principles of Sedimentology and Stratigraphy, 3rd edition., Upper Saddle River, NJ, Prentice Hall.
- Boyce W. D., McCobb L. M. E., Knight I. 2011. Stratigraphic studies of the Watts Bight Formation (St. George Group), Port au Port Peninsula, western Newfoundland. In Current Research. Government of Newfoundland and Labrador, Department of Natural Resources, Mines Branch, Report 11–1.
- Boyce, W.D. and Stouge, S. 1997. Trilobites and conodont biostratigraphy of the St. George Group at Eddies Cove West, western Newfoundland. Current Research. Newfoundland Department of Mines and Energy. Geological Survey, Report 97-1, pp. 183–200.

- Brand, U., and Veizer, J. 1980. Chemical diagenesis of a multicomponent carbonate system: 1. Trace elements. *Journal Sedimentary Petrology*, 50, pp. 1219–1236.
- Brasier, M., Corfield, R., Derry, L., Rozanov, A. and Zhuravlev, A. 1994. Multiple $\delta^{13}\text{C}$ excursions spanning the Cambrian explosion to the Botomian crisis in Siberia. *Geology*, 22(5), pp. 455.
- Buggisch, W., Keller, M., Lehnert, O. 2003. Carbon isotope record of Late Cambrian to Early Ordovician carbonates of the Argentine Precordillera. *Palaeogeography, Palaeoclimatology, Palaeoecology*, 195, pp. 357–373.
- Cawood, P. and Botsford, J. 1991. Facies and structural contrasts across Bonne Bay cross-strike discontinuity, western Newfoundland. *American Journal of Science*, 291(8), pp. 737-759.
- Cawood, P., McCausland, P. and Dunning, G. 2001. Opening Iapetus: Constraints from the Laurentian margin in Newfoundland. *Geological Society of America Bulletin*, 113(4), pp. 443-453.
- Chen, J.Y., Zhang, J.M., Nicoll, R.S. 1995. Carbon and oxygen isotopes in carbonate rocks within Cambrian–Ordovician boundary interval at Dayangcha, China. *Acta Palaeontologica Sinica* 34(4), pp. 393–409.
- Chow, N. and James, N. 1987a. Facies-Specific, Calcitic and Bimineralic Ooids from Middle and Upper Cambrian Platform Carbonates, Western Newfoundland, Canada. *SEPM Journal of Sedimentary Research*, 57.

Chow, N. and James, N. 1987b. Cambrian Grand Cycles: A northern Appalachian perspective.

Geological Society of America Bulletin, 98(4), pp. 418.

Cooper, M., Weissenberger, J. 2001. Basin evolution in western Newfoundland: New insights from hydrocarbon exploration. AAPG Bulletin, 85.

Cowan, C. and James, N. 1993. The interactions of sea-level change, terrigenous-sediment influx, and carbonate productivity as controls on Upper Cambrian Grand Cycles of western Newfoundland, Canada. Geological Society of America Bulletin, 105(12), pp. 1576-1590.

Derry, L.A., Kaufman, A.J., Jacobsen, S.B., 1992. Sedimentary cycles and environmental change in the Late Proterozoic: evidence from stable and radiogenic isotopes. *Geochimica et Cosmochimica Acta*, 56, pp. 1317–1329.

Dickson, J.A.D., 1966. Carbonate identification and genesis as revealed by staining. *Journal Sedimentary Petrology*, 36, pp. 491–505.

Fairchild, I. J., Marshall, J. D., and Bertrand-Sarfati, J. 1990, Stratigraphic shifts in carbon isotopes from Proterozoic stromatolitic carbonates (Mauritania): Influences of primary mineralogy and diagenesis: *American Journal of Science*, 290(A), pp. 46–79.

- Fan, J., Peng, P. and Melchin, M. 2009. Carbon isotopes and event stratigraphy near the Ordovician–Silurian boundary, Yichang, South China. *Palaeogeography, Palaeoclimatology, Palaeoecology*, 276(1-4), pp. 160-169.
- Fortey, R. A., Landing, E., and Skerington, D. 1982. Cambrian-Ordovician boundary sections in the Cow Head group, Western Newfoundland. In *Cambrian-Ordovician Boundary*. National Museum of Wales. (ed. M. G. Bassett and W. T. Dean), pp. 95-129.
- Glumac, B. 2002b. ABSTRACT: Stable Isotopes of Carbon as a Tool for High Resolution Stratigraphy of the Sauk II-Sauk III Sequence Boundary. *AAPG Bulletin*, 86.
- Glumac, B. and Spivak-Birndorf, M. 2002a. Stable isotopes of carbon as an invaluable stratigraphic tool: An example from the Cambrian of the northern Appalachians, USA. *Geology*, 30(6), pp. 563.
- Glumac, B. and Walker, K. 1998. A Late Cambrian positive carbon-isotope excursion in the Southern Appalachians; relation to biostratigraphy, sequence stratigraphy, environments of deposition, and diagenesis. *Journal of Sedimentary Research*, 68(6), pp. 1212-1222.
- Halverson, G.P., Hoffman, P.F., Schrag, D.P., Maloof, A.C., Rice, A.H.N. 2005. Toward a Neoproterozoic composite carbon-isotope record. *Geological Society of America Bulletin*, 117, pp. 1181–1207.
- Hiatt, E. and Pufahl, P. 2014. Cathodoluminescence petrography of carbonate rocks: application and understanding diagenesis, reservoir quality, and pore system evolution: In Coulson, I. (ed.)

Cathodoluminescence and its application to geoscience: Mineralogical Association of Canada, Short Course Series, 45, pp. 75-96.

Hibbard, J.P., van Staal, C.R., Ranking, D.G., 2007. A comparative analysis of pre-Silurian crustal building blocks of the northern and southern Appalachian orogeny. *American Journal of Science* 307, pp. 23–45.

Hurtgen, M., Pruss, S. and Knoll, A. 2009. Evaluating the relationship between the carbon and sulfur cycles in the later Cambrian ocean: An example from the Port au Port Group, western Newfoundland, Canada. *Earth and Planetary Science Letters*, 281(3-4), pp. 288-297.

Jacobi, R. 1981. Peripheral bulge—a causal mechanism for the Lower/Middle Ordovician unconformity along the western margin of the Northern Appalachians. *Earth and Planetary Science Letters*, 56, pp. 245-251.

James, N.P., Stevens, P.K. 1986. Stratigraphy and correlation of the Cambro–Ordovician Cow Head Group, western Newfoundland. *Geological Survey Canada*, 366, pp. 1–143.

James, N.P., Stevens, R.K., Barnes, C.R., Knight, I., 1989. Evolution of a Lower Paleozoic Continental-Margin Carbonate Platform, Northern Canadian Appalachians. In: Crevello, P.D. Wilson, Sarg, J.L., Read, J.F. (Eds.), *Controls on Carbonate Platform and Basin Development*. Society of Economic Paleontologists and Mineralogists Special Publication, 44, pp. 123–146.

- Ji, Z. and Barnes, C. 1994. Conodont paleoecology of the Lower Ordovician St. George Group, Port au Port Peninsula, western Newfoundland. *Journal of Paleontology*, 68(06), pp. 1368-1383.
- Jing, X., Deng, S., Zhao, Z., Lu, Y. and Zhang, S. 2008. Carbon isotope composition and correlation across the Cambrian-Ordovician boundary in Kalpin Region of the Tarim Basin, China. *Science in China Series D: Earth Sciences*, 51(9), pp. 1317-1329.
- Kaufman, A., Jacobsen, S. and Knoll, A. 1993. The Vendian record of Sr and C isotopic variations in seawater: Implications for tectonics and paleoclimate. *Earth and Planetary Science Letters*, 120(3-4), pp. 409-430.
- Kaufman, A.J., Knoll, A.H. 1995. Neoproterozoic variations in the C-isotopic composition of seawater: stratigraphic and biogeochemical implications. *Precambrian Res.* 73, pp. 27–49.
- Kennard, J. and James, N. 1986. Thrombolites and Stromatolites: Two Distinct Types of Microbial Structures. *PALAIOS*, 1(5), pp. 492.
- Kindle, C. and Whittington, H. 1958. Stratigraphy of the Cow Head region, western Newfoundland. *Geological Society of America Bulletin*, 69(3), pp. 315.
- Knight, I. and Boyce, W. D. 2002. Lower Paleozoic carbonate rocks of the northern closure of the North Brook anticline and the Spruce Pond Klippe, Georges Lake (12B/16) and Harrys River (12B/9) map areas: collected thoughts on unconnected rocks. *Current Research (2002)* Newfoundland Department of Mines and Energy, Geological Survey, Report 02-1, pp. 121–134.

- Knight, I. and James, N. 1987. The stratigraphy of the Lower Ordovician St. George Group, western Newfoundland: the interaction between eustasy and tectonics. *Canadian Journal of Earth Sciences*, 24(10), pp. 1927-1951.
- Knight, I., and Cawood P. 1991. Paleozoic geology of western Newfoundland: an exploration of a deformed Cambro-Ordovician passive margin and foreland basin, and Carboniferous successor basin. Centre for Earth Resources Research, Memorial University.
- Knight, I., Azmy, K., Boyce, D., Lavoie, D. 2008. Tremadocian Carbonates of the Lower St. George Group, Port au Port Peninsula, Western Newfoundland: Lithostratigraphic Setting of diagenetic, Isotopic, and Geochemistry Studies. Current Research Newfoundland and Labrador Department of Natural Resources Geological Survey. Report 08–1, pp. 1–43.
- Knight, I., Azmy, K., Greene, M., Lavoie, D. 2007. Lithostratigraphic Setting of Diagenetic, Isotopic, and Geochemistry Studies of Ibexian and Whiterockian Carbonates of the St. George and Table Head Groups in Western Newfoundland. Current Research Newfoundland and Labrador Department of Natural Resources Geological Survey. Report 07–1, pp. 55–84.
- Knight, I., James, N. and Lane, T. 1991. The Ordovician St. George Unconformity, northern Appalachians: The relationship of plate convergence at the St. Lawrence Promontory to the Sauk/Tippecanoe sequence boundary. *Geological Society of America Bulletin*, 103(9), pp. 1200-1225.

- Knoll, A., Kaufman, A. and Semikhatov, M. 1995. The carbon-isotopic composition of Proterozoic carbonates; Riphean successions from northwestern Siberia (Anabar Massif, Turukhansk Uplift). *American Journal of Science*, 295(7), pp. 823-850.
- Land, L. 1983. The application of stable isotopes to studies of the origin of the dolomite and problems of diagenesis of elastic sediments. In *Society for Sedimentary Geology (SEPM) Short Course Notes 10*. Edited by M. A. Arthur, T. F. Anderson, I. R. Kaplan, J. Veizer and L. S. Land. pp. 4.1-4.22.
- Landing, E., Westrop, S. and Adrain, J. 2011. The Lawsonian Stage - the *Eoconodontus notchpeakensis* FAD and HERB carbon isotope excursion define a globally correlatable terminal Cambrian stage. *Bulletin of Geosciences*, pp. 621-640.
- Lavoie, D., Burden, E. and Lebel, D. 2003. Stratigraphic framework for the Cambrian–Ordovician rift and passive margin successions from southern Quebec to western Newfoundland. *Canadian Journal of Earth Sciences*, 40(2), pp. 177-205.
- Lavoie, D., Desrochers, A., Dix, G., Knight, A., Hersi, O.S., 2012. The Great Carbonate Bank in Eastern Canada: An Overview. In: Derby, J., Fritz, R., Longacre, S., Morgan, W., Sternbach, C. (Eds.), *The Great American Carbonate Bank: The Geology and Economic Resources of Cambrian–Ordovician Sauk Megasequence of Laurentia*. American Association of Petroleum Geologists, Memoir, 98, pp. 499–524.
- Lavoie, D., Desrochers, A., Dix, G., Knight, I., and Hersi, O. 2012. The great American carbonate bank in eastern Canada: An overview, in J. R. Derby, R. D. Fritz, S. A. Longacre, W. A.

Morgan, and C. A. Sternbach, eds., The great American carbonate bank: The geology and economic resources of the Cambrian – Ordovician Sauk megasequence of Laurentia: AAPG Memoir 98, pp. 499 – 523.

Li, D., Zhang, X., Chen, K., Zhang, G., Chen, X., Huang, W., Peng, S. and Shen, Y. 2017. High-resolution C-isotope chemostratigraphy of the uppermost Cambrian stage (Stage 10) in South China: implications for defining the base of Stage 10 and palaeoenvironmental change. *Geological Magazine*, pp. 1-12.

Machel, H. G. 1985. Cathodoluminescence in calcite and dolomite and its chemical interpretation: *Geoscience Canada*, 12, pp. 139-147.

Machel, H. G., Burton, E. A. 1991. Factors Governing Cathodoluminescence in Calcite and dolomite, and Their Implications for Studies of Carbonate Diagenesis. *Luminescence microscopy and spectroscopy, qualitative and quantitative applications. SEPM Short Course*, 25, pp. 37–57.

Magaritz, M., Kirschvink, J., Latham, A., Zhuravlev, A. and Rozanov, A. (1991). Precambrian/Cambrian boundary problem: Carbon isotope correlations for Vendian and Tommotian time between Siberia and Morocco. *Geology*, 19(8), pp. 847.

Marshall, J. D. 1992. Climatic and oceanographic isotopic signals from the carbonate rock record and their preservation. *Geological Magazine* 129, pp. 143–160.

Miller, J., Ethington, R., Evans, K., Holmer, L., Loch, J., Popov, L., Repetski, J., Ripperdan, R. and Taylor, J. 2006. Proposed stratotype for the base of the highest Cambrian stage at the first appearance datum of *Cordylodus andresi*, Lawson Cove section, Utah, USA. *Palaeoworld*, 15(3-4), pp. 384-405.

Miller, J., Evans, K., Freeman, R., Ripperdan, R. and Taylor, J. 2011. Proposed stratotype for the base of the Lawsonian Stage (Cambrian Stage 10) at the First Appearance Datum of *Eoconodontus notchpeakensis* (Miller) in the House Range, Utah, USA. *Bulletin of Geosciences*, pp. 595-620.

Miller, J., Repetski, J., Nicoll, R., Nowlan, G. and Ethington, R. 2014. The conodont *Iapetognathus* and its value for defining the base of the Ordovician System. *GFF*, 136(1), pp. 185-188.

Miller, J., Ripperdan, R., Loch, J., Freeman, R., Evans, K., Taylor, J. and Tolbart, Z. 2015a. Proposed GSSP for the base of Cambrian Stage 10 at the lowest occurrence of *Eoconodontus notchpeakensis* in the House Range, Utah, USA. *Annales de Paléontologie*, 101(3), pp. 199-211.

Miller J. F., Evans K. R., Ethington R. L., Freeman R. L., Loch J. D., Popov L. E., Repetski J. E., Ripperdan R. L. & Taylor J. F. 2015b. Proposed Auxiliary Boundary Stratigraphic Section and Point (ASSP) for the base of the Ordovician System at Lawson Cove, Utah, USA. *Stratigraphy*, 12, pp. 219–36.

Narbonne, G., Kaufman, A. and Knoll, A. 1994. Integrated chemostratigraphy and biostratigraphy of the Windermere Supergroup, northwestern Canada: Implications for Neoproterozoic correlations and the early evolution of animals. *Geological Society of America Bulletin*, 106(10), pp. 1281-1292.

Nowlan, G.S. 1995 (unpublished). Variations in marine carbon isotope ratios ($\delta^{13}\text{C}$) through the Cambrian–Ordovician boundary interval, International Cambrian–Ordovician boundary working group. St. John's, Newfoundland (Canada), December, 1995.

Olanipekun, B., Azmy, K. and Brand, U. 2014. Dolomites of the Boat Harbour Formation in the Northern Peninsula, western Newfoundland, Canada: Implications for dolomitization history and porosity control. *AAPG Bulletin*, 98(4), pp. 765-791.

Pratt, B. and James, N. 1982. Cryptalgal-metazoan bioherms of early Ordovician age in the St. George Group, western Newfoundland. *Sedimentology*, 29(4), pp. 543-569.

Pratt, B. and James, N. 1986. The St George Group (Lower Ordovician) of western Newfoundland: tidal flat island model for carbonate sedimentation in shallow epeiric seas. *Sedimentology*, 33(3), pp. 313-343.

Quinn, L. 1988. Distribution and significance of Ordovician flysch units in western Newfoundland. In *Current research, part B*. Geological Survey of Canada, Paper 88-1B, pp. 119-126.

- Quinn, L. 1995. Middle Ordovician foredeep fill, in J. P. Hibbard, C. R. van Staal, and P. A. Cawood, eds., Current perspectives in the Appalachian-Caledonide orogen: Geological Association of Canada Special Paper 41, pp. 43–63.
- Ripperdan, R., Magaritz, M. and Kirschvink, J. 1993. Carbon isotope and magnetic polarity evidence for non-depositional events within the Cambrian-Ordovician Boundary section near Dayangcha, Jilin Province, China. *Geological Magazine*, 130(04), pp. 443.
- Ripperdan, R., Magaritz, M., Nicoll, R. and Shergold, J. 1992. Simultaneous changes in carbon isotopes, sea level, and conodont biozones within the Cambrian-Ordovician boundary interval at Black Mountain, Australia. *Geology*, 20(11), pp. 1039.
- Ripperdan, R., Magaritz, M., Nicoll, R. and Shergold, J. 1992. Simultaneous changes in carbon isotopes, sea level, and conodont biozones within the Cambrian-Ordovician boundary interval at Black Mountain, Australia. *Geology*, 20(11), pp. 1039.
- Rohr, D. M., Measures, E. A., Boyce, W. D. and Knight, I. 2000. Ongoing studies of Late Cambrian and Early Ordovician gastropods of western Newfoundland. In Current Research. Government of Newfoundland and Labrador, Department of Mines and Energy, Geological Survey, Report 2000-1, pp. 241-250.
- Rush, P., Chafetz, H. 1990. Fabric-retentive, Non-luminescent Brachiopods as Indicators of Original ^{13}C and ^{18}O Composition: A Test. *SEPM Journal of Sedimentary Research*, 60.

- Saltzman, M., Cowan, C., Runkel, A., Runnegar, B., Stewart, M. and Palmer, A. 2004. The Late Cambrian Spice ($\delta^{13}\text{C}$) Event and the Sauk II-SAUK III Regression: New Evidence from Laurentian Basins in Utah, Iowa, and Newfoundland. *Journal of Sedimentary Research*, 74(3), pp. 366-377.
- Schidlowski, M., and Aharon, P. 1992, Carbon cycle and carbon isotope record: Geochemical impact of life over 3.8 Ga of Earth history, in Schidlowski, M., Golubic', S., Kimberley, M.M., McKirdy, D.M., and Trudinger, P.A., eds., *Early Organic Evolution: Implications for Mineral and Energy Resources*: New York, Springer-Verlag, pp. 147–175.
- St. Julien, P. and Hubert, C. 1975. Evolution of the Taconian orogen in the Quebec Appalachians. *American Journal of Science*, 275-A, pp. 337-362.
- Stenzel, S., Knight, I. and James, N. 1990. Carbonate platform to foreland basin: revised stratigraphy of the Table Head Group (Middle Ordovician), western Newfoundland. *Canadian Journal of Earth Sciences*, 27(1), pp. 14-26.
- Stevens, R. K. 1970. Cambro-Ordovician flysch sedimentation and tectonics in west Newfoundland and their possible bearing on a protoAtlantic Ocean, in Lajoie, J., ed. *Flysch sedimentology in North America: Geological Association of Canada Special Paper No. 7*, pp. 165-177.
- Stockmal, G., Slingsby, A. and Waldron, J. 1998. Deformation styles at the Appalachian structural front, western Newfoundland: implications of new industry seismic reflection data. *Canadian Journal of Earth Sciences*, 35(11), pp. 1288-1306.

Stouge, S. 1982. Preliminary conodont biostratigraphy and correlation of the Lower and Middle Ordovician carbonates of the St. George Group, Great Northern Peninsula, Newfoundland. Mineral Dev. Div., Dept. Mines & Energy, Gvt. Newfoundland & Labrador, Rept. 82-3, pp. 59.

Stouge, S. 1984. Conodonts of the Middle Ordovician Table Head Formation, western Newfoundland. *Fossils and Strata*. 16, pp. 1-145.

Terfelt, F., Bagnoli, G., Stouge, S. 2012. Re-evaluation of the conodont *Iapetognathus* and implications for the base of the Ordovician System GSSP. *Lethaia* 45, pp. 227–237.

Terfelt, F., Eriksson, M. and Schmitz, B. 2014. The Cambrian–Ordovician transition in dysoxic facies in Baltica — diverse faunas and carbon isotope anomalies. *Palaeogeography, Palaeoclimatology, Palaeoecology*, 394, pp. 59-73.

Thomas, W. 1977. Evolution of Appalachian-Ouachita salients and recesses from reentrants and promontories in the continental margin. *American Journal of Science*, 277(10), pp. 1233-1278.

Tucker, M. E., Wright, V. P. 1990. *Carbonate Sedimentology*. Blackwell Scientific Publications, Oxford, UK.

- Urey, H. 1947. The thermodynamic properties of isotopic substances. *Journal of the Chemical Society (Resumed)*, pp. 562.
- Veizer, J. 1999. $^{87}\text{Sr}/^{86}\text{Sr}$, $\delta^{13}\text{C}$ and $\delta^{18}\text{O}$ Evolution of Phanerozoic Oceans. *Mineralogical Magazine*, 62A(3), pp. 1586-1586.
- Veizer, J., 1983. Chemical Diagenesis of Carbonates. In: Arthur, M.A., Anderson, T.F., Kaplan, I.R., Veizer, J., Land, L.S. (Eds.), *Theory and application of trace element technique, Stable Isotopes in Sedimentary Geology*. Society of Economic Paleontologists and Mineralogists (SEPM) Short Course Notes, 10, pp. III-1–III-100.
- Waldron, J., Anderson, S., Cawood, P., Goodwin, L., Hall, J., Jamieson, R., Palmer, S., Stockmal, G. and Williams, P. 1998. Evolution of the Appalachian Laurentian margin: Lithoprobe results in western Newfoundland. *Canadian Journal of Earth Sciences*, 35(11), pp. 1271-1287.
- Wang, L. 2017. Chemostratigraphy of the uppermost Cambrian at the Ordovician GSSP. Graduate. Brock University.
- Westrop, S. 1992. Upper Cambrian (Marjuman–Steptoean) trilobites from the Port Au Port Group, western Newfoundland. *Journal of Paleontology*, 66(02), pp. 228-255.
- Williams, H. 1975. Structural Succession, Nomenclature, and Interpretation of Transported Rocks in Western Newfoundland. *Canadian Journal of Earth Sciences*, 12(11), pp. 1874-1894.

Williams, H. 1979. Appalachian Orogen in Canada. *Canadian Journal of Earth Sciences*, 16(3), pp. 792-807.

Williams, H. 1995. *Geology of the Appalachian-Caledonian Orogen in Canada and Greenland*. [Ottawa, Ontario]: Energy, Mines and Resources Canada.

Zhu, M., Babcock, L. and Peng, S. 2006. Advances in Cambrian stratigraphy and paleontology: Integrating correlation techniques, paleobiology, taphonomy and paleoenvironmental reconstruction. *Palaeoworld*, 15(3-4), pp. 217-222.

APPENDIX 1

Elemental and isotopic geochemical compositions of the East Isthmus Bay carbonates.

Sample ID	Distance	$\delta^{13}\text{C}$	$\delta^{18}\text{O}$	CaCO_3	MgCaO_3	Sr	Mn	Fe
#	(m)	(‰ VPDB)	(‰ VPDB)	%	%	(ppm)	(ppm)	(ppm)
EI-161	160.0	-0.5	-8.2	99.4	0.6	278	61	190
EI-159	158.0	-1.6	-7.8	99.2	0.8	399	55	371
EI-157a	156.5	-1.0	-8.4					
EI-156	155.0	-0.8	-8.2					
EI-154	153.0	-0.3	-6.0					
EI-152	151.0	0.2	-8.2	99.1	0.9	322	117	468
EI-150	149.0	-0.7	-8.2	99.4	0.6	314	40	270
EI-148	147.0	-0.2	-6.9					
EI-146	145.0	-0.1	-8.1	94.9	5.1	358	53	180
EI-144a	143.5	-0.7	-8.1					
EI-143	142.0	-0.7	-6.7					
EI-139	138.0	-1.9	-8.1	98.7	1.3	918	96	2184
EI-136	135.0	-1.4	-6.0	63.1	36.9	233	149	7182
EI-134	133.0	-1.8	-7.8					
EI-132	131.0	-2.5	-7.8	99.1	0.9	427	55	264
EI-129b	128.0	-0.5	-6.9	66.1	33.9	158	162	3386
EI-129	127.0	-0.7	-7.6					
EI-127	125.0	-0.8	-9.8					
EI-125	123.5	-1.4	-6.1					
EI-123	121.0	-1.8	-7.7	65.4	34.6	111	262	4638
EI-121	119.0	-1.4	-10.3					
EI-119	117.0	-1.4	-7.3					
EI-114	112.0	-1.0	-5.5	58.5	41.5	69	116	932
EI-112	110.0	-1.3	-5.9					
EI-110	108.0	-1.3	-7.6	60.3	39.7	77	291	1854
EI-108	106.0	-1.3	-6.7					
EI-105	103.0	-1.0	-5.1	59.9	40.1	91	164	1790
EI-103	101.0	-1.2	-5.8					
EI-101	99.0	-1.1	-8.0					
EI-99	97.0	-1.6	-8.1	60.7	39.3	87	158	1362
EI-97	95.0	-1.3	-5.1					
EI-95	93.0	-1.5	-6.1					
EI-93	91.0	-1.4	-6.4					
EI-90	88.0	-1.4	-6.3					
EI-88	86.0	-1.6	-6.4					
EI-85	83.0	-2.1	-7.7	98.9	1.1	535	97	218
EI-80	82.0	-1.2	-7.4	98.2	1.8	493	175	248
EI-77	81.0	-1.5	-8.0					

EI-74	79.0	-1.6	-5.7					
EI-72	77.0	-2.1	-6.2	59.3	40.7	96	164	1096
EI-70	75.0	-1.6	-5.8					
EI-68	73.0	-1.8	-7.4					
EI-66	71.0	-1.2	-9.8					
EI-64	69.0	-1.1	-6.0	60.3	39.7	124	146	644
EI-62	67.0	-1.1	-9.1					
EI-60	65.0	-1.0	-5.5					
EI-59	63.0	-1.0	-5.1					
EI-58	62.0	-0.8	-6.7	64.7	35.3	121	306	1831
EI-57	60.5	-0.9	-7.1					
EI-56	59.5	-0.9	-6.8					
EI-55	58.5	-1.2	-8.0					
EI-54	57.5	-1.8	-5.8	64.1	35.9	202	207	1509
EI-53	56.0	-1.5	-6.7					
EI-52	55.5	-1.7	-9.5					
EI-51	54.5	-1.6	-6.3					
EI-50	53.0	-1.4	-5.6					
EI-49	52.5	-1.2	-6.6	67.4	32.6	194	288	2013
EI-48	50.0	-1.2	-7.3					
EI-46	49.0	-1.5	-6.6					
EI-44	47.5	-1.5	-6.9					
EI-43	47.0	-1.3	-6.8					
EI-42	46.0	-1.0	-7.4					
EI-41	45.0	-1.5	-11.3	59.7	40.3	37	139	1248
EI-40	44.0	-0.7	-7.6	63.9	36.1	81	565	2561
EI-39	42.0	-0.8	-7.2					
EI-38	40.0	-1.3	-6.7					
EI-36	39.0	-0.8	-7.0					
EI-35	37.5	-1.7	-6.8	69.5	30.5	184	374	4622
EI-34	37.0	-1.0	-8.2					
EI-33	35.5	-0.4	-6.6	63.1	36.9	152	340	2715
EI-31	35.0	-1.1	-8.9	59.0	41.0	75	279	1499
EI-29	33.0	-0.6	-7.8					
EI-28	30.5	-0.7	-6.8					
EI-27	29.0	-0.5	-5.6	60.1	39.9	189	368	2862
EI-26	28.5	-1.1	-5.8					
EI-24	27.5	-1.1	-5.1	58.2	41.8	84	198	1603
EI-23	26.0	-0.9	-6.3					
EI-22	25.0	-0.8	-5.8					
EI-21	23.5	-0.6	-7.8	59.9	40.1	88	123	2397
EI-20	23.0	-0.8	-6.8					
EI-19	22.0	-1.2	-7.0					
EI-18	20.0	-1.1	-6.4					
EI-16	18.5	-1.0	-5.3					
EI-14	17.0	-1.6	-6.8	62.6	37.4	131	314	5897

EI-12	15.0	-1.0	-5.9					
EI-10	12.5	-1.1	-5.2					
EI-9	9.5	-0.7	-5.6	59.2	40.8	91	157	4872
EI-7	8.0	-1.3	-6.3					
EI-6	6.0	-1.3	-5.4					
EI-5	4.0	-1.6	-6.1	62.4	37.6	146	356	6042
EI-3	2.0	-1.5	-5.5					
EI-1	0.5	-1.5	-5.6					

APPENDIX 2

Elemental and isotopic geochemical compositions of the Broom Point carbonates.

Sample ID	Distance	$\delta^{13}\text{C}$	$\delta^{18}\text{O}$	CaCO_3	MgCaO_3	Sr	Mn	Fe
#	(m)	(‰ VPDB)	(‰ VPDB)	%	%	(ppm)	(ppm)	(ppm)
BP-37	142.5	0.8	-6.8	98.7	1.3	721	89	888
BP-35	140	-0.2	-6.6					
BP-34	138	-0.4	-6.6	99.0	1.0	340	249	3152
BP-33	137.5	0.0	-6.8					
BP-31	136	1.5	-6.4	98.2	1.8	399	75	1120
BP-29	135	1.6	-6.9					
BP-28	133.5	1.6	-6.7	98.2	1.8	622	119	1814
BP-26	132	-0.5	-7.1					
BP-25	125	0.3	-6.9	97.8	2.2	562	104	2053
BP-24	148.5	-0.4	-6.5					
BP-23	146.5	-0.4	-6.5	99.0	1.0	308	113	1493
BP-22	140	-0.3	-6.7					
BP-21	137.5	0.6	-6.5	98.5	1.5	586	70	1962
BP-20	136	0.3	-6.4					
BP-19	131	-1.8	-6.6	97.5	2.5	290	200	3354
BP-18c	130	-2.0	-6.3					
BP-18c	129	0.5	-6.6					
BP-17	126.5	-2.1	-6.4	98.8	1.2	352	169	1760
BP-16	120.5	-2.1	-6.2					
BP-15a	119.5	-1.2	-6.6					
BP-15	114	0.5	-6.8	97.7	2.3	489	167	1613
BP-14	109	-0.2	-6.5					
BP-13	102	-1.6	-6.9	98.8	1.2	320	151	3298
BP-12c	98.5	0.1	-6.6					
BP-12	97.5	0.7	-6.7					
BP-11	94	-1.0	-6.4					
BP-10	93.5	-2.3	-6.4	98.5	1.5	352	164	1705
BP-9	87	-1.0	-6.4					
BP-8	84	0.6	-6.8	98.5	1.5	580	89	1617
BP-7a	78	-0.1	-6.9	98.7	1.3	407	186	1843
BP-6d	75	-1.2	-6.7					
BP-6b	73.5	-1.0	-6.7					
BP-6a	67.5	-0.2	-6.6	98.9	1.1	420	184	964
BP-5	56	-1.8	-7.0	98.7	1.3	255	328	1438
BP-4	45	-1.1	-6.6	98.4	1.6	227	380	4726
BP-3	40.5	-0.5	-6.5					
BP-2	38	-0.9	-6.9	98.7	1.3	252	118	1343
BP-1	35	-0.3	-7.2					

CHAPTER VII

Manuscript submitted to Canadian Journal of Earth Sciences (in review)

Carbon-isotope stratigraphy of the Berry Head (Port au Port Group) and Watts Bight (St. George Group) formations, western Newfoundland and the correlative significance

Sebastian Scorrer*, Karem Azmy, and Svend Stouge

Abstract: Carbon-isotope stratigraphy of the Furongian (Stage 10; Upper Cambrian) and Tremadocian (lowermost Ordovician) reveals distinct variations from the carbonates of the Berry Head and Watts Bight formations of the East Isthmus Bay section that accumulated in a shallow-marine setting on the eastern Laurentian platform/passive margin in western Newfoundland, Canada. The East Isthmus Bay $\delta^{13}\text{C}$ values show insignificant correlation with their Sr ($R^2 = 0.04$), Mn ($R^2 = 0.001$), and Fe ($R^2 = 0.02$) counterparts, implying preservation of at least near-primary C-isotope compositions. The investigated section is largely fossil poor but the $\delta^{13}\text{C}$ profile shows a pattern with distinct variations that can be matched with those of the western Laurentian Lawson Cove Auxiliary Boundary Stratigraphic Section and Point (ASSP) section, Utah, USA. Therefore, a conclusive conodont biozonal match was possible to reconstruct by matching the $\delta^{13}\text{C}$ profile with its counterpart from the Lawson Cove ASSP section. At the base of the East Isthmus Bay section, the $\delta^{13}\text{C}$ profile exhibits a broad excursion (the top of the Herlilnmaria-Red Tops Boundary, HERB Event), which can be matched with the base of the *Eoconodontus* Zone (mid-Furongian), followed by an enrichment trend through the *Cordylodus intermedius* Zone (top Furongian). A positive excursion (*Hirsutodontus simplex* spike or HSS) is recorded in the upper *Cordylodus intermedius* Zone (the top Cambrian), and a prominent positive peak

characteristic for the upper *Cordylodus lindstromi* Zone is recorded from the top of the investigated section. The $\delta^{13}\text{C}$ values of the Newfoundland carbonates are generally $\sim 1\text{‰}$ VPDB lower than those of Lawson Cove, which is likely attributed to a relative higher productivity and/or organic burial in the Utah region.

Introduction

In the last decade, the $\delta^{13}\text{C}$ profiles of Upper Cambrian marine carbonates of Port au Port Peninsula, western Newfoundland (e.g., Salzman *et al.*, 2004; Hurtgen *et al.*, 2009), documented the presence of the global distinct carbon-isotope event called the Steptoean positive carbon isotope excursion (or SPICE) in the Petit Jardin Formation at Felix Cove, Port au Port Peninsula. The excursion has been dated by trilobites (*Aphelaspis*, *Dunberbergia*, and *Elvinia* zones), to the Steptonian Stage of the Upper Cambrian (Westrop, 1992; Cowan and James, 1993; Knight and Boyce, 2002; Salzman *et al.*, 2004), on the south coast of Port au Port Peninsula (Fig. 1). Hurtgen *et al.*, (2009) presented both $\delta^{34}\text{S}$ and $\delta^{13}\text{C}$ isotope data from the Port au Port Group and recorded two $\delta^{13}\text{C}$ excursions, where one was referred to the SPICE event (Salzman *et al.*, 2004). The authors investigated the March Point and Felix Cove formations of the Port au Port Group and their studies focused on sections exposed in the steep coastal cliffs along the south coast of the Port au Port Peninsula.

Azmy and Lavoie (2009) constructed the $\delta^{13}\text{C}$ -isotope profile for the St. George Group (Lower Ordovician), western Newfoundland and Azmy *et al.*, (2010) discussed its correlation along the Laurentian margin with northeast Greenland. The current investigation focuses on the Upper Cambrian to Lower Ordovician carbonates exposed East of Isthmus Bay on the southwestern coast of Newfoundland.

The purpose of the current investigation is (1) to present the carbon-isotope stratigraphy of the Furongian (Upper Cambrian) Berry Head Formation of the Port au Port Group extending into the Tremadocian (Lower Ordovician) Watts Bight Formation of the St. George Group to fill the gap between the $\delta^{13}\text{C}$ curve of Hurtgen *et al.*, (2009) and that of Azmy and Lavoie (2009), and (2) to discuss correlation of the conodont biozonation scheme with the mainly barren (fossil-poor) carbonates of the Berry Head and Watts Bight formations of western Newfoundland by matching the $\delta^{13}\text{C}$ isotope curves, following the approach promoted by Glumac *et al.*, (2002a; 2002b).

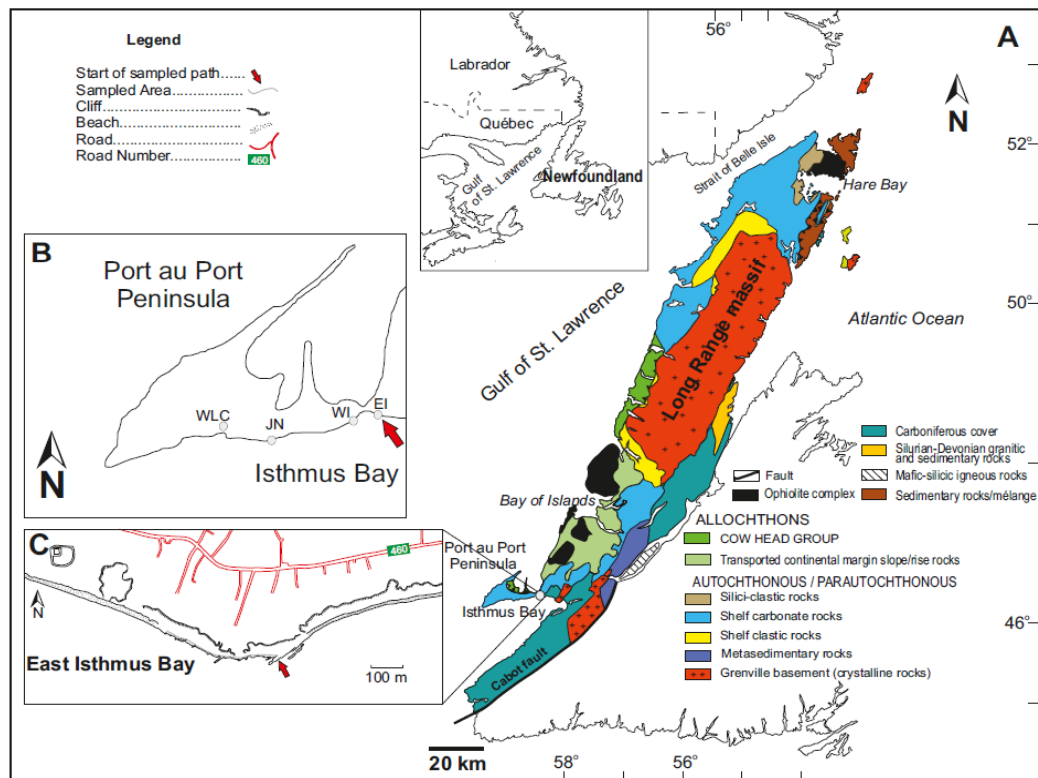


Fig. 1. (A) Map of western Newfoundland, Canada, showing the location of the investigated section, and (B) Localities where the boundary between the Berry Head and Watts Bight formations is exposed on the Port au Port Peninsula (Modified from Ji and Barnes, 1994; EI: East Isthmus Bay, WI: West Isthmus Bay, JN: Jerrys Nose, WLC: Highway cut west of Lower Cove). Red arrow points at the study area (EI, known as East Isthmus Bay section). (C) East Isthmus Bay section's coastline (48° 33' 5.5" N; 58° 42' 4.5" W).

Geological setting and stratigraphy

The Furongian (Upper Cambrian) to Tremadocian (Lower Ordovician) carbonates in western Newfoundland represent the Canadian segment of the extensive peritidal to shallow-marine carbonates that covered most of the Laurentian palaeocontinent (James *et al.*, 1989; Knight and Boyce, 2002; Lavoie *et al.*, 2003, 2013). The carbonates accumulated on the equatorial Laurentian mixed carbonate-clastic platform in a passive margin setting along the eastern Iapetus Ocean (Chow and James, 1987a; James *et al.*, 1989; Cowan and James, 1993; Lavoie *et al.*, 2013). Today, these deposits are extensively preserved in coastal and inland exposures in western Newfoundland (Knight and Boyce, 2002).

On the west coast of western Newfoundland, the peritidal to shallow marine, carbonate sedimentary rocks are referred to as the Port au Port and St. George groups (Fig. 2; James and Stevens, 1986; James *et al.*, 1989; Ji and Barnes, 1994; Lavoie *et al.*, 2013). The Port au Port Group comprises the March Point, Petit Jardin (with five members) and Berry Head formations (Fig. 2; James and Stevens, 1986; James *et al.*, 1989; Lavoie *et al.*, 2013). The sequence generally consists of limestones, dolomitic limestones and dolomites which contain shallow-marine carbonate components such as limemud, bioclastics, ooids, and oncoids (Chow and James, 1987b; Knight and James, 1987) associated with abundant microbial stromatolite and thrombolite building organisms (cyanobacteria) in the Cambrian accumulated in intertidal to subtidal environments. In the Lower Ordovician, extensive *Renalcis* mounds appeared (Pratt and James, 1982, 1986; Knight *et al.*, 2008). The biostratigraphic ages of the Port au Port Group carbonates are constrained from the trilobite *Bolaspidella* Zone (Series 3; Cambrian) at the base through the Furongian Series (Upper Cambrian) into lower Middle Ordovician (Whiterockian). They are mainly based on shelly fossil assemblages of trilobites, cephalopods, gastropods and brachiopods (e.g. Westrop, 1992; Rohr *et al.*, 2000; Boyce *et al.*, 2011) as well as conodonts (Barnes and Tuke, 1970;

Stouge, 1982; Ji and Barnes, 1994; Boyce and Stouge, 1997).

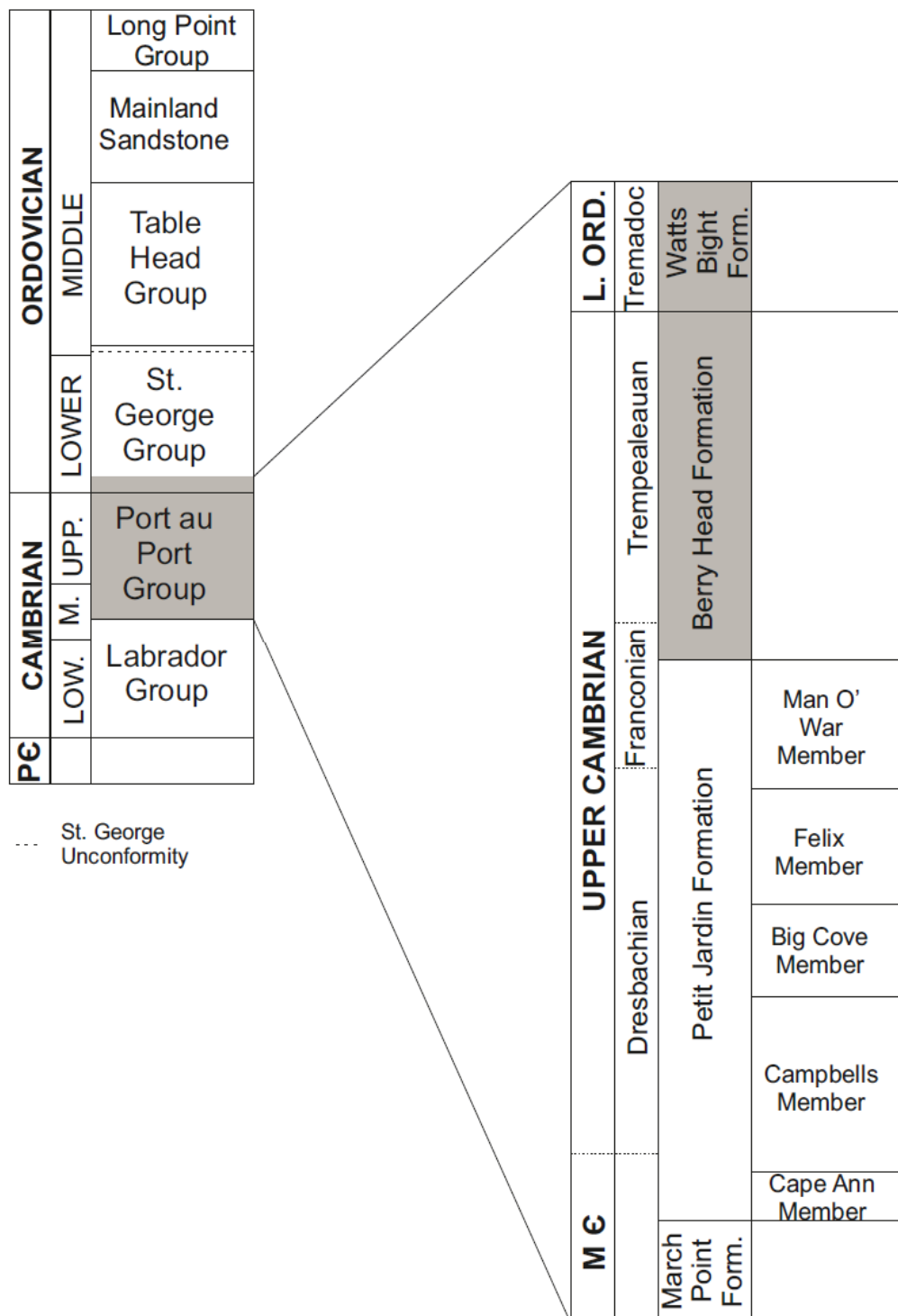


Fig. 2. A schematic framework of the different stratigraphic units spanning the East Isthmus Bay section. Highlighted area shows the approximate interval the investigated section covers.

The study area

The East Isthmus Bay section (Ji and Barnes, 1994) is a coastal cliff exposure situated at the southern coast of Newfoundland and to the east of the Port au Port Peninsula (Fig. 1; 48° 33' 5.5" N; 58° 42' 4.5" W). Ji and Barnes (1994) recorded a meagre and undiagnostic fauna composed of mainly long-range conodont species (e.g. *Teridontus nakamurai*, *Cordylodus lindstromi* and species of *Semiacontiodus*) from the uppermost part of the succession. The possible presence of *Cordylodus lindstromi* indicates that the top beds in the section should be referred to the *Cordylodus lindstromi* Zone (lowermost Ordovician).

The succession at the East Isthmus Bay section is ~ 200 m thick and composed of dolostone, dolomitic limestone and limestone (Fig. 3), with several horizons of oolites, thrombolites and stromatolites. Shale/siltstone beds and chert at certain levels with also some minor conglomeratic interbeds at the bottom of the section (Fig. 3). These lithologies suggest shallow-water environment of deposition particularly in the upper part of the section.

Ooids were observed in some thin sections (e.g., sample EI-72 and EI-132, Fig. 4A), which have been interpreted in previous Port au Port Group studies to accumulate *in situ* (Cowan and James, 1993). The development of massive, high-energy thrombolitic mound complexes in the upper part of the section supports the interpretation of a shallow marine setting.

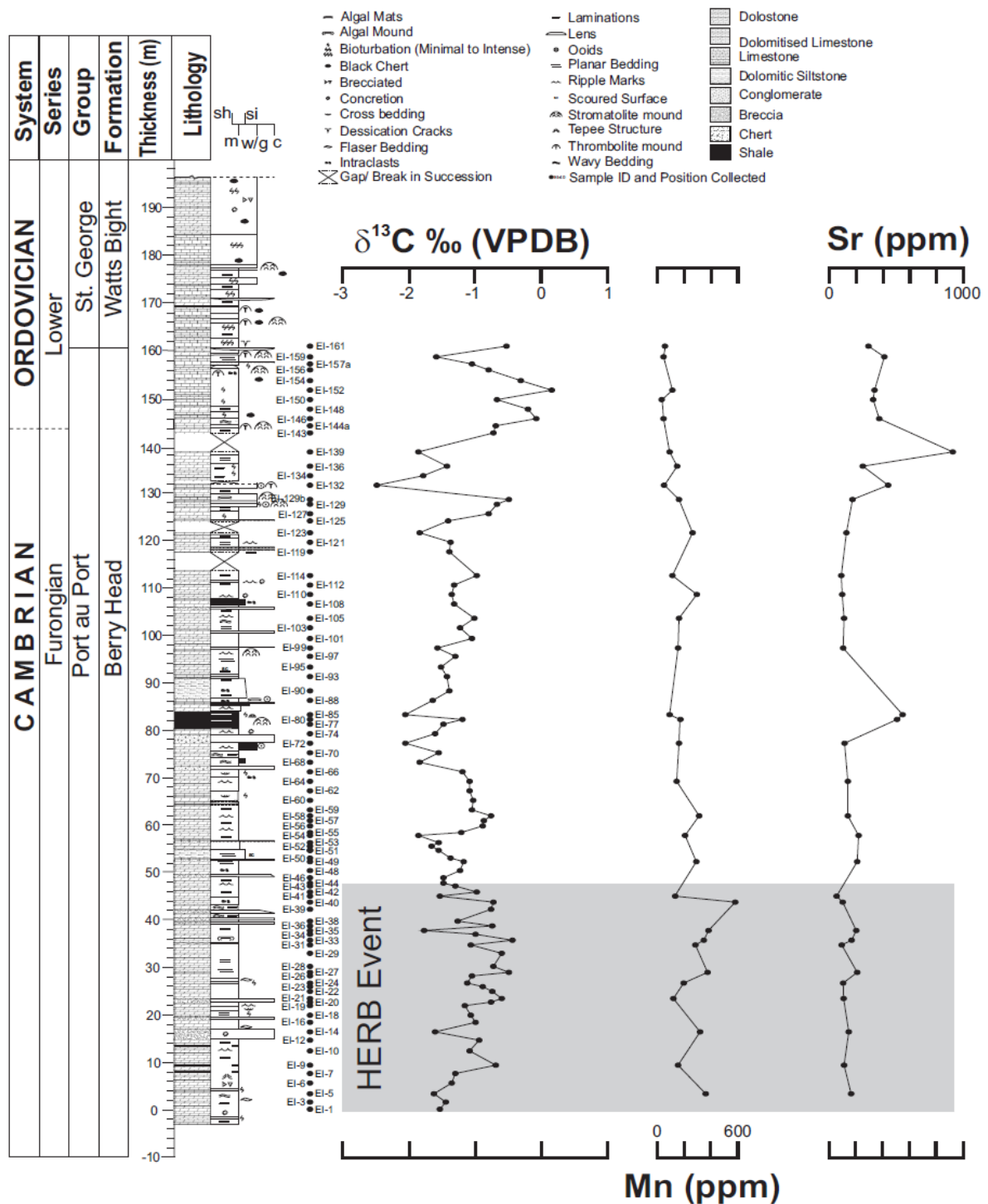


Fig. 3. Stratigraphic framework and detailed measured section with the positions of investigated samples along with the carbon-isotope, Mn and Sr profiles of the investigated Upper Cambrian to lowermost Ordovician section East of Isthmus Bay, western Newfoundland. Highlighted area shows the top of the HERB Event.

Material and methods

Ninety-two carbonate samples were collected (at sampling intervals between 20 and 100 cm) from the late Cambrian to early Ordovician East Isthmus Bay section. Thin sections were cut, stained with a mixture of potassium ferricyanide and alizarine red solution (Dickson, 1966), and examined petrographically using a polarizing microscope. Cathodoluminescence (CL) observations were performed using a Technosyn 8200 MKII cold cathodoluminoscope operated at 8 kV accelerating voltage and 0.7 mA current.

Mirror-image slabs of thin sections were prepared and polished for microsampling. The slabs were washed with deionized water and dried at 40°C overnight prior to microsampling. Guided by the observations from petrographic examination of the thin sections, samples were extracted carefully from the most micritic spots in the clean mirror-image slabs using a low-speed microdrill, avoiding cement and veins.

For C- and O-isotope analyses, about 200 µg of powder sample was reacted in an inert atmosphere with ultrapure concentrated (100 %) orthophosphoric acid at 70°C in a Thermo–Finnigan GasBench II. The liberated CO₂ was automatically delivered to a ThermoFinnigan DELTA V plus isotope ratio mass spectrometer in a stream of helium, where the gas was ionized and measured for isotope ratios. Uncertainties of better than 0.1 ‰ (2σ) for the analyses were determined by repeated measurements of NBS-19 ($\delta^{18}\text{O} = -2.20$ ‰ and $\delta^{13}\text{C} = +1.95$ ‰ vs. VPDB) and L-SVECS ($\delta^{18}\text{O} = -26.64$ ‰ and $\delta^{13}\text{C} = -46.48$ ‰ vs. VPDB). The isotopic values ($\delta^{13}\text{C}$ and $\delta^{18}\text{O}$) were expressed as per mil (‰) relative to the Vienna Pee Dee Belemnite (VPDB) (Table 1, Appendix 1).

For trace element analyses, a subset of sample powder (~ 10 mg each) was digested in 0.2 M HNO₃ for 28 hours and analysed for major and minor elements using an Elan DRC II ICP-MS (Perkin Elmer SCIEX) at Memorial University of Newfoundland. The relative

uncertainties of the measurements are better than 5 %, and results (Appendix 1) are normalized to a 100 % carbonate basis (e.g., Brand and Veizer, 1980; Veizer et al. 1999; Azmy *et al.*, 2014).

Table 1. Summary of geochemical statistics.

	$\delta^{13}\text{C}$ (‰ VPDB)	$\delta^{18}\text{O}$ (‰ VPDB)	CaCO_3 %	MgCO_3 %	Fe (ppm)	Mn (ppm)	Sr (ppm)
<i>n</i>	92	92	32	32	32	32	32
STDV	0.5	1.2	16.9	16.9	1907	121	184
Median	-1.2	-6.8	63.5	36.5	1696	163	149
Average	-1.2	-7.0	72.3	27.7	2155	199	214
Max	0.16	-5.07	99.4	41.8	7182	565	918
Min	-2.47	-11.26	58.2	0.6	180	40	37

Results

Petrography

Petrographic investigation shows that the sampled carbonates from the East Isthmus Bay section have mainly retained at least their near-micritic texture (~ 4–20 μm ; Figs. 4B, D) except for some minor recrystallization caused by dolomitization in the lower part of the succession. They appear dull to non-luminescent (Fig. 4C) under cathodoluminescence. The sampled carbonates are dominated by fine-grained carbonate mudstones with minor oolitic grainstone interbeds. The bottom of the East Isthmus Bay section is dolomitized and composed mainly of fenestral dolomicrites with minor beds of crystalline dolomite and breccia.

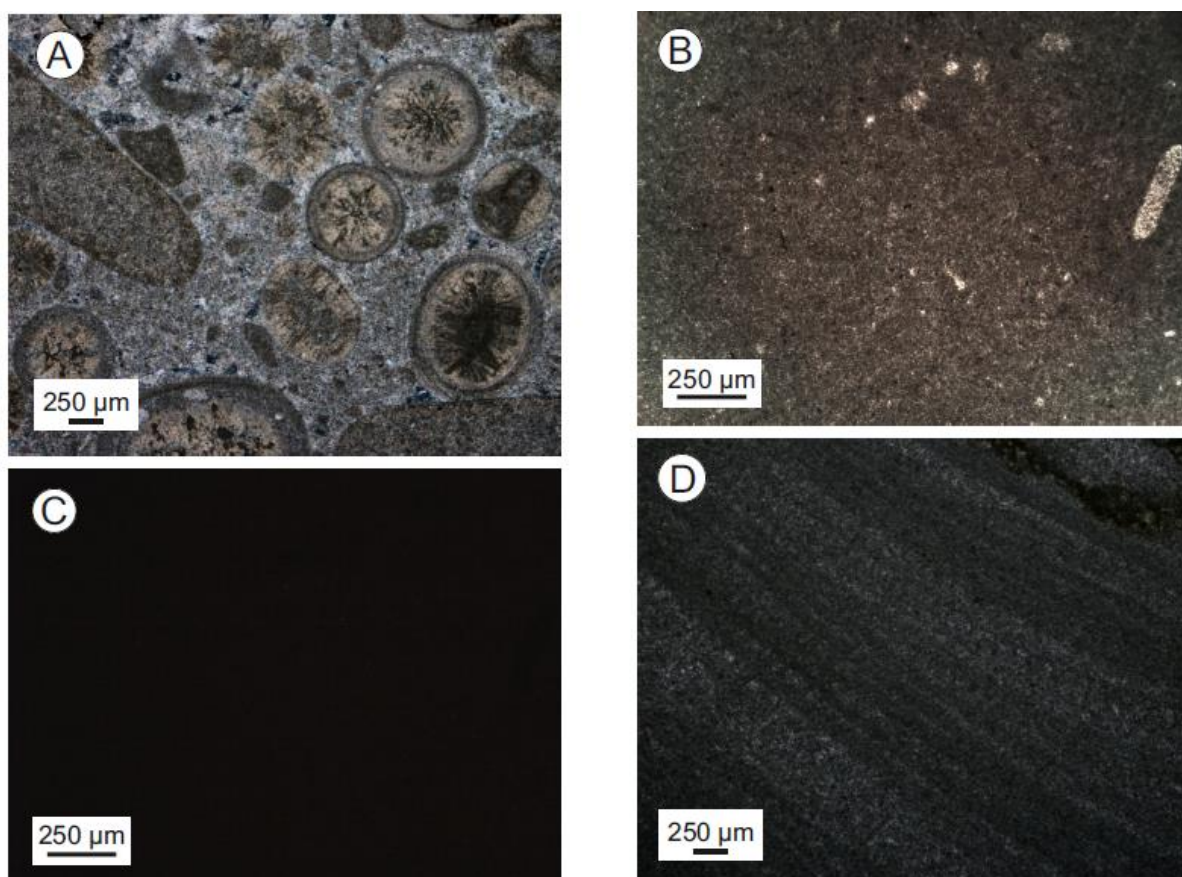


Fig. 4. Photomicrographs of various petrographic features of the East Isthmus Bay section showing (A) radial-concentric ooids (Sample EI-132, XPL), (B) micritic lime mudstone (Sample EI-139, PPL), (C) CL image of (B) that appears non-luminescent (Sample EI-139), and (D) near-micritic laminated limestone (Sample EI-77, XPL).

Stable isotopes

The geochemical characteristics of the investigated carbonates are tabulated in Appendix 1 and their statistics are summarized in Table 1. The $\delta^{13}\text{C}$ values of the East Isthmus Bay carbonates are slightly more depleted (-1.2 ± 0.5 ‰ VPDB, $n = 92$, Table 1; Fig. 3) relative to their Lawson Cove counterparts (0.4 ± 0.5 ‰ VPDB, $n = 113$, Miller *et al.*, 2015b). When compared to the $\delta^{13}\text{C}$ signatures, the $\delta^{18}\text{O}$ values show a relatively wider range of values from -11.3 to -5.1 ‰ VPDB (-7.0 ± 1.2 ‰ VPDB, $n = 92$; Table 1). The $\delta^{13}\text{C}$

values of the investigated carbonates show insignificant correlation with those of the $\delta^{18}\text{O}$ ($R^2 = 0.0003$, Fig. 5) and most of values fall within the range documented for best-preserved carbonates of the late Cambrian (Veizer *et al.*, 1999).

The C-isotope profile of the East Isthmus Bay section shows two negative excursions. The lower excursion is broad (~ 2 ‰ VPDB), recorded in the lowermost portion of the section (Fig. 3) and the upper excursion (at 132 m, Fig. 3) is sharper (-2.47 ‰ VPDB), recorded in the upper portion of the section.

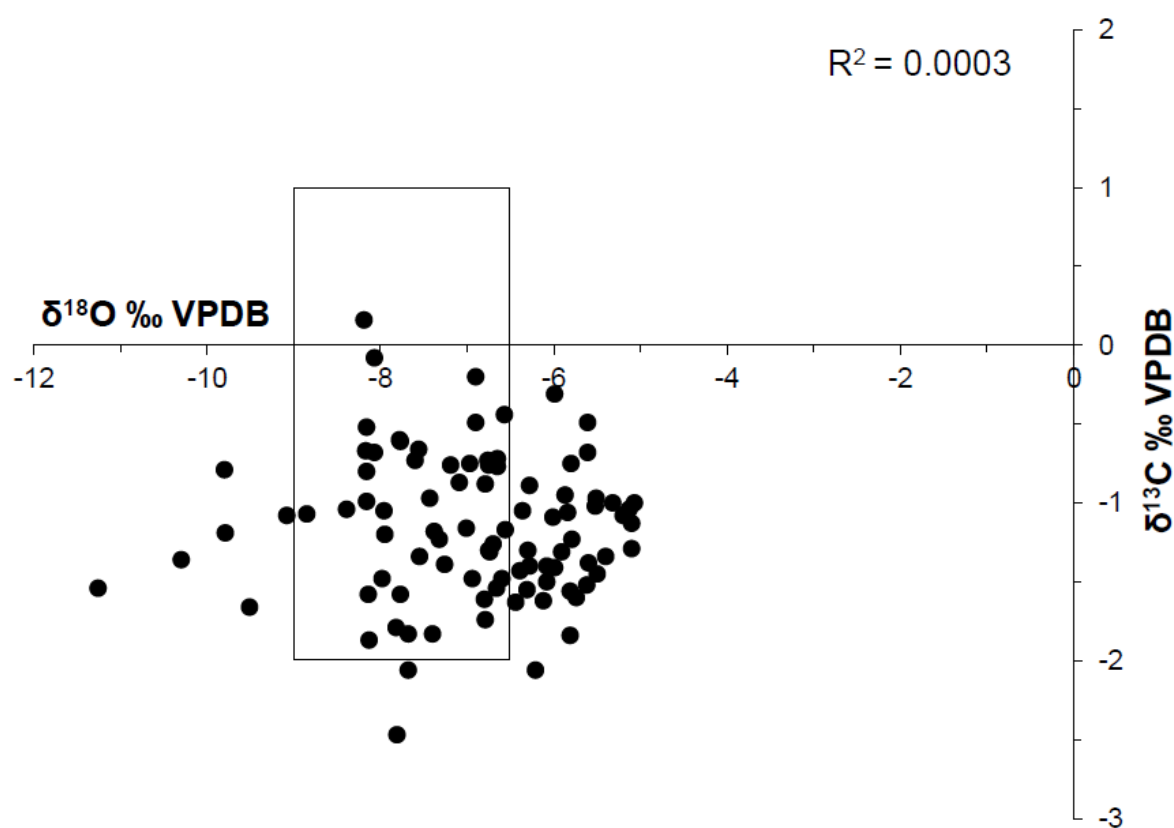


Fig. 5. Scatter plot showing correlation of the $\delta^{13}\text{C}$ with their $\delta^{18}\text{O}$ counterparts. The square represents the composition documented for the best-preserved carbonates from the Late Cambrian (Veizer *et al.* 1999).

Manganese and strontium

The Mn concentrations show an overall gradual decrease upward, with the lowest values in the upper part of the section (Fig. 3). There is little variation between 100 and 300 ppm from the lowermost interval to 120 m on the section, except for a high value of ~ 550 ppm at 44 m, but the Mn concentration decreases generally below 100 ppm for the remainder of the section (Fig. 3; Appendix 1). On the contrary, the Sr concentrations are nearly constant at ~ 200 ppm in the lower to middle intervals, except for a large interrupting peak at 83 m of ~ 500 ppm, but they are consistently higher (~ 400 ppm) in the upper interval (above the ~ 120 m horizon), except for one peak of ~ 900 ppm at 140 m (Fig. 3; Appendix 1).

The Sr concentrations are poorly correlated with their Mn counterparts ($R^2 = 0.18$, Fig 6A) and both elements exhibit insignificant correlation with their $\delta^{13}\text{C}$ counterparts ($R^2 = 0.04$ and 0.001 , respectively; Fig. 6B, C). Similarly, Fe shows an insignificant correlation with the $\delta^{13}\text{C}$ counterparts ($R^2 = 0.02$, Fig. 6D). Moreover, the Sr and Mn concentrations are also insignificantly correlated with their $\delta^{18}\text{O}$ counterparts ($R^2 = 0.06$ and 0.05 , respectively). In addition, the Mn/Sr values are poorly correlated with their $\delta^{13}\text{C}$ ($R^2 = 0.001$) and $\delta^{18}\text{O}$ ($R^2 = 0.005$) counterparts.

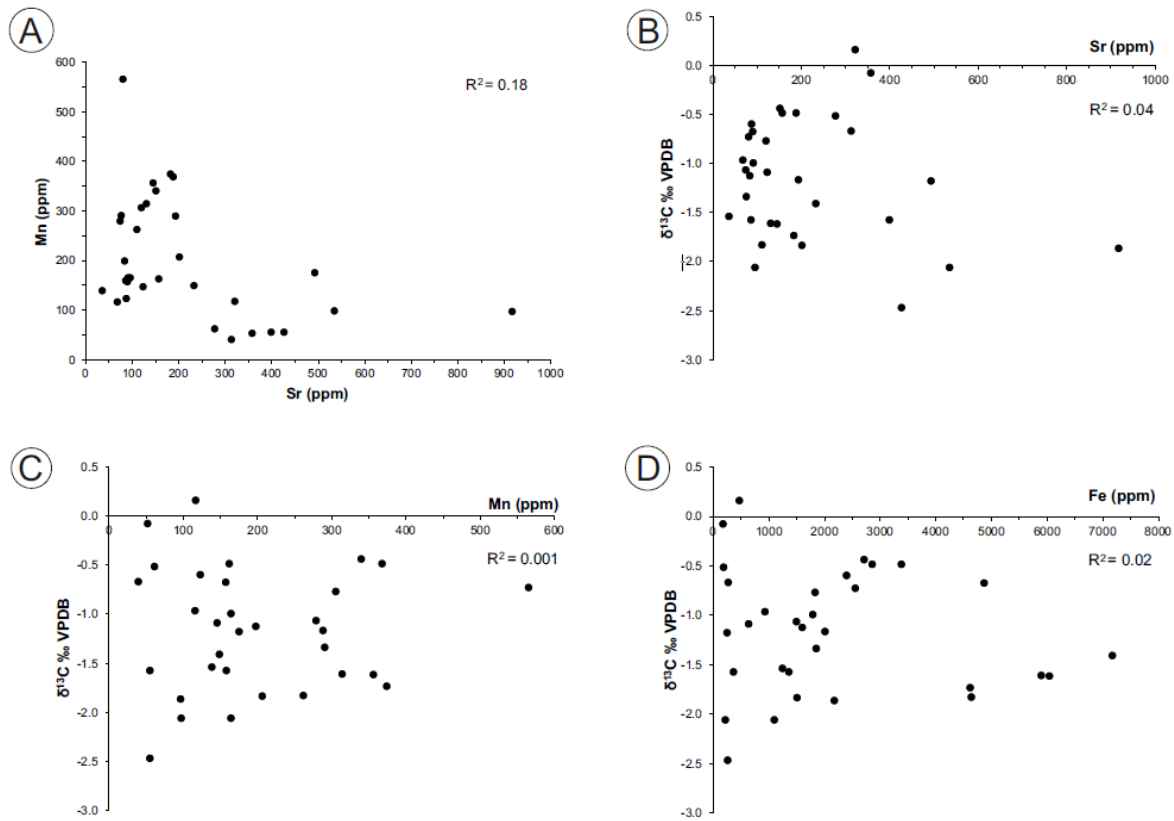


Fig. 6. Scatter plot showing correlation of (A) Mn with Sr, and (B) Sr, (C) Mn, and (D) Fe with their $\delta^{13}\text{C}$ counterparts for the investigated samples.

Discussion

Evaluation of diagenetic influence

The scarcity of preservation of ancient sediments, particularly those from the Paleozoic, makes the evaluation of the petrographic and geochemical preservation of the investigated carbonates a foundation for carbon-isotope chemostratigraphic correlations.

Petrographic investigation shows that the sampled carbonates from the studied section have mainly retained at least their near-primary sedimentary fabrics (Fig. 4A–D), except for minor recrystallization caused by dolomitization in the lower parts of the succession.

Although most of the East Isthmus Bay section consists of dolomites (mainly dolomicrites), the reset of $\delta^{13}\text{C}$ signatures requires high water-rock interaction ratio, which is always associated with significant recrystallization and significant increase in crystal size (Veizer, 1983; Banner and Hanson, 1990). The micritic/ near-micritic grain size (Fig. 4B, D) of investigated carbonates and the preservation of fabric, such as the ooids internal structure (Fig. 4A, radial-concentric ooids, Chow and James, 1987b) argue against significant reset of the $\delta^{13}\text{C}$ signatures. Also, the investigated carbonates appear dull to non-luminescent under cathodoluminescence (Fig. 4C).

It is well established that, during burial of sediments, the diagenetic fluids react with marine sediments under anoxic conditions through dissolution-reprecipitation processes that result in recrystallization (generally associated with aggrading neomorphism) and changes in the geochemical composition of the diagenetic carbonate phase where Mn and Fe is enriched in the secondary carbonate, but Sr is progressively depleted (Veizer, 1983; Veizer *et al.*, 1999). However, the investigated samples were extracted from mainly carbonate mudstones and dolomicrites that generally retained micritic to near-micritic grain size and their sedimentary fabrics, thus suggesting a high degree of textural preservation, which is also supported by their non- to dull CL (Fig. 4C). In addition, the Sr, Mn, and Fe contents (diagenetic proxies) exhibit insignificant correlation with their $\delta^{13}\text{C}$ counterparts ($R^2 = 0.04$, 0.001, and 0.02, respectively; Fig. 6B–D) suggesting the preservation of at least near-primary carbon-isotope compositions of the investigated carbonates. The relative contents of the Mn and Fe in carbonates have been found to control their luminescence (CL) under a cold cathodoluminoscope (Machel and Burton, 1991). High Mn concentrations in carbonates activate bright CL whereas, on the contrary, the enrichment of Fe quenches the luminescence and results in dull to non-CL (Machel and Burton, 1991). The dull to non-CL exhibited by the investigated carbonates (Fig. 4C) supports the preservation of primary geochemical

signatures, which is consistent with the near-micritic grain size and fabric retention. However, cathodoluminescence of carbonates has to be taken with caution because high Fe contents can cause non-luminescence in altered carbonates (see Rush and Chafetz, 1990). Therefore, other techniques are always applied to confirm the preservation of carbonates.

Impact of diagenesis on the $\delta^{13}\text{C}$ composition of carbonates is relatively less than that on the $\delta^{18}\text{O}$ counterparts, particularly at low water/rock interaction ratio (reflected by near-micritic grain size and restricted recrystallization) because diagenetic fluids do not usually have high amounts of dissolved CO_2 , which may reset the $\delta^{13}\text{C}$ signatures significantly (Veizer, 1983; Banner and Hanson, 1990). Unless the process of dolomitization occurs under conditions of significantly high water/rock interaction ratios, the $\delta^{13}\text{C}$ of the dolomite reflects the nature of the precursor carbonate (Tucker and Wright, 1990). Freshwater diagenesis is another alteration process that delivers ^{13}C -depleted carbon from soil CO_2 together with ^{18}O -depleted oxygen from meteoric water (Allan and Matthews, 1982). Such diagenesis is often associated with meteoric cements that have low values of both $\delta^{13}\text{C}$ and $\delta^{18}\text{O}$ and generates the apparent covariance of the C- and O-isotopic values (e.g. Allan and Matthews, 1982; Marshall, 1992). The poor correlation between the $\delta^{18}\text{O}$ and $\delta^{13}\text{C}$ values of the investigated carbonates (Fig. 5) and the falling of most of these values within the range documented for the best preserved marine carbonates of the Late Cambrian (Fig. 5; Veizer *et al.*, 1999) strongly support the preservation of at least near-primary signatures of the investigated carbonates.

Match to the Lawson Cove ASSP section, Utah, USA

The systematic sampling of the investigated section allows the reconstruction of a continuous $\delta^{13}\text{C}$ profile from the Furongian (Upper Cambrian) into the Tremadocian (Lower

Ordovician) in the East Isthmus Bay section (Fig. 3) and the correlation with the equivalent section, from Laurentia, the Lawson Cove ASSP section (Utah, USA; Miller *et al.*, 2011, 2014). The two sections consist of shallow-marine carbonates deposited on the platform of Laurentia, but the Lawson Cove section is much less dolomitized and has a nearly complete conodont record tied to the $\delta^{13}\text{C}$ isotope profile (Miller *et al.*, 2015a, 2015b).

The $\delta^{13}\text{C}$ values at East Isthmus Bay are generally ~ 1 ‰ VPDB lower than those of the Lawson Cove counterparts (Table 1; Miller *et al.*, 2015b, their text-figure 14), which is likely attributed to the local paleo-oceanographic conditions such as productivity and/or organic carbon burial. The $\delta^{13}\text{C}$ profiles of both sections (East Isthmus Bay and Lawson Cove) have comparable features of synchronous peaks of distinct negative and positive excursions that allow a possible correlation of the conodont-poor section in western Newfoundland (Fig. 7). For consistency, the numbering of C-isotope peaks on the profiles of the correlated sections in this study (Fig. 7) follows the format of Miller *et al.*, (2015b). The lower negative excursion (~ 2 ‰ VPDB) that peaks in the bottom of East Isthmus Bay section is close to the base of the *Eoconodontus* conodont Zone (Fig. 7), though this excursion is not complete in the investigated section and can therefore be correlated with the top of the HERB Event (Miller *et al.*, 2011, 2014; also known as TOCE – the Top of Cambrian Excursion; Zhu *et al.*, 2006). The upper negative excursion (Fig. 7; Peak 13) can be reliably correlated with the upper subzone of the *Cordylodus intermedius* Zone. The following sharp increase (Peak 14) appears to match the spike seen in the upper *Cordylodus lindstromi* Zone of the Lawson Cove. The intermediate but characteristic excursions (Peaks 9 to 11) can be matched respectively with the base and the upper part of the *Cordylodus proavus* Zone. The overlying positive peak (Peak 12), here named HSS (= *Hirsutodontus simplex* spike, i.e. following Chen *et al.*, 1995), lies within the lower *Cordylodus intermedius* Zone.

This match using the near-primary $\delta^{13}\text{C}$ -isotope variations improve the relative dating

of the fossil-poor, Furongian (Upper Cambrian) carbonates of the Berry Head Formation (Port au Port Group) and its lateral equivalents.

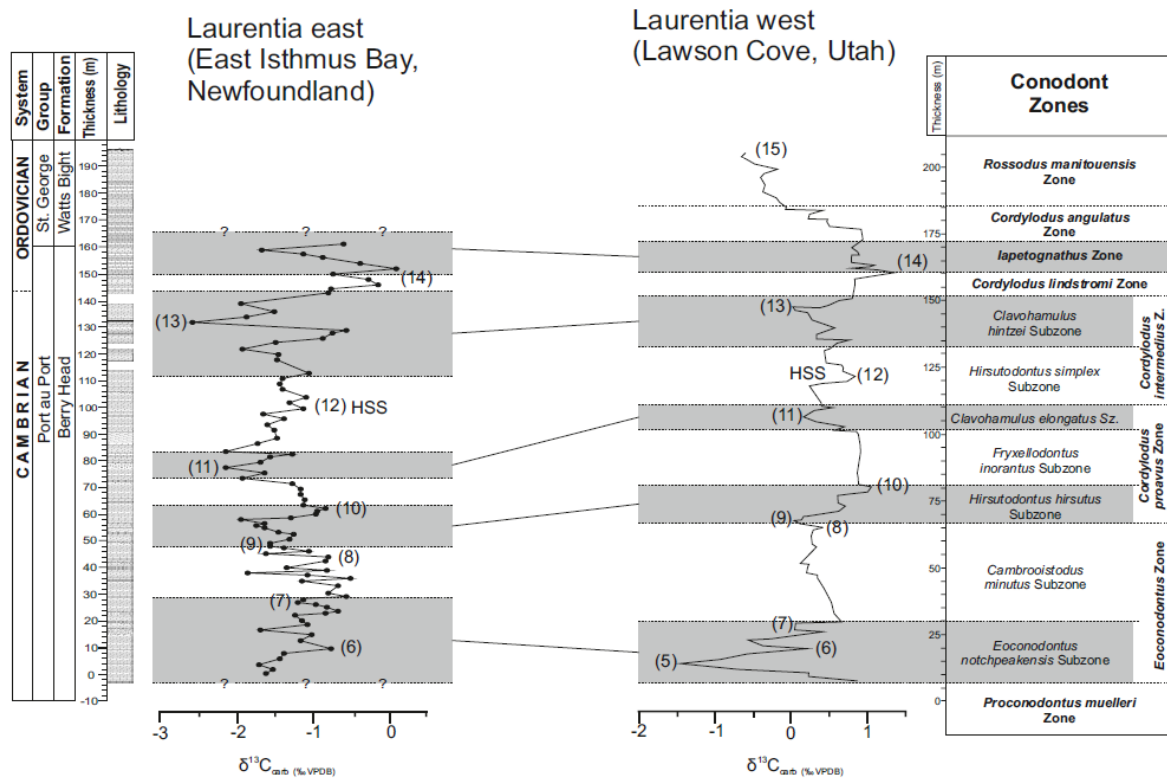


Fig. 7. The correlation of the $\delta^{13}\text{C}$ profiles of the East Isthmus Bay section, western Newfoundland, Canada, with that of Lawson Cove, Utah, USA. Conodont biostratigraphy in Utah is from Miller et al. (2015b). The construction of the conodont biostratigraphy at East Isthmus Bay is based on the C-isotope correlation. Detail in text.

Conclusions

Samples were collected at narrow intervals from the near-micritic carbonates of the East Isthmus Bay section of Berry Head and Watts Bight formations in western Newfoundland, Canada. Petrographic examination and geochemical analyses suggest preservation of at least near-primary $\delta^{13}\text{C}$ signatures. The $\delta^{13}\text{C}$ profile shows two main negative excursions, a broad one in the lower section (Furongian, Upper Cambrian) and a

sharper counterpart in the upper part of the section (uppermost Cambrian).

The main negative excursions and the bracketed minor peaks in between can be correlated with counterparts on the well-established equivalent profile of the Lawson Cove ASSP section, Utah, USA. The match suggests that the large lower negative excursion seen in the lower East Isthmus Bay section can be correlated with the *Eoconodontus notchpeakensis* Subzone of the *Eoconodontus* Zone (Furongian, Upper Cambrian) in the Lawson Cove section and the large upper negative excursion can be correlated with the top of the *Cordylodus intermedius* Zone (top Cambrian) in the Lawson Cove section.

The large positive excursion (Peak 14) at the top of the East Isthmus Bay section probably corresponds to the largest positive excursion recorded in the upper subzone of the *Cordylodus lindstromi* Zone of the Lawson Cove (Miller *et al.*, 2015b).

The positive and negative peaks between the two major negative excursions on the East Isthmus Bay C-isotope profile can be matched with equivalent counterparts in the Lawson Cove profile allowing for a secure match with the conodont biozonation scheme between the *Eoconodontus notchpeakensis* Subzone of the *Eoconodontus* Zone and *Iapetognathus* Zone.

Local variations in paleo-oceanographic conditions likely resulted in a slight decrease (~ 1 ‰ VPDB) in the $\delta^{13}\text{C}$ values at East Isthmus Bay relative to those of their Lawson Cove counterparts.

The current study provides a continuous carbon-isotope profile from the top of Port au Port Group extending into the base of the St. George Group that allows better regional correlation for the sections with poor biostratigraphic controls.

References

- Allan, J. and Matthews, R. 1982. Isotope signatures associated with early meteoric diagenesis. *Sedimentology*, 29(6), pp. 797-817.
- Azmy, K. and Lavoie, D. 2009. High-resolution isotope stratigraphy of the Lower Ordovician St. George Group of western Newfoundland, Canada: implications for global correlation. *Canadian Journal of Earth Sciences*. 46, pp. 1–21.
- Azmy, K., Stouge, S., Christiansen, J.L., Harper, D.A.T., Knight, I., Boyce, D. 2010. Carbon-isotope stratigraphy of the Lower Ordovician succession in Northeast Greenland: implications for correlations with St. George Group in western Newfoundland (Canada) and beyond. *Sedimentary Geology*. 225, pp. 67–81.
- Azmy, K., Stouge, S., Brand, U., Bagnoli, G., and Ripperdan, R. 2014. High-resolution chemostratigraphy of the Cambrian–Ordovician GSSP: Enhanced global correlation tool. *Palaeogeography, Palaeoclimatology, Palaeoecology*, 409: 135-144.
- Banner, J. L. and Hanson, G. N. 1990. Calculation of simultaneous isotopic and trace element variations during water-rock interaction with applications to carbonate diagenesis. *Geochimica et Cosmochimica Acta*, 54(11), pp. 3123–37.

- Barnes, C.R. and Tuke, M.F. 1970. Conodonts from the St. George Formation (Ordovician), northern Newfoundland. Geological Survey of Canada, Bulletin 187, pp. 79–97.
- Boyce, W.D. and Stouge, S. 1997. Trilobites and conodont biostratigraphy of the St. George Group at Eddies Cove West, western Newfoundland. Current Research. Newfoundland Department of Mines and Energy. Geological Survey, Report 97-1, pp. 183–200.
- Boyce W. D., McCobb L. M. E., Knight I. 2011. Stratigraphic studies of the Watts Bight Formation (St. George Group), Port au Port Peninsula, western Newfoundland. *In* Current Research. Government of Newfoundland and Labrador, Department of Natural Resources, Mines Branch, Report 11–1.
- Brand, U., and Veizer, J. 1980. Chemical diagenesis of a multicomponent carbonate system: 1. Trace elements. *Journal Sedimentary Petrology*, 50, pp. 1219–1236.
- Chen, J.Y., Zhang, J.M., Nicoll, R.S. 1995. Carbon and oxygen isotopes in carbonate rocks within Cambrian–Ordovician boundary interval at Dayangcha, China. *Acta Palaeontologica Sinica* 34(4), pp. 393–409.

- Chow, N. and James, N. 1987a. Cambrian Grand Cycles: A northern Appalachian perspective. *Geological Society of America Bulletin*, 98(4), pp. 418.
- Chow, N. and James, N. P. 1987b. Facies-Specific, Calcitic and Biomineralic Ooids from Middle and Upper Cambrian Platform Carbonates, Western Newfoundland, Canada. *SEPM Journal of Sedimentary Research*, 57.
- Cowan, C. and James, N. 1993. The interactions of sea-level change, terrigenous-sediment influx, and carbonate productivity as controls on Upper Cambrian Grand Cycles of western Newfoundland, Canada. *Geological Society of America Bulletin*, 105(12), pp. 1576–1590.
- Dickson, J. 1966. Carbonate identification and genesis as revealed by staining. *Journal Sedimentary Petrology* 36, pp. 491–505.
- Glumac, B. and Spivak-Birndorf, M. 2002a. Stable isotopes of carbon as an invaluable stratigraphic tool: An example from the Cambrian of the northern Appalachians, USA. *Geology*, 30(6), pp. 563.
- Glumac, B. 2002b. ABSTRACT: Stable Isotopes of Carbon as a Tool for High Resolution Stratigraphy of the Sauk II-Sauk III Sequence Boundary. *AAPG Bulletin*, pp. 86.

- Hurtgen, M., Pruss, S. and Knoll, A. 2009. Evaluating the relationship between the carbon and sulfur cycles in the later Cambrian ocean: An example from the Port au Port Group, western Newfoundland, Canada. *Earth and Planetary Science Letters*, 281(3-4), pp. 288–297.
- James, N.P., and Stevens, P.K. 1986. Stratigraphy and correlation of the Cambro–Ordovician Cow Head Group, western Newfoundland. *Geological Survey Canada*, 366: 1–143.
- James, N. P., Stevens, R. K., Barnes, C. R., and Knight, I. 1989. Evolution of a Lower Paleozoic Continental-Margin Carbonate Platform, Northern Canadian Appalachians. In: Crevello, P.D. Wilson, Sarg, J.L., Read, J.F. (Eds.), *Controls on Carbonate Platform and Basin Development*. Society of Economic Paleontologists and Mineralogists Special Publication, 44: 123–146.
- Ji, Z. and Barnes, C. 1994. Conodont paleoecology of the Lower Ordovician St. George Group, Port au Port Peninsula, western Newfoundland. *Journal of Paleontology*, 68(06): 1368-1383.
- Knight, I. and Boyce, W. D. 2002. Lower Paleozoic carbonate rocks of the northern closure of the North Brook anticline and the Spruce Pond Klippe, Georges Lake (12B/16) and Harrys River (12B/9) map areas: collected thoughts on unconnected rocks. *Current Research (2002) Newfoundland Department of Mines and Energy, Geological Survey, Report 02-1*, pp. 121–134.

- Knight, I. and James, N. P. 1987, Stratigraphy of the Saint George Group (Lower Ordovician): The interaction between eustasy and tectonics: *Canadian Journal of Earth Sciences*, 24, pp. 1927–1952.
- Knight, I., Azmy, K., Boyce, D., Lavoie, D. 2008. Tremadocian Carbonates of the Lower St. George Group, Port au Port Peninsula, Western Newfoundland: Lithostratigraphic Setting of diagenetic, Isotopic, and Geochemistry Studies. Current Research Newfoundland and Labrador Department of Natural Resources Geological Survey. Report 08–1, pp. 1–43.
- Lavoie, D., Burden, E. and Lebel, D. 2003. Stratigraphic framework for the Cambrian–Ordovician rift and passive margin succession from southern Quebec to western Newfoundland. *Canadian Journal of Earth Sciences*, 40(2), pp. 177-205.
- Lavoie, D., Desrochers, A., Dix, G., Knight, A. and Hersi, O.S. 2013. The Great Carbonate Bank in Eastern Canada: An Overview. In: Derby, J., Fritz, R., Longcare, S., Morgan, W., Sternbach, C. (Eds.), *The Great American Carbonate Bank: The Geology and Economic Resources of Cambrian–Ordovician Sauk Megasequence of Laurentia*. American Association of Petroleum Geologists, Memoir, 98: 499–524.
- Machel, H.G., and Burton, E.A. 1991. Factors Governing Cathodoluminescence in Calcite and dolomite, and Their Implications for Studies of Carbonate Diagenesis.

Luminescence microscopy and spectroscopy, qualitative and quantitative applications.
SEPM Short Course, 25: 37–57.

Marshall, J. D. 1992. Climatic and oceanographic isotopic signals from the carbonate rock record and their preservation. *Geological Magazine* 129, 143–160.

Miller, J., Evans, K., Freeman, R., Ripperdan, R. and Taylor, J. 2011. Proposed stratotype for the base of the Lawsonian Stage (Cambrian Stage 10) at the First Appearance Datum of *Eoconodontus notchpeakensis* (Miller) in the House Range, Utah, USA. *Bulletin of Geosciences*, pp.595-620.

Miller, J., Repetski, J., Nicoll, R., Nowlan, G., and Ethington, R. 2014. The conodont *Iapetognathus* and its value for defining the base of the Ordovician System. *GFF*, 136(1): 185-188.

Miller, J., Evans, K., Freeman, R., Ripperdan, R and Taylor, J. 2015a. The proposed GSSP for the base of Cambrian Stage 10 at the First Appearance Datum, of the conodont *Eoconodontus notchpeakensis* (Miller, 1969) in the House Range, Utah, USA. *GFF*, 136(1), pp. 189-192.

Miller J. F., Evans K. R., Ethington R. L., Freeman R. L., Loch J. D., Popov L.
E., Repetski J. E., Ripperdan R. L. & Taylor J. F. 2015b. Proposed Auxiliary

Boundary Stratigraphic Section and Point (ASSP) for the base of the Ordovician System at Lawson Cove, Utah, USA. *Stratigraphy*, 12, 219–36.

Pratt, B. and James, N. 1982. Cryptalgal-metazoan bioherm of early Ordovician age in the St George Group, western Newfoundland. *Sedimentology*, 29(4), pp.543-569.

Pratt, B. and James, N. 1986. The St George Group (Lower Ordovician) of western Newfoundland: tidal flat island model for carbonate sedimentation in shallow epeiric seas. *Sedimentology*, 33(3), pp. 313-343.

Rohr, D.M., Measures, E.A., Boyce, W.D. and Knight, I. 2000. Ongoing studies of Late Cambrian and Early Ordovician gastropods of western Newfoundland. In *Current Research*. Government of Newfoundland and Labrador, Department of Mines and Energy, Geological Survey, Report 2000-1, pages 241-250.

Rush, P. and Chafetz, H. 1990. Fabric-retentive, Non-luminescent Brachiopods as Indicators of Original ^{13}C and ^{18}O Composition: A Test. *SEPM Journal of Sedimentary Research*, 60.

Saltzman, M. R., Cowan, C. A., Runkel, A. C., Runnegar, B., Stewart, M. C. and Palmer, A. R. 2004. The Late Cambrian Spice ($\delta^{13}\text{C}$) event and the Sauk II–Sauk III regression: New evidence from Laurentian basins in Utah, Iowa, and Newfoundland: *Journal of Sedimentary Research*, 74, pp. 366–377.

Stouge, S. 1982. Preliminary conodont biostratigraphy and correlation of the Lower and Middle Ordovician carbonates of the St. George Group, Great Northern Peninsula, Newfoundland. Mineral Dev. Div., Dept. Mines & Energy, Gvt. Newfoundland & Labrador, Rept. 82-3, pp. 59.

Tucker, M. E. and Wright, V. P. 1990. Carbonate Sedimentology. Blackwell Scientific Publications, Oxford, UK.

Veizer, J. 1983. Chemical Diagenesis of Carbonates. In: Arthur, M.A., Anderson, T.F., Kaplan, I.R., Veizer, J., Land, L.S. (Eds.), Theory and application of trace element technique, Stable Isotopes in Sedimentary Geology. Society of Economic Paleontologists and Mineralogists (SEPM) Short Course Notes, 10: III-1–III-100.

Veizer, J., Ala, D., Azmy, K., Bruckschen, P., Bruhn, F., Buhl, D., Carden, G., Diener, A., Ebner, S., Goddard, Y., Jasper, T., Korte, C., Pawellek, F., Podlaha, O., Strauss, H., 1999. $^{87}\text{Sr}/^{86}\text{Sr}$, $\delta^{18}\text{O}$ and $\delta^{13}\text{C}$ evolution of Phanerozoic seawater. Chem. Geol. 161, 59–88.

Westrop, S. 1992. Upper Cambrian (Marjuman-Steptoean) trilobites from the Port au Port Group, western Newfoundland. Journal of Paleontology. 66(02), pp. 228–255.

Zhu, M., Babcock, L. and Peng, S. 2006. Advances in Cambrian stratigraphy and paleontology: Integrating correlation techniques, paleobiology, taphonomy and paleoenvironmental reconstruction. *Palaeoworld* 15, pp. 217–222.